UNIVERSITY OF CALIFORNIA

Los Angeles

Achieving the "Dual Targets" of CO_2 emission reduction and air quality improvement for Chinese cities

A dissertation submitted in partial satisfaction

of the requirements for the degree

Doctor of Environmental Science and Engineering

by

Li Zhang

2021

ABSTRCT OF THE DISSERTATION

Achieving the “Dual Targets” of CO_2 emission reduction and air quality improvement for Chinese cities

by

Li Zhang

Doctor of Environmental Science and Engineering

University of California, Los Angeles, 2021

Professor Yifang Zhu, Chair

China is facing the challenges of both climate change and air pollution. To tackle the challenges, China has set specific goals, such as the CO_2 emission peak target by 2030 and the "Beautiful China" target by 2035, to reduce greenhouse gases and air pollutant emissions. Cities in China play an important role as they are the fundamental units to implement reduction policies. In this dissertation, we investigate the pathway for Chinese cities to achieve the dual targets of CO_2 emission reduction and air quality improvement. This work is divided into the following five chapters: an overview (Chapter 1), three chapters of original research (Chapters 2 – 4), conclusions and future work (Chapter 5).

We first make a comprehensive assessment of air quality and CO_2 emission changes from 2015 to 2019 for 335 Chinese cities, using the city-level data of $PM_{2.5}$ and O_3 concentrations and CO_2 emissions. We select important regions for air pollution control in China and categorize all cities

into different classes according to their development levels. Then we compare the changes of air quality and CO_2 emission by region or city class. We find that $PM_{2.5}$ concentrations decrease remarkably from 2015 to 2019 due to mandatory city-level $PM_{2.5}$ reduction targets, especially in the Beijing-Tianjin-Hebei and Yangtze River Delta regions. Nonetheless, O_3 concentrations increase in 91% of Chinese cities and CO_2 emissions increase in 69% of the cities. The changes in CO_2 emissions are significantly lower in developed cities compared to developing cities, which is mainly driven by the reduction in energy intensity and the improvement in energy structure. Our findings indicate a lack of synergy in air quality improvement and CO_2 emission reduction in China under the current policy framework. To tackle the challenges of both air pollution and CO_2 mitigation, we suggest that cities set mandatory city-level CO_2 emission reduction targets and reinforce energy-related measures in future policies.

To address the inconsistency in current CO_2 and air pollutants emission inventories, we then develop a unified emission inventory including both emissions. We also identify the co-hotspots of both CO_2 and air pollutants emissions at a high spatial resolution (1×1 km^2). Using Guangzhou city as a case, we find that the stationary combustion sector and the transportation sector are the main contributors to CO_2 and air pollutants emissions, together accounting for 95%, 67%, and 93% of total CO_2, SO_2, and NO_x emissions. The co-hotspots analysis shows that more than 66% of total CO_2 and air pollutants emissions are originated from the top 10% emission grids. Our findings enable accurate identification of high-emission grids, which improve the precision and effectiveness in the collaborative control of CO_2 and air pollutants.

Lastly, we propose a pathway for Chinese cities to reach the dual targets of CO_2 emission reduction and air quality improvement. Using Yantai city as a case, we develop an integrated assessment model that couples the emission projection, air quality, and health assessment. We find

that strict energy-related measures can help Yantai meet the national annual $PM_{2.5}$ standard of 35 $\mu g/m^3$ by 2030 and achieve the carbon neutrality goals by 2060. Energy-related measures contributed to 53% and 79% of $PM_{2.5}$ reduction in 2035 and 2060, exhibiting an increasing potential in improving air pollutants emissions compared to the advanced end-of-pipe controls. We find that the future health benefit from improved air quality will likely compensate for the abatement cost of implementing energy measures, with a net monetized benefit of 1.9 billion Chinese yuan in 2060. Our findings could provide a reference for Chinese cities to deal with the dual challenges in the future.

Overall, we find a lack of synergy in air quality improvement and CO_2 emission reduction in China under the current policy framework. The unified emission inventory and co-hotspots analysis provide a basis to design collaborative control strategies. The proposed dual targets pathway can guide Chinese cities to address both challenges in future policy design.

The dissertation of Li Zhang is approved.

Timothy Malloy

Suzanne E Paulson

Irwin H Suffet

Yifang Zhu, Committee Chair

University of California, Los Angeles

2021

Table of Contents

List of Figures

List of Tables

ACKNOWLEDGMENTS

My sincerest appreciation and deepest gratitude go to my advisor, Dr. Yifang Zhu, for her support and encouragement throughout my doctoral studies. She has always been willing to listen to my ideas, findings, and challenges, and, and provide me with invaluable advice to make progress. She is the true definition of the role model. This work would not have been possible without her patience, enthusiasm, and guidance.

I would like to express my sincere thanks to my committee members, Dr. Timothy Malloy, Dr. Suzanne E Paulson, and Dr. Irwin H Suffet for their constant efforts, detailed feedback, and great guidance on this dissertation work. Special thanks to Dr. Bofeng Cai and Dr. Yu Lei at CAEP for their expertise, guidance, and support throughout my doctoral research. I also want to extend my thanks to Harrison Levy and Dr. Cully Nordby in the Environmental Science and Engineering Program.

I also want to thank all my coauthors for their contribution and help throughout our collaboration work. Special thanks to Muchuan Niu and Pengcheng Wu for the stimulating ideas and continuous assistance. I would like to extend my appreciation to Dr. Yan Lin, Nickie Cammisa, Amanda Wagner, and all my fellow colleague at UCLA and CAEP for their help throughout this dissertation work.

Finally, my warm and heartfelt thanks go to my family for their tremendous support and continuous encouragement. Thanks for the emotional, intellectual and financial support in both work and life. I thank my wife Jing Deng for her unconditional love and support. I would not be here without all of you.

Vita

Education

University of California, Los Angeles, CA 2017–present

D.Env candidate in Environmental Science Engineering

Harvard University, Boston, MA 2015–2017

M.S. in Environmental Health

Tsinghua University, Beijing, China 2011–2015

B.S. in Building Science Engineering

Professional Experience

Chinese Academy of Environmental Planning, Beijing, China 2019–present

Research Intern at Center for Carbon Neutrality

Environmental Resource Management China, Shanghai, China 2016

Environmental Consultant Intern

Selected Publications

Li Zhang, Libin Cao, Yu Lei, Bofeng Cai, Guangxia Dong. (in press) "The research on the synergy effects of air pollution control and CO_2 emissions reduction and policy implication." in Green Book of Climate Change (2021). 2021, Social Science Academic Press (China).

Li Zhang, Xin Wan, Hanying Jiang, Xuan Li, Shaodong Xu, Bofeng Cai. "Study on quantitative evaluation on the status of CO_2 emissions (In Chinese)." *Environment Engineering*, 2021, 39 (10), 1–7.

Li Zhang, Lin Yan, Yifang Zhu. "Transport and Mitigation of Exhaled Electronic Cigarette Aerosols in a Multizone Indoor Environment." *Aerosol Air Quality Research*. 2020, 20: 2536–2547.

Li Zhang, Zixuan Xie, Libin Cao, Qiaong Wu, Bofeng Cai. "Discussion on evaluation method on carbon dioxide emissions peaking for Chinese cities (In Chinese)." *Environment Engineering*, 2020, 38 (11), 1–5+43.

Bofeng Cai, **Li Zhang**, Chuyu Xia, Lu Yang, Hui Liu, Lingling Jiang, Libin Cao, Yu Lei, Gang Yan, Jinnan Wang (Accepted). "A new model for China's CO_2 emission pathway using the top-down and bottom-up approaches". *Chinese Journal of Population, Resources and Environment*, 2021.

Mengbing Du, Xiaoling Zhang, Lang Xia, Libin Cao, Zhe Zhang, **Li Zhang**, Heran Zheng, Bofeng Cai (Accepted). " The China Carbon Watch (CCW) system: a rapid accounting of household carbon emissions in China at the provincial level." *Renewable and Sustainable Energy Reviews*, 2021.

Selected Presentations

Li Zhang and Bofeng Cai. "Evaluation on the CO_2 emission peak." Oral presentation at *the Dual Targets Pathway for Chinese Cities Annual Conference* (Oct 2021), Beijing

Li Zhang, Yan Lin, Yifang Zhu. "Assessment and Mitigation of Exhaled Electronic Cigarette Aerosols in a Multi-zone Indoor Environment." Poster presentation at *the American Association for Aerosol Research (AAAR) 37th Annual Conference* (Oct 2019), Portland, Oregon

Patents

Libin Cao, Bofeng Cai, **Li Zhang**. "A quick calculation system of industrial CO_2 emissions". *China National Intellectual Property Administration*, No. CN111859045B, granted on Apr. 16th, 2021.

Fellowships & Awards

Tobacco-Related Disease Research Program Student Research Supplement Award, University of California, Los Angeles, 2018

Harvard Chan Central Grant Award, Harvard University, 2015–2016

University Research Scholarship, Tsinghua University, 2014

Chapter 1

Overview

The recent climate system is changing at an unprecedented rate over centuries to millennia (Masson-Delmotte et al. 2021). According to the Intergovernmental Panel on Climate Change (IPCC) Sixth Assessment Report (Masson-Delmotte et al. 2021), over the period 2011 to 2020, the global surface temperature is 1.09 °C higher than the pre-industrial level. Unquestionably, human influence has warmed the atmosphere, ocean, and land and affected many climate extremes in every region around the globe, such as heatwaves, heavy precipitation, droughts, and tropical cyclone (Masson-Delmotte et al. 2021). Anthropogenic emissions, particularly greenhouse gases (GHG), are considered to cause changes in the climate system (Stocker et al. 2013). Human-induced CO_2 emissions from fossil fuel combustion and industrial processes account for about 78% of the total GHG emissions increase from 1970 to 2010 (Stocker et al. 2013). It is estimated that global warming of 2 °C will be exceeded by the end of the 21st century unless extensive reductions in CO_2 and other GHG emissions occur.

China, as the world's largest carbon dioxide (CO_2) emitter since 2005 (1), has taken a leading role in battling against climate change. In the Nationally Determined Contribution (NDC) of the Paris Agreement in 2015, China pledges to peak CO_2 emissions around 2030 at the latest and lower CO_2 emissions per unit of Gross Domestic Product (GDP), namely the carbon intensity, by 60 – 65% by 2030 compared to 2005 (NDRC 2015; The Guardian 2016). The NDC targets are further strengthened in the Climate Ambition Summit in 2020. More specifically, China claims to implement more aggressive actions against climate change by reaching CO_2 emission peak before

2030 and carbon neutrality before 2060, lowering the carbon intensity by over 65% by 2030 from the 2005 level, increasing the share of non-fossil fuels in primary energy consumption to around 25% by 2030, increasing the forest stock volume by 6 billion m^3 by 2030 from the 2005 level, and increasing the total installed capacity of wind and solar power to over 1.2 billion kW by 2030 (Climate Ambition Summit 2020). In support of the national climate goals, the white paper "Responding to Climate Change: China's Policies and Actions" is published in 2021 (State Council Information Office of the People's Republic of China 2021), which set up requirements in all major sectors, such as transforming and upgrading the industrial structure, improving the energy mix through innovation, controlling GHG emissions in key industries (iron and steel, building material, chemical, and non-ferrous metal sectors), and promoting a low-carbon transportation system and reducing non-CO_2 GHG emissions. In summary, a considerable amount of efforts have been made in China to curb climate change.

Fossil fuel combustion and industrial processes emit CO_2 emissions, accounting for roughly 92% of the total GHG emissions in China (China Ministry of Ecology and Environment 2018). In the meantime, they also produce air pollutants (Oh et al. 2019; Lu et al. 2020), including $PM_{2.5}$ (particulate matter with an aerodynamic diameter ≤ 2.5 μm) and precursors of ozone (O_3). Previous studies have reported that both $PM_{2.5}$ and O_3 are associated with adverse effects on human health (Brunekreef and Holgate 2002; Burnett et al. 2018). To tackle air pollution issues, extensive efforts have been made in the past decade (Zheng et al. 2017; Zhang et al. 2019). China has introduced strict clean air policies since 2013, including the Air Pollution Prevention and Control Action Plan (2013) (State Council of the People's Republic of China 2013) and the Three-Year Action Plan for Winning the Blue Sky Defense Battle (2018) (State Council of the People's Republic of China 2018), with special requirements in important regions including the Beijing-Tianjin-Hebei and the

surrounding region (BTH, the 2+26 cities), the Yangtze River Delta region (YRD), and the Pearl River Delta region (PRD). Further, the 2035 "Beautiful China" target is proposed to require most cities in China to achieve the annual $PM_{2.5}$ standard (< 35 μg/m^3) by 2035 (Xinhua 2020). Despite the past efforts in controlling air pollution, the current situation is still not optimistic. In 2019, almost half of Chinese cities still fail to meet the national annual $PM_{2.5}$ standard (China National Environmental Monitoring Centre 2021). In addition, increasingly severe O_3 pollution, especially in the summertime, has been observed in China in recent years (Li et al. 2019a, b; Xing et al. 2019), and a 1-3 ppb increase per year is reported in megacity clusters (Miao et al. 2021). The above evidence suggests China also faces strict air pollution challenge in addition to the climate change challenge.

Previous studies suggest that control measures that reduce CO_2 emissions could also reduce air pollutant concentrations and vice versa, as many air pollutants and CO_2 are emitted from the same sources, such as fossil fuel burning (Oh et al. 2019; Lu et al. 2020). Therefore, well-designed mitigation policies could potentially achieve the co-benefit of reducing CO_2 emissions (Jiang et al. 2013; Lu et al. 2019) and improving air quality (Markandya et al. 2009; Nemet et al. 2010; West et al. 2013; Xie et al. 2018; Li et al. 2019d) simultaneously. While studies have evaluated either the air quality improvement or CO_2 emission reductions in China, they usually treat them as two separate issues. Besides, only a few studies are conducted at the city level (Wang et al. 2019; Jiang et al. 2021), with most studies focusing on the national or regional levels (Cai et al. 2017; Zhang et al. 2019). A comprehensive understanding of both issues at the city-level resolution is important as cities are the fundamental units to implement reduction policies in China (Chen et al. 2020a). As the Chinese government has announced to pursue a synchronized control of air pollution and CO_2 emissions, the analysis at the city level with both air pollution and CO_2 emission assessment

will be fundamental for China to achieve the ambitious climate and air quality goals. Besides, we believe it is meaningful to investigate the pathway that helps Chinese cities to understand the relationship between CO_2 emissions and air pollutants emissions and finally achieve the "dual targets" of CO_2 emission reduction and air quality improvement, which can directly support the city's design of control strategies and policies in the future.

In Chapter 2, we make a comprehensive assessment of air quality and CO_2 emission changes for all Chinese cities from 2015 to 2019 by using the data of $PM_{2.5}$ and O_3 concentrations and CO_2 emissions with city-level resolution. Both the international climate pledge and the national air quality goals have necessitated the need to first make a detailed and synchronized assessment of the current situations in China. Here we select important regions for air pollution control in China, including the BTH, the YRD, the PRD, the Fenwei Plain region (FWP), and the Cheng-Yu District region (CYD). We also categorize all cities into different classes based on the cities' development level (GDP, permanent population, and industrial structure). Then we make comparisons for the changes of air quality and CO_2 emissions by region or city class. We find the unsynchronized reduction trends under the current policies when comparing $PM_{2.5}$ and O_3 concentrations and CO_2 emissions in parallel. We find that $PM_{2.5}$ concentrations decrease remarkably from 2015 to 2019, especially in the BTH and YRD regions, which shows the effectiveness of current pollution control policies with city-level mandatory $PM_{2.5}$ reduction targets. Nonetheless, we find that O_3 concentrations increase in most cities and CO_2 emissions increase in 69% of the cities. The CO_2 emission changes show distinct patterns among different city classes, mainly driven by the city's economic level, energy intensity, and energy structure. Our findings indicate a lack of synergy in air quality improvement and CO_2 emission reduction under the current policy framework and

underscore the importance of addressing both challenges holistically in future policies by reinforcing energy-related measures and setting mandatory CO_2 reduction targets at the city level.

The lack of synergy in reduction trends of air quality and CO_2 emission under the current policies in Chapter 2 leads us to the question of how to address both challenges simultaneously, which puts more requirements on effective emission control strategies. Previous studies report that the comprehensive emission inventory is crucial to conduct effective controls on air pollutants and CO_2 (D'Avignon et al. 2010; Crippa et al. 2020), as it provides the basic emission characteristics, the major contribution of different sources, and the spatial profile of the emissions(Qi et al. 2017; Bai et al. 2020). At present, there is unbalanced development between the CO_2 and air pollutants emission inventories in China. The air pollutants emission inventories are well established and provide sufficient support to tackle the air pollution problem (Zhang et al. 2009; Li et al. 2017). In the meantime, the CO_2 emission inventory in China is far from developed. Although previous studies (WRI China 2015; C40 Cities 2021; CDP 2021) have developed the CO_2 emission inventory at the provincial or city level, inventories are often developed for research purposes and the data were not publicly available(Xu 2018). The above unsynchronized development greatly prevents cities from understanding the CO_2 emission characteristics and formulating targeted control measures, thus greatly hindering China's ability to achieve its ambitious CO_2 mitigation goals. In addition, few studies have investigated the inconsistency in the structures and classification of current CO_2 and air pollutants emission inventories. As to the spatial distribution, previous studies usually treat two inventories separately, so the spatial information of both emissions cannot be obtained simultaneously. Such information is important in understanding the spatial pattern of CO_2 and air pollutants emissions and conducting site-specific management to control both emissions collaboratively.

In Chapter 3, using Guangzhou city as a case, we develop a unified emission inventory including both CO_2 and air pollutants emissions to address the issues on data sources, inventory structure, and spatial distribution in current inventories. Further, we map both emissions at a high spatial resolution (1×1 km^2), which allows us to identify high emission grids for both emissions, namely the "co-hotspots". We find that CO_2 and air pollutants emissions are mainly originated from the stationary combustion and the transportation sectors. The co-hotspots analysis shows that most CO_2 and air pollutants emissions are attributed to the top 10% emission grids. Our findings provide important guidance for designing and implementing collaborative control strategies on CO_2 and air pollutants emissions for Chinese cities.

Another issue related to Chinese cities is how the city can achieve the dual targets through ambitious CO_2 and air pollution mitigation pathways. Previous studies use integrated modeling frameworks to investigate the co-benefits in major sectors. Most studies are conducted at global (West et al. 2013), national (Xie et al. 2018), and provincial (Dong et al. 2015) scales, which cannot provide sufficient support for Chinese cities to deal with the strict challenges of climate change and air pollution. Therefore, we believe it is important to conduct a city-level co-benefit analysis that proposes the mitigation pathway to achieve the "dual targets" of CO_2 emission reduction and air quality improvement. From a broader perspective, considering the unique role of Chinese cities as the fundamental units to implement reduction policies (Chen et al. 2020a), the effectiveness of the city-level mitigation pathway is crucial to fulfilling China's international climate pledge and ambitious air quality targets.

In Chapter 4, we propose a pathway for Chinese cities to achieve the dual targets of CO_2 emission reduction and air quality improvement. Using Yantai city as a case, we couple an integrated assessment model that combines the emission projection, air quality, and health impact

analysis. Our approach considers different levels of energy-related measures and end-of-pipe controls, which allows us to understand their mitigating effects on CO_2 and air pollution. We find that city-level air quality and CO_2 reduction targets are feasible through energy-related measures and end-of-pipe controls. Energy-related measures exhibit an increasing potential in reduction air pollutants as well as its dominant contribution to mitigate CO_2 emissions; while advanced end-of-pipe controls will contribute to improve air quality in the short term. We find that the future health benefit from improved air quality will likely compensate for the implementation cost of energy measures. Our findings could serve as an example for other Chinese cities to tackle climate and air quality problems in the future.

Chapter 2

A systematic assessment of city-level climate change mitigation and air quality improvement in China

2.1 Abstract

To tackle the challenges of both climate change and air pollution, China has set specific goals, such as reaching the CO_2 emission peak by 2030 and the "Beautiful China" target by 2035, to reduce greenhouse gases and air pollutant emissions. Although previous studies had evaluated air quality improvement and CO_2 emission reductions in China, the two issues were usually treated separately and the analyses were often conducted for selected regions or at the national level. Thus, a detailed and synchronized assessment of China's air quality and CO_2 emissions at the city level is lacking. Here we used city-level data to evaluate the changes in $PM_{2.5}$ and O_3 concentrations and CO_2 emissions from 2015 to 2019 for 335 Chinese cities. We selected important regions for air pollution control in China and also categorized all cities into different classes according to their development levels. Then we made comparisons for the changes of air quality and CO_2 emissions by region or city class. We found that $PM_{2.5}$ concentration decreased remarkably from 2015 to 2019, especially in the BTH (-27%) and YRD (-21%) regions, which demonstrated the effectiveness of current control policies with city-level mandatory $PM_{2.5}$ reduction targets. Nonetheless, O_3 concentrations had increased in 91% of Chinese cities and CO_2 emissions had increased in 69% of the cities from 2015 to 2019. We also found that the changes of CO_2 emissions showed distinct patterns among different city classes that the changes were significantly lower in

developed cities compared to developing cities, which was mainly driven by the reduction in energy intensity and the improvement in energy structure. Our study indicates a lack of synergy in air quality improvement and CO_2 emission reduction in China. To address the challenges of both climate change and air pollution simultaneously, we suggest that cities set mandatory city-level CO_2 emission reduction targets and reinforce energy policies in future policies and control strategies.

2.2 Introduction

Given the fast industrialization and urbanization, China has become the world's largest CO_2 emitter in 2005 (BP 2021). It is estimated that CO_2 emissions in China will keep rising by more than 50% in the next 15 years without strict and proper mitigations (Liu et al. 2015). CO_2 emissions from fossil fuel combustion and industrial processes accounted for roughly 92% of the total GHG emissions in China (China Ministry of Ecology and Environment 2018). In the meantime, fossil fuel combustion and industrial processes also produced air pollutants (Oh et al. 2019; Lu et al. 2020), including $PM_{2.5}$ (particulate matter with an aerodynamic diameter ≤ 2.5 μm) and precursors of O_3. Both $PM_{2.5}$ and O_3 have been shown to have adverse effects on human health (Brunekreef and Holgate 2002; Burnett et al. 2018). Considerable amount of efforts had been made in the past decade to tackle air pollution issues in China (Zheng et al. 2017; Zhang et al. 2019). Yet, almost half of Chinese cities still failed to meet the national annual ambient air quality standard of 35 $\mu g/m^3$ for $PM_{2.5}$ in 2019 (China National Environmental Monitoring Centre 2021). Further, increasingly severe O_3 pollution, especially in the summertime, has been observed in China in recent years (Li et al. 2019a, b; Xing et al. 2019), and a 1-3 ppb increase per year was reported in megacity clusters (Miao et al. 2021).

China had proposed a series of goals and mitigation policies to reduce CO_2 emissions and to improve air quality. In the NDC of the Paris Agreement in 2015, China pledged to reduce CO_2 emissions per unit of GDP, namely the CO_2 emission intensity, by 60-65% by 2030 compared to 2005 (NDRC 2015; The Guardian 2016). Recently in the Climate Ambition Summit, China claimed to implement more aggressive actions against climate change by reaching CO_2 emission peak before 2030 and carbon neutrality by 2060 (Climate Ambition Summit 2020). More specifically, according to China's Thirteenth Five-Year Plan, a 12 – 20% reduction in the CO_2

emission intensity was set at the provincial level (State Council of the People's Republic of China 2016). Moreover, "China's pilot low-carbon city" initiative (National Development and Reform Commission 2010) was launched to promote low-carbon actions at the city level. On the other hand, China had already introduced strict clean air policies since 2013, including the Air Pollution Prevention and Control Action Plan (2013) (State Council of the People's Republic of China 2013) and the Three-Year Action Plan for Winning the Blue Sky Defense Battle (2018) (State Council of the People's Republic of China 2018). The 2035 "Beautiful China" target was also proposed to require most cities in China to achieve the annual $PM_{2.5}$ standard (< 35 $\mu g/m^3$) by 2035 (Xinhua 2020). These efforts had resulted in marked improvements in ambient air quality in China (Cai et al. 2017; Ding et al. 2019; Zhang et al. 2019), including a 33% reduction in $PM_{2.5}$ concentrations between 2013 and 2017, which was associated with a reduction of roughly 47,000 $PM_{2.5}$-related premature deaths in the same span of time (Huang et al. 2017b).

Previous studies suggested that control measures that reduce CO_2 emissions could also reduce air pollutant concentrations and vice versa, as many air pollutants and CO_2 were emitted from the same sources, such as fossil fuel burning (Oh et al. 2019; Lu et al. 2020). Therefore, well-designed mitigation policies could potentially reduce CO_2 emissions (Jiang et al. 2013; Lu et al. 2019) and improve air quality (Markandya et al. 2009; Nemet et al. 2010; West et al. 2013; Xie et al. 2018; Li et al. 2019d) simultaneously. However, previous studies that evaluated either the air quality improvement or CO_2 emission reductions in China often treated them as two separate issues. Furthermore, such studies were usually conducted at the regional or national levels (Cai et al. 2017; Zhang et al. 2019), with few studies focusing on the city level (Wang et al. 2019; Jiang et al. 2021). As a result, a comprehensive evaluation at the city-level resolution that quantifies the changes for both air quality and CO_2 emissions is still missing. As the Chinese government has announced to

pursuit a synchronized control of both air pollution and CO_2 emissions in the coming years, the analysis at the city level with both air quality and CO_2 emissions assessment will be fundamental for China to achieve its goal on climate mitigation and air pollution control.

In this Chapter, we assessed the changes for both CO_2 emissions and air quality for 335 Chinese cities from 2015 to 2019. We emphasized the differences observed among different pollutants and CO_2 for different regions and different city classes. Our results provide insights for future policy that accommodates both climate and air quality control targets in China.

2.3 Methods

2.3.1 Data source

CO_2 emission data for all cities in China were compiled by the China City Greenhouse Working group (CCG) (CCG 2020) and sourced from CHRED 3.0 database (Cai et al. 2018a, 2019b, a; CHRED 2020). Air quality data were sourced from the China National Environmental Monitoring Centre (China National Environmental Monitoring Centre 2021). In China, O_3 concentrations were reported in mass concentration (unit: $\mu g/m^3$) at a reference meteorological condition with an ambient temperature of 298 K and an ambient pressure of 1013 hPa. To facilitate the comparison with reported O_3 concentrations in most countries (unit: ppb), we thus converted the collected O_3 concentrations with the coefficient of 1.95 $\mu g/m^3$ to 1 ppb. The exact data are shown in **Table A 1**. City-level GDP, permanent population, and industrial structure data from 2015 to 2019 were obtained from the Statistical Bulletin on the National Economic and Social Development of each city (National Bureau of Statistics 2020a) and the statistical yearbook of each province or city (National Bureau of Statistics 2020b). To exclude inflation and other price increases, GDP was converted to constant prices in 2015.

2.3.2 Identification of the periods of CO_2 emissions

Overall, we identified three periods of CO_2 emission, including the period of growth, plateau, and decline (Jiang et al. 2021). **Figure 2. 1** shows the schematic diagram of different periods of CO_2 emission.

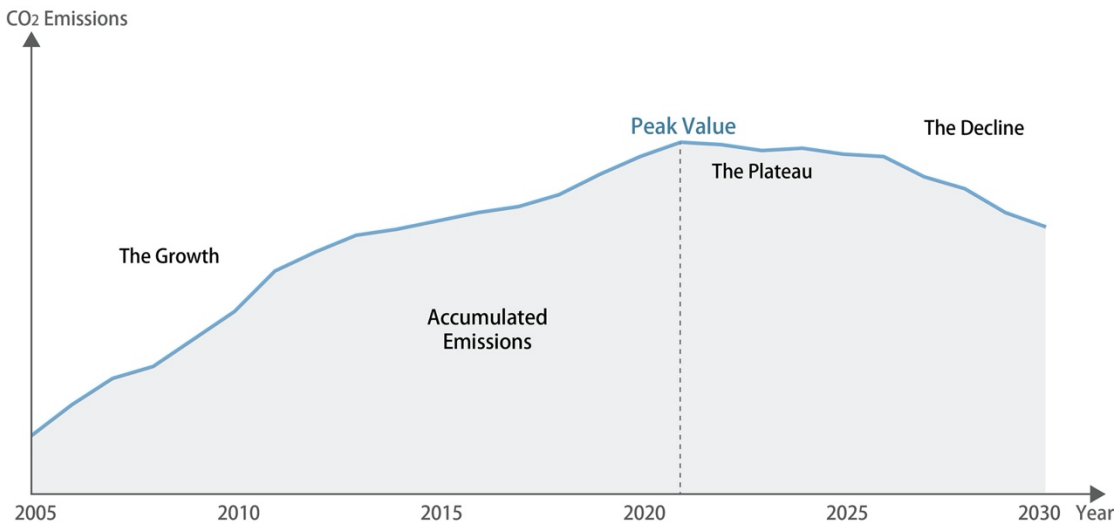

Figure 2. 1 A schematic diagram on the different periods of CO_2 emission

We used the Mann-Kendall trend test to determine the periods of CO_2 emission based on the 15-year data, as shown in **Figure 2. 2**. We first identified the maximum CO_2 emission from 2005 to 2019 as the "peak value", then applied the Mann-Kendall trend test, which was used to test for significant decreasing trends, and finally determined the periods based on the test results of both total and direct CO_2 emission. The period of growth was defined when the CO_2 emission was increasing continuously from 2005 to 2019. The period of plateau was defined when the CO_2 emission was around the maximum emission level in recent years. The period of decline was defined when the CO_2 emission decreased after reaching the maximum emission level. The total CO_2 emission included direct CO_2 emission from fossil fuel combustion and indirect CO_2 emission from electricity use. Before using the Mann-Kendall trend test, we needed at least five data points of yearly CO_2 emission after reaching the "peak value". According to the Levin and UNEP report (Levin and Rich 2017; UNEP 2018) and Gilbert statistical rule (Richard O. Gilbert 1987), if data points were less than five, they would not be enough to prove that it was not a false decline or plateau period (C40 2018).

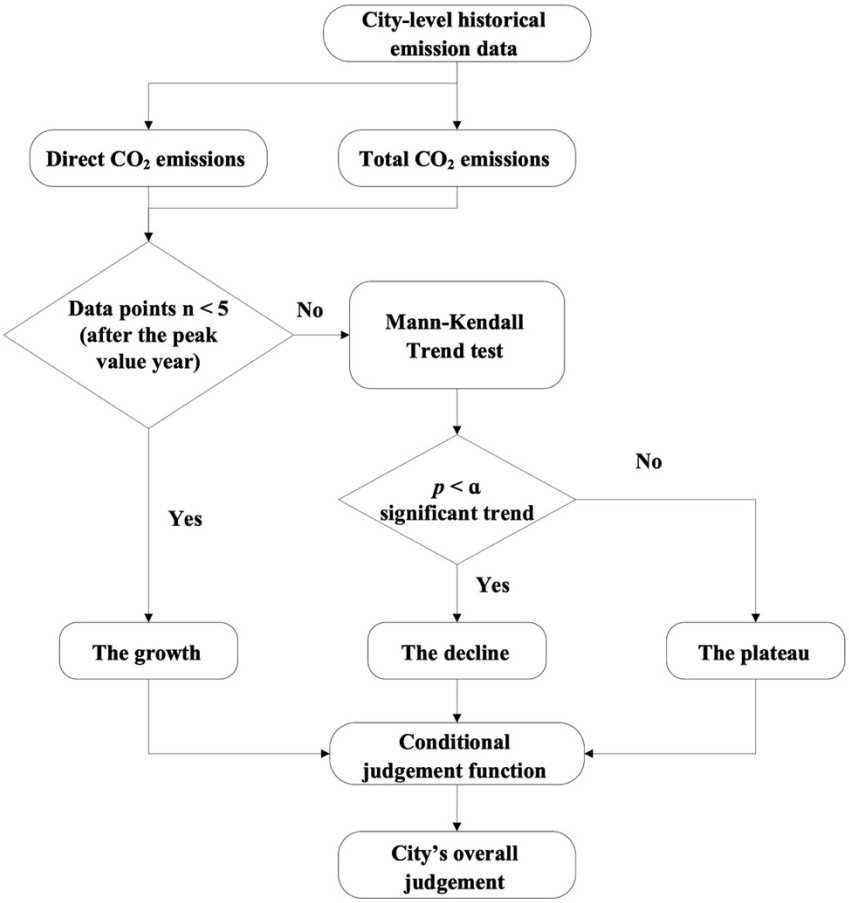

Figure 2. 2 Systematic assessment model on the periods of CO_2 emission

Figure 2. 3 presents the CO_2 emissions for representative cities from 2005 to 2019. The green, purple, and grey background colors represent the cities in the period of decline, plateau, and growth of CO_2 emission, respectively. For example, the total CO_2 emission in Kunming city reached the maximum emission in 2010, and the data points after the maximum year are nine (more than five). The Mann-Kendall test result was significant with a p-value less than 0.05. Therefore, we concluded that the total CO_2 emissions of Kunming showed a significant downward trend and Kunming's total CO_2 emission have reached the period of decline. A similar analysis was conducted for the direct CO_2 emission of Kunming, and the result was significant as well. Thus, we concluded that Kunming reached the period of decline of CO_2 emission. For Yichang, the direct

and total CO_2 emission reached the maximum emission in 2012 and the Mann-Kendall test result did not show a significant downward trend for CO_2 emission after 2012. Thus, we concluded that Yichang was in the period of plateau of CO_2 emission. In contrast, Yantai's direct and total CO_2 emission was increasing from 2005 to 2019 and we concluded that Yantai was in the period of growth of CO_2 emission.

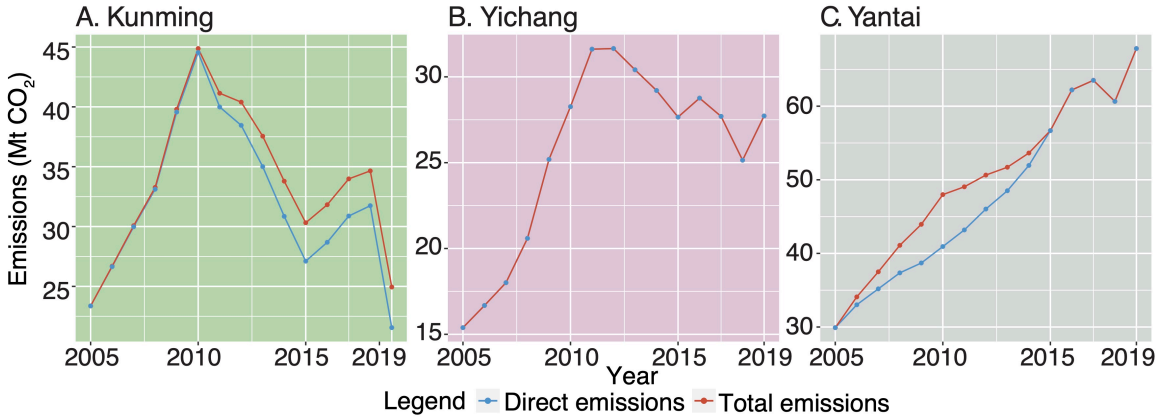

Figure 2. 3 The CO_2 emissions for representative cities from 2005 to 2019 with identification results. The green, purple, and grey background colors represent the cities in the decline, plateau, and growth period of CO_2 emission, respectively.

2.3.3 K-means clustering analysis for five classes of cities

To better understand the characteristics of Chinese cities, all 335 cities were grouped into five classes using the cluster analysis based on the attribute characteristics, including the GDP, permanent population, and proportion of secondary industry and tertiary industry (Hartigan and Wong 1979). K-means clustering is a vector quantization method. It searches for a pre-determined number of clusters in an unlabeled dataset, where each observation belongs to the nearest mean. The process includes (1) pre-dividing the dataset into *k* groups, (2) randomly selecting *k* objects as

the cluster centers, (3) calculating the distance between each object and each cluster center, and (4) assigning each object to the nearest cluster center. The distance is calculated by the following formulas:

$$\mu_i = \frac{1}{|C_i|}\sum_{x \in C_i} x \qquad \textbf{[2-1]}$$

$$E = \sum_{i=1}^{k}\sum_{x \in C_i}|x - \mu_i|^2 \qquad \textbf{[2-2]}$$

where μ_i represents the mean value of cluster C_i, x represents the selected attribute characteristics of every unit, i represents the cluster number, $\in$ represents belongs to, E represents the sum of squared errors within the cluster, which is usually adopted as the standard measure function. By calculating the distance between each object and each cluster center for the different number of clusters, we finally selected 5 clusters as the optimal k, as shown in **Figure 2. 4**. The summary of characteristics for cities in Classes 1-5 is shown in **Table 2. 1**.

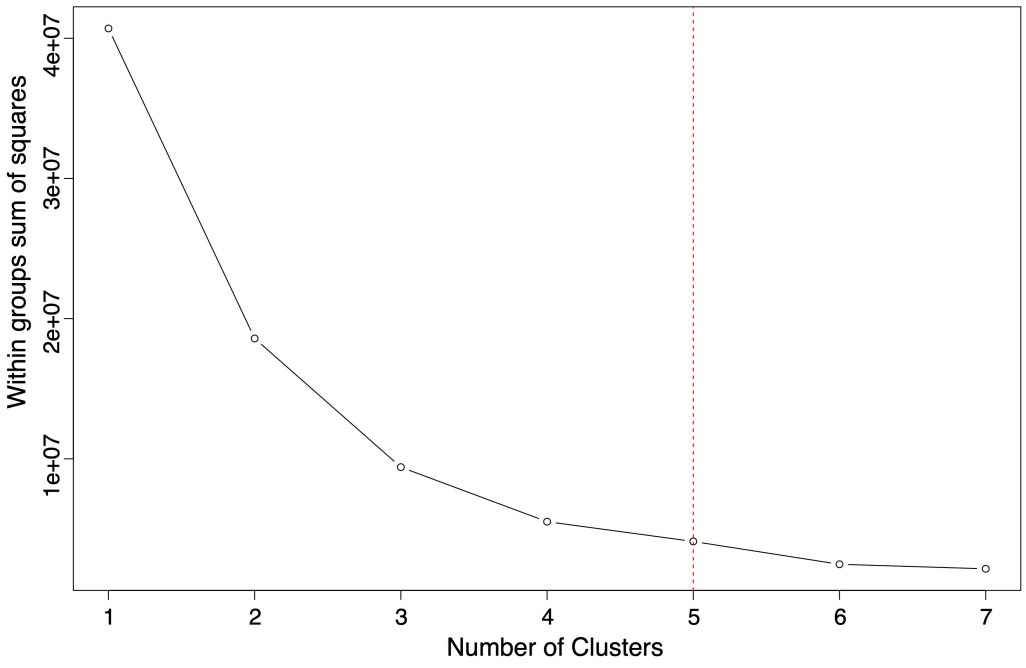

Figure 2. 4 Within groups sum of squares for cluster analysis

Table 2. 1 Summary statistics for cities in Class 1-5

City Class	*Annual CO_2 emission (Million ton)*	*CO_2 emission per capita (Ton)*	*GDP per capita (10^4 RMB)*	*Population (Million)*	*CO_2 emission per GDP (ton/10^4 RMB)*
Class 1	111 (54, 144)	5 (4, 7)	12 (9, 14)	21 (16, 24)	0.5 (0.3, 0.6)
Class 2	55 (34, 71)	6 (3, 8)	8 (4, 10)	9 (8, 10)	0.9 (0.5, 1.2)
Class 3	32 (16, 41)	6 (3, 8)	6 (4, 7)	5 (5, 6)	1.3 (0.6, 1.6)
Class 4	28 (10, 34)	10 (3, 12)	6 (4, 7)	3 (3, 3)	1.7 (0.8, 2.0)
Class 5	16 (3, 21)	18 (4, 17)	6 (3, 8)	1 (1, 1)	2.6 (1.0, 3.2)

2.3.4 Dunn's test

Dunn's test (Dunn 1964) was used to compare the changes of air pollutant concentrations and CO_2 emissions among different regions or different city classes. We first used the Shapiro–Wilk normality test to check the normality of the data (Royston 1982) (**Table 2. 2**). Then, based on the normality results, Dunn's test was used to compare the changes among multiple pairwise groups. The groups included different regions (BTH, YRD, PRD, FWP, CYD, and the other) (**Table 2. 3**) or different city classes (Classes 1 to 5) (**Table 2. 4**). Shapiro.test and Dunn.test functions of the R 3.6.3 version were applied to perform the statistical tests. The significance level was set at $p < 0.05$.

Table 2. 2 Shapiro–Wilk normality test results

Parameters	P-value
$PM_{2.5}$	2.26E-7
O_3	2.20E-16
CO_2	4.51E-5

Table 2. 3 Dunn's test results (Z statistic) for (A) $PM_{2.5}$, (B) O_3, and (C) CO_2 among different regions

(A) $PM_{2.5}$

Region	BTH	CYD	FWP	PRD	YRD	Other
BTH						
CYD	-1.27					
FWP	-4.70 ****	-3.26 **				
PRD	-3.30 ***	-2.08 *	0.91			
YRD	-1.66	-0.03	3.73 ***	2.33 *		
Other	-2.66 **	-0.52	3.70 ***	-2.15 *	0.74	

(B) O_3

Region	BTH	CYD	FWP	PRD	YRD	Other
BTH						
CYD	3.42 ***					
FWP	-0.34	-3.05 **				
PRD	0.05	-2.53 *	0.31			
YRD	2.63 **	-1.45	2.25 *	1.70		
Other	4.81 ****	-0.43	3.51 ***	-2.78 **	-1.87	

(C) CO_2

Region	BTH	CYD	FWP	PRD	YRD	Other
BTH						
CYD	-0.68					
FWP	1.64	2.03 *				
PRD	-0.08	0.44	-1.39			
YRD	-0.08	0.66	-1.77	0.03		
Other	1.63	-0.44	-2.89 **	0.89	1.79	

Note: significance level *: p <= 0.05; **: p <= 0.01; ***: p <= 0.001; ****: p <= 0.0001.

Table 2. 4 Dunn's test results (Z statistic) for (A) $PM_{2.5}$, (B) O_3, and (C) CO_2 among cities in Class 1-5

(A) $PM_{2.5}$

City Class	1	2	3	4	5
1					
2	-0.77				
3	-1.61	-1.83			
4	-1.68	-2.05 *	-0.13		
5	-1.06	-0.59	1.48	1.75	

(B) O_3

City Class	1	2	3	4	5
1					
2	-0.98				
3	-0.98	0.06			
4	0.01	2.42 *	2.96 **		
5	0.09	2.44 *	2.89 **	0.24	

(C) CO_2

City Class	1	2	3	4	5
1					
2	-2.20 *				
3	-2.15 *	0.26			
4	-2.67 **	-0.87	-1.44		
5	-2.65 **	-0.86	-1.34	-0.07	

Note: significance level *: p <= 0.05; **: p <= 0.01; ***: p <= 0.001; ****: p <= 0.0001.

2.3.5 Logarithmic mean Divisia index decomposition analysis

To further understand the driving forces of changes of CO_2 emissions, we used the logarithmic mean Divisia index (LMDI) that decomposed the CO_2 emissions into factors of population, GDP per capita, energy intensity, and energy structure (Ang 2005) as follows:

$$C = \sum_j \frac{C_j}{E_j} \times \frac{E_j}{E} \times \frac{E}{GDP} \times \frac{GDP}{P} \times P = \sum_j U_j \times M_j \times I \times GP \times P \quad \textbf{[2-3]}$$

$$\Delta C = C^t - C^{t-1} = \Delta U + \Delta M + \Delta I + \Delta GP + \Delta P \quad \textbf{[2-4]}$$

$$\Delta U = \sum_j \frac{C_j^t - C_j^{t-1}}{\ln C_j^t - \ln C_j^{t-1}} \ln \frac{U_j^t}{U_j^{t-1}} \quad \textbf{[2-5]}$$

$$\Delta M = \sum_j \frac{C_j^t - C_j^{t-1}}{\ln C_j^t - \ln C_j^{t-1}} \ln \frac{M_j^t}{M_j^{t-1}} \quad \textbf{[2-6]}$$

$$\Delta I = \sum_j \frac{C^t - C^{t-1}}{\ln C^t - \ln C^{t-1}} \ln \frac{I^t}{I^{t-1}} \quad \textbf{[2-7]}$$

$$\Delta GP = \sum_j \frac{C^t - C^{t-1}}{\ln C^t - \ln C^{t-1}} \ln \frac{GP^t}{GP^{t-1}} \quad \textbf{[2-8]}$$

$$\Delta P = \sum_j \frac{C^t - C^{t-1}}{\ln C^t - \ln C^{t-1}} \ln \frac{P^t}{P^{t-1}} \quad \textbf{[2-9]}$$

where C represents the CO_2 emission, E represents the energy consumption, GDP represents the city-level GDP, P represents the permanent population, j represents the fuel type, U represents the CO_2 emission factor, M represents the fuel mix, I represents the energy intensity, GP represents the GDP per capita, t and $t-1$ represents the year 2019 and 2015.

2.4 Results

2.4.1 Overall changes in air quality and CO_2 emissions

Figure 2. 5 shows the percent changes of air pollutant concentrations ($PM_{2.5}$ and O_3) and CO_2 emissions for 335 cities in China in 2019 compared to 2015 (excluding three provincial-controlled divisions and Danzhou city due to data availability). In **Figure 2. 5A – B**, the blue color represents cities that had met the China's national air quality standard of the corresponding air pollutants in 2019; and the orange color represents the ones that had not. In **Figure 2. 5C**, green, purple, and grey represents the different CO_2 emission states of the cities, i.e., the periods of decline, plateau, and growth of CO_2 emissions, respectively (see **Method** for details). Among the analyzed pollutants, $PM_{2.5}$ concentration decreased in 88% (N = 295) of the 335 Chinese cities with an average reduction of 23% in 2019 compared to 2015 (**Figure 2. 5A**). Nonetheless, almost half (47%, N = 158) of the cities still failed to meet China's national $PM_{2.5}$ standard (i.e., annual average of 35 $\mu g/m^3$) by 2019 (**Figure 2. 5A**), which was much looser compared to the $PM_{2.5}$ standard of the World Health Organization (WHO; annual mean $PM_{2.5}$ concentration < 5 $\mu g/m^3$) (World Health Organization 2021). The national $PM_{2.5}$ standard was exceeded by 20% in 100 cities (**Table A 1**) and by 50% in 49 cities. In contrast, as presented in **Figure 2. 5B,** O_3 concentration increased in 304 (91%) Chinese cities and 103 (31%) of them failed to meet the national O_3 standard (the 90th percentile of daily 8-h maximum concentrations <160 $\mu g/m^3$, converts to 82 ppb at 298 K and an ambient pressure of 1013 hPa). Among the 103 non-attainment cities, 21 exceeded the O_3 standard by 20%. The increasing trend of O_3 concentrations in China could be driven by the ineffective control of volatile organic compounds (VOCs) emissions (i.e., a major O_3 precursor) given the sharp NO_x emission decrease under VOC-limited conditions (Li et al. 2019c). For CO_2,

231 cities had increased emissions from 2015 to 2019, and 56 cities showed over 50% increase during this period (**Figure 2. 5D**). Among all 335 cities, only 20% (N = 67) were in the period of decline or plateau of CO_2 emissions.

By comparing the changes of $PM_{2.5}$ and CO_2, we found that 27% of the cities (N = 90) had reduced both (co-reduction) in 2019 compared to 2015, with an average reduction of 23% for $PM_{2.5}$ and 22% for CO_2 emissions, respectively (**Figure 2. 5A**). For the remaining 73% of the cities (N = 245), CO_2 emissions increased by an average of 33%, while $PM_{2.5}$ concentration decreased by an average of 18%. Overall, our results showed a lack of synchronized city-level co-reduction of CO_2 and $PM_{2.5}$ under current climate change and air pollution control policies in China.

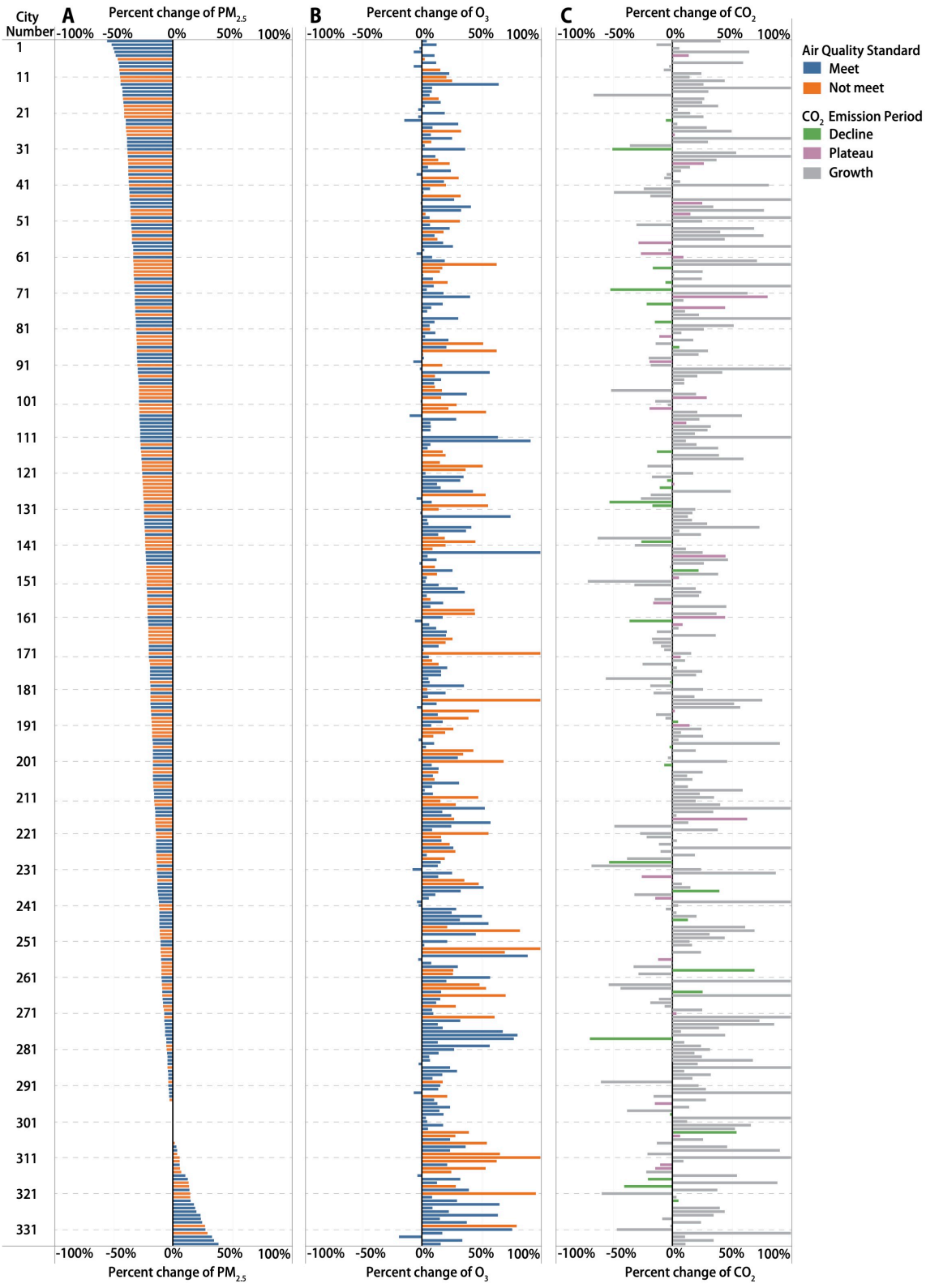

Figure 2. 5 Percent change of CO_2 emissions and air pollutant concentrations for 335 cities in China in 2019 compared to 2015. (A) $PM_{2.5}$; (B) O_3; (C) CO_2. Panels A-B: The blue color- cities

met the air quality standard in 2019; the orange color - cities did not meet the air quality standard in 2019. The national standards of $PM_{2.5}$ and O_3 are 35 μg/m^3 and 82 ppb, respectively. Panel C: The green, purple, and grey color - cities in the period of decline, plateau, and growth of CO_2 emissions. Outliers (< 5% of the data) exceed -100% or 100% were not shown in this figure.

2.4.2 Spatial characteristics of air quality improvement and CO_2 emission reduction

Figure 2. 6 presents the spatial distribution of air quality improvement and CO_2 emission reduction for the 335 cities in China. In **Figure 2. 6A – B and Figure 2. 6D – E**, non-attainment cities for $PM_{2.5}$ and O_3 were shown in pink dots in 2015 or 2019. The black, brown, rose red, red, and blue polygons represent the BTH, the YRD, the PRD, the FWP, and the CYD, respectively, which are important regions for air pollution control in China (**Figure 2. 6C and Figure 2. 6F**). The green check mark and the purple triangle represent the cities in the period of decline or plateau of CO_2 emissions, and the rest of the cities are in the period of growth of CO_2 emissions (**Figure 2. 6I**). City-level $PM_{2.5}$, O_3, and CO_2 data in 2015 and 2019 can be found in **Table A 1.**

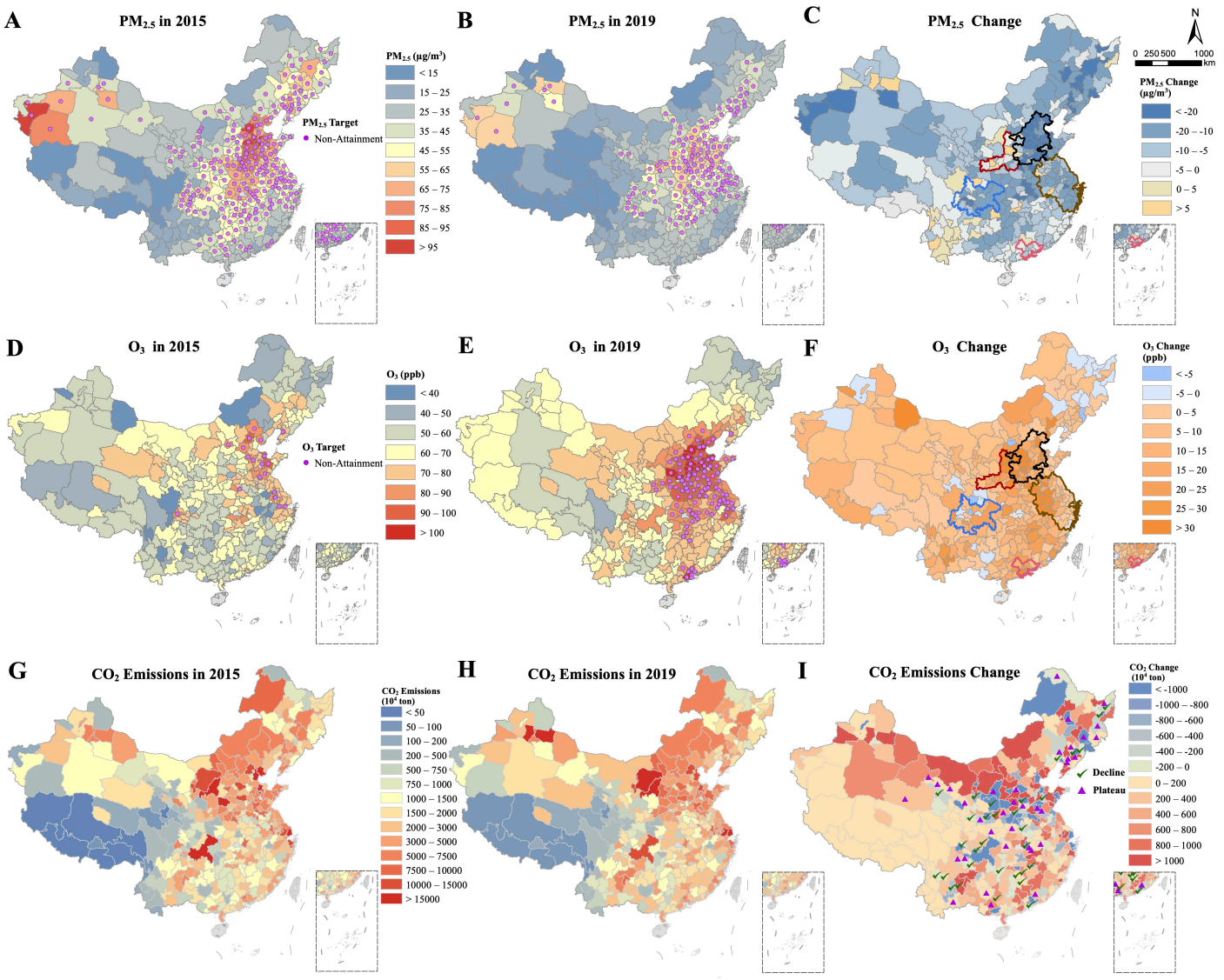
A
PM2.5 in 2015
PM2.5 (μg/m3)
< 15
15 – 25
25 – 35
35 – 45
45 – 55
55 – 65
65 – 75
75 – 85
85 – 95
> 95
PM2.5 Target
Non-Attainment
B
PM2.5 in 2019
C
PM2.5 Change
N
0 250 500 1000
km
PM2.5 Change (μg/m3)
< -20
-20 – -10
-10 – -5
-5 – 0
0 – 5
> 5
D
O3 in 2015
O3 (ppb)
< 40
40 – 50
50 – 60
60 – 70
70 – 80
80 – 90
90 – 100
> 100
O3 Target
Non-Attainment
E
O3 in 2019
F
O3 Change
O3 Change (ppb)
< -5
-5 – 0
0 – 5
5 – 10
10 – 15
15 – 20
20 – 25
25 – 30
> 30
G
CO2 Emissions in 2015
CO2 Emissions (10^4 ton)
< 50
50 – 100
100 – 200
200 – 500
500 – 750
750 – 1000
1000 – 1500
1500 – 2000
2000 – 3000
3000 – 5000
5000 – 7500
7500 – 10000
10000 – 15000
> 15000
H
CO2 Emissions in 2019
I
CO2 Emissions Change
CO2 Change (10^4 ton)
< -1000
-1000 – -800
-800 – -600
-600 – -400
-400 – -200
-200 – 0
0 – 200
200 – 400
400 – 600
600 – 800
800 – 1000
> 1000
Decline
Plateau

Figure 2. 6 The spatial pattern of $PM_{2.5}$, O_3, and CO_2 for 335 cities in China from 2015 to 2019. (A) $PM_{2.5}$ in 2015; (B) $PM_{2.5}$ in 2019; (C) Changes of $PM_{2.5}$ concentration from 2015 to 2019; (D) O_3 in 2015; (E) O_3 in 2019; (F) Changes of O_3 concentration from 2015 to 2019. The pink dots in (A) or (B) represent the cities not meeting the national $PM_{2.5}$ standard (35 $\mu g/m^3$) in 2015 or 2019. The pink dots in (D) or (E) represent the cities not meeting the national O_3 standard (82 ppb) in 2015 or 2019, respectively. The black, brown, rose red, red, and blue polygons in (C) and (F) represent BTH - the Beijing-Tianjin-Hebei and the surrounding region, YRD - the Yangtze River Delta region, PRD - the Pearl River Delta region, FWP - the Fenwei Plain region, and CYD - the Cheng-Yu District region, respectively. (G) CO_2 emissions in 2015; (H) CO_2 emissions in 2019; (I) Changes of CO_2 emissions from 2015 to 2019. The green check mark or the purple triangle in (I) represent the cities in the period of decline or plateau of CO_2 emissions, the rest of the cities are in the period of growth of CO_2 emissions.

As shown in **Figure 2. 6A – C**, only 106 Chinese cities had met the national $PM_{2.5}$ standard in 2015, which were mainly located in the southern (Fujian and Guangdong provinces) and southwest (Yunnan province) areas in China. In 2019, 72 additional cities had met the $PM_{2.5}$ standard, which were mainly located in the northeastern (Heilongjiang, Jilin province and Inner Mongolia Autonomous Region), western (Gansu province), central (Sichuan province), and southern (Guangdong and Guangxi province) areas. Although the largest $PM_{2.5}$ reduction was observed in the BTH region (-27 $\mu g/m^3$) (**Figure 2. 6B – C**), none of the cities in this region had met the national $PM_{2.5}$ standard in 2019. Similarly, none of the cities in the FWP region had met the $PM_{2.5}$ standard in 2019. Besides, only 27% and 31% of the cities in the YRD and CYD regions had met the $PM_{2.5}$ standard in 2019. In comparison, all cities in the PRD region had met the $PM_{2.5}$ national standard in 2019.

As shown in **Figure 2. 6D – F**, the average national O_3 concentration increased rapidly from 63 ppb in 2015 to 76 ppb in 2019. From 2015 to 2019, the most prominent increase in O_3 concentration (absolute concentration change) was observed in the FWP and BTH regions (+12 ppb), followed by the PRD (+10 ppb), the YRD (+8 ppb), and the CYD (+4 ppb) regions, respectively (**Figure 2. 6F**). The number of non-attainment cities for O_3 increased by more than five times from 2015 (19 cities) to 2019 (103 cities), with half of the additional non-attainment cities located in the BTH, YRD, PRD, and FWP regions. In 2019, 100%, 61%, 78%, and 82% of the cities in the BTH (N = 28), PRD (N = 7), YRD (N = 25), and FWP (N = 9) regions exceeded the national O_3 standard, and 61% of the cities in the BTH region (N = 17) exceeded the standard by over 20%. Our results showed that the O_3 pollution worsened from 2015 to 2019 in China, which calls for effective control strategies immediately (Li et al. 2019b; Xing et al. 2019).

For CO_2 (**Figure 2. 6G – H**), cities with high emissions were mainly located in the northern

(Hebei and Shandong provinces) and northeastern (Inner Mongolia Autonomous Region) regions, while cities with lower emissions were mainly located in the southwestern (Tibet and Yunnan provinces) areas. The amount of national CO_2 emissions increased from 9334 Mt (Million ton) in 2015 to 9890 Mt in 2019. An increase of more than 10 Mt was observed in 42 cities, which were mainly located in Hebei, Inner Mongolia, Shandong, and Shanxi provinces (**Figure 2. 6I**). Based on our results (see **Method** for details), only 31 cities had reached a period of decline of CO_2 emissions and 36 cities had reached the plateau by 2019 (**Figure 2. 6I**). These cities together contributed to 17% of the national CO_2 emissions in 2019. All other cities (N = 268) were still in the period of growth and contributed to 83% of CO_2 emissions in China.

2.4.3 Regional differences of air quality improvement and CO_2 emission reduction

Figure 2. 7A – C showed the changes of air pollutant concentrations and CO_2 emissions by region, including the BTH, CYD, YRD, PRD, FWP, and the other regions, from 2015 to 2019. Dunn's test (Dunn 1964) was performed to compare the changes of air pollutant concentrations and CO_2 emissions among different regions and the test results are shown in **Table 2. 3**.

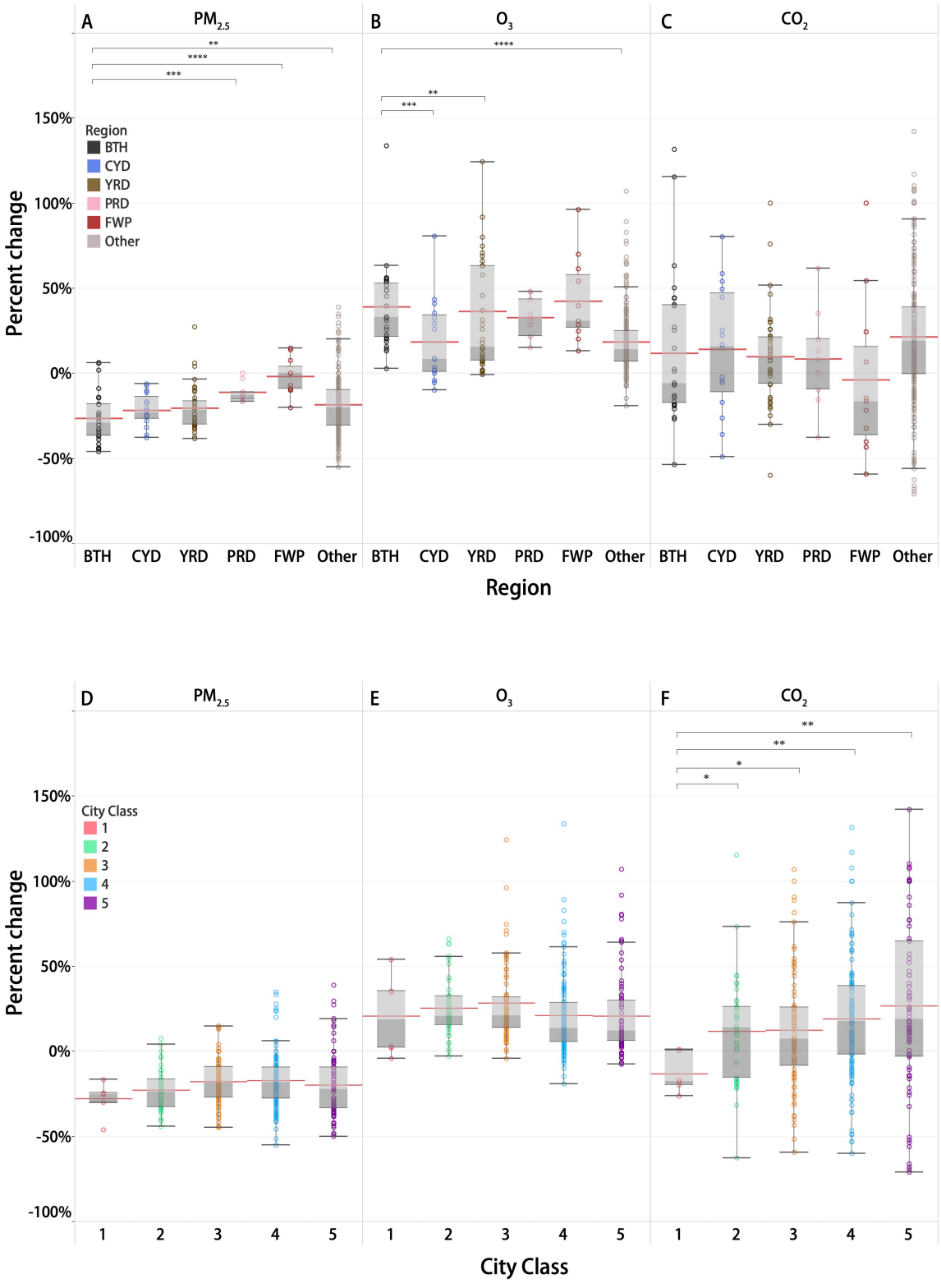

Figure 2. 7 The comparison of percent changes of air pollutant concentrations and CO_2 emissions for different regions (A-C) and classes of cities (D-F) in China from 2015 to 2019. (A, D) $PM_{2.5}$;

(B, E) O_3; and (C, F) CO_2 emissions. Regions included BTH - the Beijing-Tianjin-Hebei and the surrounding region, PRD - the Pearl River Delta region, YRD - the Yangtze River Delta region, FWP - the Fenwei Plain region, CYD - the Cheng-Yu District region, and the other region - the remaining cities. City Classes 1-5 represent the cities identified by the cluster analysis (see Method for details). Significance level *: p <= 0.05; **: p <= 0.01; ***: p <= 0.001; ****: p <= 0.0001.

Among all regions, the BTH region had the most prominent decrease in $PM_{2.5}$ (-27%) (**Figure 2. 7A**) since the most stringent requirements and control strategies were implemented there (State Council of the People's Republic of China 2018; Zhang et al. 2019). PRD and FWP regions showed less decrease in $PM_{2.5}$ (-11% and -2%, respectively) compared to the BTH region (**Table 2. 3**). In contrast, O_3 concentrations increased across all regions. As demonstrated in **Figure 2. 7B**, the most dramatic O_3 increase (percent change) was observed in the FWP region (+42%) in 2019 compared to 2015, followed by the BTH (+39%), YRD (+36%), PRD (+33%), CYD (+18%), and the other regions (+18%). In contrast to the noticeable differences in air pollutant concentrations changes among different regions, CO_2 emissions showed less differences except for the FWP region, where a decrease of 4% was observed. For other regions, the CO_2 emission increase was in the range of 8% to 21% (**Figure 2. 7C**).

To better understand the characteristics of CO_2 emission across different cities in China, we categorized all cities into five classes (Class 1-5) using the clustering analysis (Hartigan and Wong 1979) based on the cities' development level. The summary statistics for clustering analysis are shown in **Table 2. 1**. We further compared the changes of air pollutant concentrations and CO_2 emissions by city class from 2015 to 2019 (**Figure 2. 7D – F**). Dunn's test was performed to compare the changes among different city classes and the test results are shown in **Table 2. 4**.

Different CO_2 emission characteristics were observed for different city classes. Class 1 cities (N = 6) with the highest GDP per capita (average value of 12E4 RMB, **Table 2. 1**) had higher CO_2

emissions, with an average of 111 Mt in 2019. However, the change of CO_2 emissions was significantly lower for Class 1 cities from 2015 to 2019 compared to cities in the other four classes (**Table 2. 4**). Class 2 (N = 42) and Class 3 (N = 84) cities were characterized by higher-than-average development level across the nation, with an average GDP per capita of 8E4 RMB and 6E4 RMB (**Table 2. 1**), respectively. These two classes together contributed to half of the total CO_2 emissions in China, with an average CO_2 emissions of 55 Mt (Class 2) and 32 Mt (Class 3) in 2019 and the same average change rate of +12% from 2015 to 2019 (**Figure 2. 7F**). Our results showed that only 18% of the cities in Classes 2 & 3 were in the period of decline or plateau, such as Shenzhen. In comparison, for Classes 4 & 5 cities, the amount of CO_2 emissions was relatively low, with an average of 28 Mt and 16 Mt in 2019, respectively. Cities in these classes were relatively less developed, which were mainly located in the central and western parts of China. However, increasing trends in CO_2 emissions were found for these cities. There were 48% (N = 23) and 50% (N = 39) of the cities in Classes 4 & 5 showing CO_2 emission increases over 20% from 2015 to 2019 (**Table A 1**). In spite of a relatively low total CO_2 emissions, Classes 4 & 5 cities had much higher average per capita CO_2 emissions of 10 tons and 18 tons, respectively, compared to cities in Classes 1 - 3 (around 6 tons) (**Table 2. 1**). Thus, special attention should be paid to the cities in Classes 4 & 5 as the economic development might further increase their CO_2 emissions substantially.

Figure 2. 7D – E provide the distribution of the changes for air pollutant concentrations by city class. In contrast to the significant differences of CO_2 emissions, the differences in air pollutant concentration changes, including $PM_{2.5}$ and O_3, were less significant across different city classes (**Table 2. 4**). From 2015 to 2019, the average $PM_{2.5}$ decreased in the range of 17% to 28% for cities in different classes. In contrast, O_3 concentration increased by an average of 21% to 28% in

2019 compared to 2015.

To investigate the driving forces of CO_2 emission changes, we used the LMDI to decompose the CO_2 emissions into factors of population, GDP per capita, energy intensity, and energy structure (Ang 2005). As shown in **Figure 2. 8**, the reduction in energy intensity was the most important factor for CO_2 emission reduction, while the increase in GDP per capita was the driving factor for CO_2 emission increase. The effect of energy intensity was the most prominent in Class 1 cities (around -33%), followed by Classes 2 - 3 (around -15%) and Classes 4 - 5 cities (around -7%) (**Figure 2. 8E – H**). Besides, the effect of improved energy structure on CO_2 reduction was most obvious in Class 1 cities (-5%) compared to other city classes, but to a less extent than energy intensity. GDP per capita was the main positive driving force, leading to over 20% of CO_2 emission increase for all city classes. We also compared the driving forces of CO_2 emission change by region (**Figure 2. 8A – D**). The reduced CO_2 emissions in the FWP region was mainly driven by the energy intensity factor (-22%) due to the strict control on coal consumption (Ministry of Ecology and Environment of the People's Republic of China 2018).

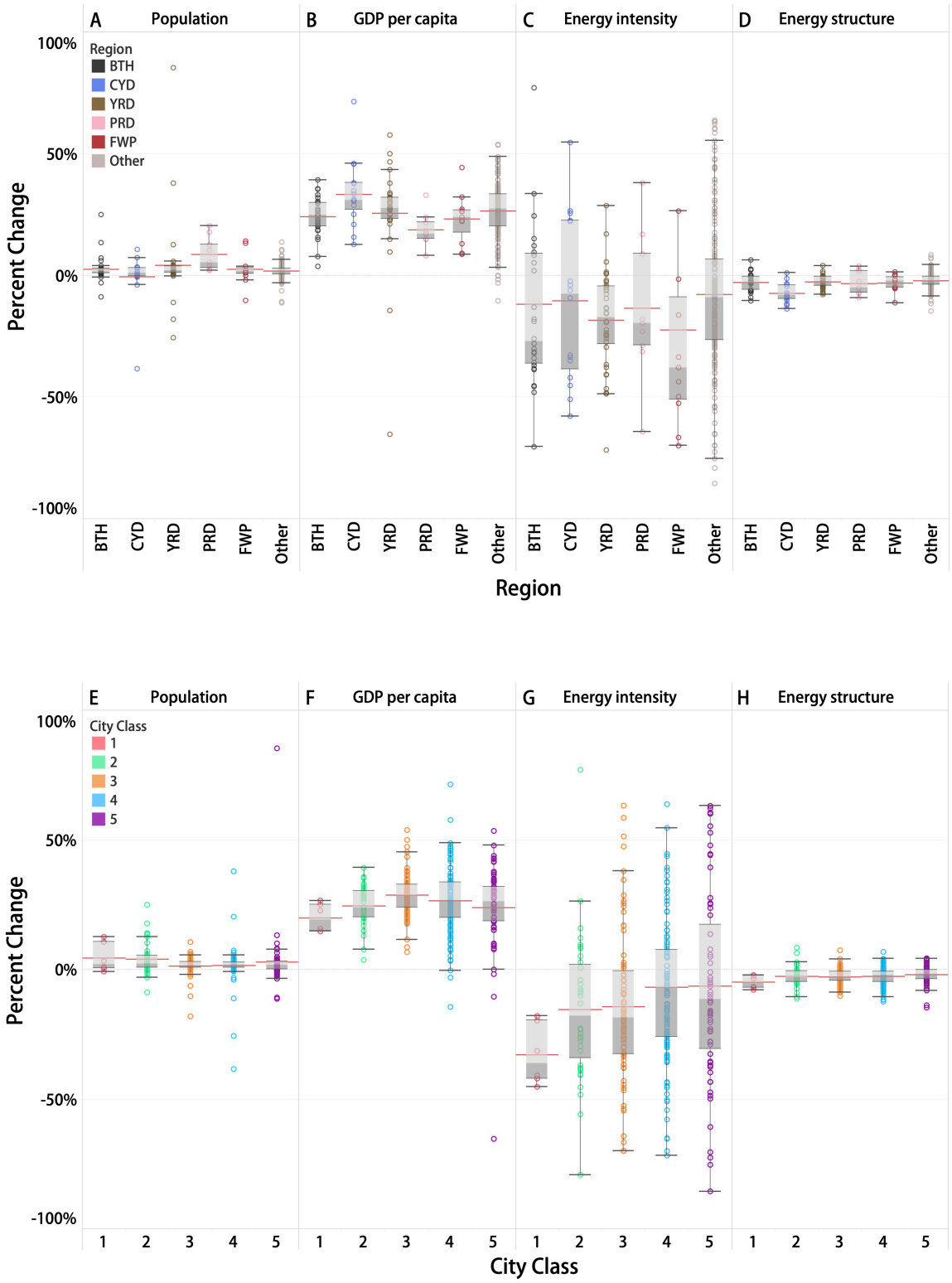

Figure 2. 8 The logarithmic mean Divisia index (LMDI) decomposition factors of (A, E) Population, (B, F) GDP per capita, (C, G) Energy intensity, and (D, H) Energy structure to the

changes of CO_2 emissions for different regions (A-D) and classes of cities (E-H) in China from 2015 to 2019. Regions included BTH - the Beijing-Tianjin-Hebei and the surrounding region, PRD - the Pearl River Delta region, YRD - the Yangtze River Delta region, FWP - the Fenwei Plain region, CYD - the Cheng-Yu District region, and the other region - the remaining cities. City Classes 1-5 represent the cities identified by the cluster analysis (see Method for the detail).

2.5 Discussion

China is facing both challenges of climate change and air pollution. Our study presented one of the first attempts to comprehensively assess city-level air quality improvements and CO_2 emission reductions simultaneously, using data from 335 Chinese cities in 2015 and 2019. We compared the changes of $PM_{2.5}$ and O_3 concentrations and CO_2 emissions in parallel, which allowed us to realize the unsynchronized reduction trends under the current policies. Our results showed an average reduction of 22% in $PM_{2.5}$ (**Figure 2. 6A – C)** and an average increase of 21% and 6% in O_3 concentrations and CO_2 emissions (**Figure 2. 6D – I**) for 335 Chinese cities.

The changes in air pollutant concentrations had distinct patterns across different regions. Air pollutant concentrations were affected by self-emissions (Ge et al. 2018), regional transport from surrounding areas (Chang et al. 2019a), and meteorology conditions (Chen et al. 2020b). In China, pollution control policies were implemented based on regional joint prevention and control (State Council of the People's Republic of China 2013, 2018; Ministry of Ecology and Environment of the People's Republic of China 2017). Cities and their surrounding cities within the same region often set mandatory reduction goals with the uniform stringency level, which improved the effectiveness of pollution control. In the past years, control policies accentuated the importance of $PM_{2.5}$ in particular by targeting $PM_{2.5}$ control at the city level. Policies were implemented mainly through end-of-pipe controls (Geng et al. 2021), which were driven by the strengthened emission standards (Zhang et al. 2019). As a result, noticeable reductions in $PM_{2.5}$ were found, especially for cities in the BTH (-23 $\mu g/m^3$) and YRD regions (-11 $\mu g/m^3$) (**Figure 2. 6A – C**).

In contrast, CO_2 emission changes varied substantially among different city classes at different development stages. Our results showed that CO_2 emissions were driven by the city's economic

level, energy intensity, and energy structure, indicating a weak association with the geographical region. Energy intensity was the most dominant driving force of CO_2 emission compared with other factors. The reduction in energy intensity was more obvious in developed cities, suggesting a boosting economic development that utilized the energy more efficiently (Martínez et al. 2019). However, for less developed cities in China, CO_2 emissions increased rapidly due to economic development and less improvement in energy intensity (**Figure 2. 8E – H**). Thus, future low carbon policies should prioritize the promotion on improving energy intensity and energy structure for less developed cities (Zhang et al. 2019; Xing et al. 2020). Currently, CO_2 mitigations were self-motivated at the city level, such as the "China's pilot low-carbon city" initiative (National Development and Reform Commission 2010). However, our results found limited effectiveness of the initiative as no obvious difference in CO_2 emission changes was observed between pilot low-carbon cities and non-pilot low-carbon cities (**Figure A 1**). To achieve the goal of CO_2 emission peak before 2030 and carbon neutrality by 2060, China should consider deriving future CO_2 mitigation policies from its own successful experience in $PM_{2.5}$ control, such as setting mandatory city-level emission reduction targets as cities are the fundamental units to implement various policies in China (Chen et al. 2020a).

Although great improvement was observed in $PM_{2.5}$, limited effects were found for city-level co-reduction of CO_2 and $PM_{2.5}$ under the current policies. Only 29 cities met the national $PM_{2.5}$ standard and reached the period of plateau or decline of CO_2 emissions. The remaining cities faced either air pollution or increasing CO_2 emission problem, or both. Current policies used strict end-of-pipe controls that reduced air pollutant emissions effectively (Geng et al. 2021). For example, the implementation of the ultra-low emission standard could reach a 98% removal efficiency for $PM_{2.5}$ in the power sector (Zheng et al. 2018). However, the end-of-pipe control measure could in

contrast increase CO_2 emissions due to increased energy consumption (Zhao et al. 2017). As the implementation of the advanced end-of-pipe control devices in major sectors increases, the reduction potential of end-of-pipe controls is shrinking and their effectiveness on air quality improvements is decreasing (Xing et al. 2020; Geng et al. 2021). Considering the above, the implementation of low carbon policies, such as clean energy transition and industrial structure optimization, is urgently needed as they could bring co-benefits of improving air quality and reducing CO_2 emissions (Wang et al. 2015; Xing et al. 2020). Existing energy policies that have the potential to exhibit effectiveness in addressing both challenges in the long run should be reinforced for further improvement (Xing et al. 2020; Geng et al. 2021). Indeed, some cities in China had already benefited from such existing energy policies. For example, Shenzhen city in the PRD region obtained the co-reductions of CO_2 and $PM_{2.5}$ by implementing strict low-carbon policies in the power, industry, transportation, and building sectors (Development and Reform Commission of Shenzhen Municipality 2012). The transition to clean energy and improved energy efficiency led to a 20% reduction in $PM_{2.5}$ from 2015 to 2019 and allowed Shenzhen to reach the period of decline of CO_2 emissions.

Chapter 3

A new method of hotspot analysis on the management of CO_2 and air pollutants, a case in Guangzhou city, China

3.1 Abstract

Emission inventory plays an important role in deigning effective emission control strategies. Currently, there is unbalanced development of CO_2 and air pollutants emission inventories in China and the spatial information of both cannot be obtained simultaneously, which prevents constructing a collaborative control. In this Chapter, we used Guangzhou city as a case to develop a unified emission inventory including both CO_2 and air pollutants. We then utilized spatial mapping methods to identify the co-hotspots of both CO_2 and air pollutants at a high spatial resolution (1×1 km^2). The results showed that CO_2 and air pollutants were mainly originated from point sources in the stationary combustion sector and line sources in the transportation sector. These two sectors contributed to 95%, 67%, and 93% of total CO_2, SO_2, and NO_x emissions, respectively. Besides, more than 66% of total CO_2 or air pollutants emissions were attributed to top 10% emission grids (up to 86% for CO_2 and SO_2). However, our results showed weak spatial autocorrelations for these high emission grids. The co-hotspot analysis enabled an accurate identification of high-emission grids, which improves the precision and effectiveness of site-

specific management. Our study underscores the importance of managing CO_2 and air pollutants simultaneously at the city level.

3.1 Introduction

China faces both challenges of climate change and air pollution. To battle against the climate challenge, China, as the world's largest CO_2 emitter (BP 2021), pledged to implement aggressive actions to reach the CO_2 emission peak before 2030 and carbon neutrality by 2060 in the Climate Ambition Summit (Climate Ambition Summit 2020). On the other hand, China implemented strengthened clean air policies to address air pollution (State Council of the People's Republic of China 2013, 2018). Despite the noticeable improvement in air quality, air pollution is still a severe problem in China. To address challenges of both CO_2 mitigation and air pollution control, effective emission control strategies are needed. Studies have suggested that a comprehensive emission inventory is crucial for effective emission control strategies and policies (D'Avignon et al. 2010; Crippa et al. 2020). A comprehensive emission inventory provides foundations to formulate effective environmental management plans based on the emission characteristics, the major contribution of different sources, and the spatial profile of the emissions (Qi et al. 2017; Bai et al. 2020).

Currently, there is an unbalanced development between CO_2 and air pollutants emission inventories in China. In the past decade, the air pollutants emission inventories have been well established (Zhang et al. 2009; Li et al. 2017) which provided comprehensive and sufficient support for China to address its air pollution problem. For example, the Multi-resolution Emission Inventory for China (MEIC) provided an open-access dataset that estimates the anthropogenic emissions in China (MEIC 2021). The latest version was developed in 2021, with an update to the 2020 inventory and a spatial resolution of 27×27 km^2. In contrast, the CO_2 emission inventory in China is far from developed. The national GHG inventory was only updated to the year of 2014,

and the 2016 version was still under development (China Ministry of Ecology and Environment 2018). Further, the guideline for provincial greenhouse gas inventory was published back in 2010 (NDRC 2011). Some studies (WRI China 2015; C40 Cities 2021; CDP 2021) tried to construct the CO_2 emission inventory at the provincial or city level. However, these inventories were developed for research purposes and the data were not publicly available (Xu 2018). The inventory results were not comparable among different studies due to different inventory scopes and calculation methods applied, which limited the broader application of these inventories (Xu 2018). A lack of a systematic CO_2 emission inventory in China prevents cities from understanding the emission characteristics and formulating targeted control measures, and thus, greatly hinders China's ability to achieve its ambitious CO_2 mitigation goals.

Considering the differences between CO_2 and air pollutants emission inventories, two challenges should be addressed to better facilitate city-level CO_2 emission reduction and air pollution control. First, there was a mismatch in the sectors of CO_2 and air pollutants emission inventories. Currently, the CO_2 emission inventory mainly referred to the 2006 IPCC Guidelines for National Greenhouse Gas Inventory (Eggleston H.S. et al. 2016), the 2019 Refinement to the 2006 IPCC Guidelines for National Greenhouse Gas Inventory (IPCC 2019), and Guidelines for Provincial Greenhouse Gas Inventory (NDRC 2011), while the air pollutants emission inventory mainly referred to the technical guidelines issued by the Ministry of Ecology and Environment (MEE 2014a, b). As such, two independent categories of guidelines led to distinct inventory structures and classification, and a unified emission inventory was missing. Second, spatial information of both CO_2 and air pollutants emissions was lacking. Traditionally, we could map the emissions of CO_2 (Cai et al. 2018a) or air pollutants (Qi et al. 2017; Bai et al. 2020) at a high spatial resolution by utilizing spatial mapping methods. However, previous studies usually treat

them separately, so the spatial information of both emissions cannot be obtained simultaneously. Missing such information may prevent us from understanding the spatial pattern of CO_2 and air pollutants emissions. Accordingly, site-specific management to control CO_2 and air pollutants emissions collaboratively cannot be conducted effectively.

To bridge the above gaps, we developed a unified emission inventory of CO_2 and air pollutants to address the core issues on data sources, inventory structure, and spatial distribution. Based on the unified emission inventory, we mapped both emissions inventories at a high spatial resolution (1×1 km^2), which allowed us to identify high emission grids for both emissions, namely the "co-hotspots". Obtaining a unified emission inventory with co-hotspots was fundamental to understanding the emission characteristics of CO_2 and air pollutants spatially. It could provide better support for designing and implementing collaborative control strategies for Chinese cities.

3.3 Method

Figure 3. 1 presents the flowchart of the development of a unified emission inventory and the identification of the co-hotspots. Based on the existing CO_2 and air pollutants emission data, a unified emission inventory was established by reclassifying both emission inventories at the same sub-sector level. The spatial mapping methods (Cai et al. 2018a, 2019b) were used to allocate the unified emission inventory. Finally, the co-hotspots of both CO_2 and air pollutants emissions were identified according to their ranks across all spatial grids.

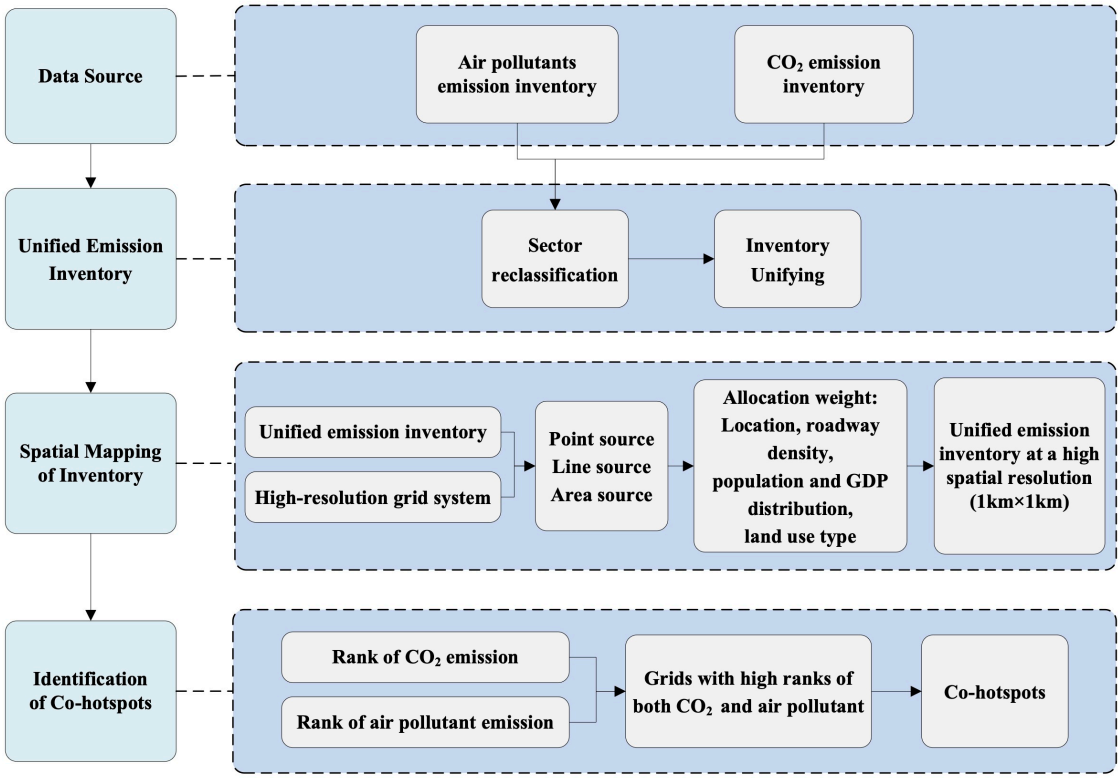

Figure 3. 1 A flowchart of the overall framework to develop a unified emission inventory and identify the co-hotspots

3.3.1 Study area

Guangzhou city is a developed city located in the Pearl River Delta region and a national low-carbon pilot city in China. We used Guangzhou as a representative case to develop the method in this Chapter. The air quality in Guangzhou has improved in recent years. The $PM_{2.5}$ concentrations reduced from 36 μg/m^3 in 2015 to 30 μg/m^3 in 2019 due to strict air pollution control measures. However, the CO_2 emissions in Guangzhou have increased steadily since 2005. The basic information of Guangzhou city, including the districts, population, and roadway distribution, is presented in **Figure 3. 2**. We included 7556 grids with 1 × 1 km^2 resolution based on the administrative boundary of Guangzhou city and chose the study year 2018.

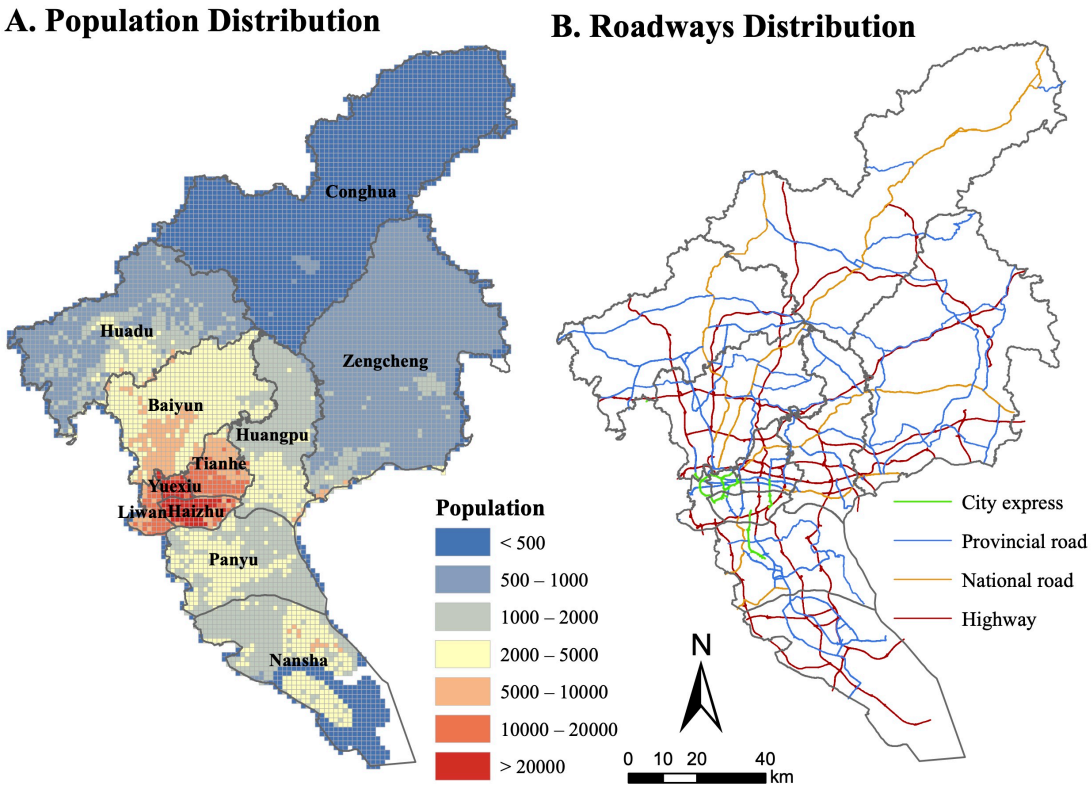

Figure 3. 2 The distributions of (A) population and (B) roadways in Guangzhou in 2018.

3.3.2 Data source

The CO_2 emission inventory was compiled by the CCG (CCG 2020) and sourced from the CHRED 3.0 database (Cai et al. 2018a, 2019b, a). CHRED 3.0 Database was compiled by utilizing bottom-up, enterprise-level point-source data. We focused on CO_2 emissions from fossil fuel combustion and industrial processes, instead of those from land use, land-use change, and forestry. The air pollutants emission inventory was compiled by referring to the technical guidelines issued by the Ministry of Ecology and Environment (MEE 2014a, b) and city-level environmental statistics (National Bureau of Statistics 2020c). Overall, seven air pollutants (SO_2, NO_x, $PM_{2.5}$, PM_{10}, VOCs, CO, and NH_3) were included, covering emissions from point, line, and area sources. The gridded population data were sourced from the Resource and Environment Science and Data Center compiled by the Institute of Geographic Sciences and Natural Resources Research, Chinese Academy of Sciences (CAS) (CAS Institute of Geographic Sciences and Natural Resources Research 2021).

3.3.3 Establish a unified emission inventory of CO_2 and air pollutants

To establish a unified emission inventory, we examined the data sources, emission inventory structure, and classification at the sub-sector level. Originally, there were six major emission sectors (industry energy, industrial processes, agriculture, transportation, residential building, and service building) in the CO_2 emission inventory and ten major emission sectors (stationary combustion, industrial processes, agriculture, transportation, solvent use, waste disposal, fuel oil storage and transportation, dust, biomass burning, and other emission sources) in the air pollutants emission inventory. Using the classification of the air pollutants emission inventory as the standard,

we reclassified the sectors of the CO_2 emission inventory by matching the same sub-sectors so that CO_2 and air pollutants emissions from the same emission source were categorized into the same sub-sector. Then, we established a unified emission inventory that integrated both CO_2 and air pollutants emissions.

3.3.4 Spatial mapping of the unified emission inventory and the spatial autocorrelation pattern

Based on the unified emission inventory with emissions from point sources, line sources, and area sources, we allocated emissions into specific grids and obtained a high-resolution emission inventory using the ArcGIS platform. For each grid, detailed information including CO_2 and air pollutants emissions with sectoral classification could be obtained. The detailed methods of the spatial mapping process can be found in our previous work (Cai et al. 2018a, 2019b). Briefly, point source emissions, such as power plants or industries, were assigned to the grid based on the location information. We calibrated the locations of point sources using longitude and latitude data obtained from the Accurate Position Indicator geocoding system for precise spatial location control. For line source emissions, such as the road transportation sub-sector, the emissions were allocated to the grid based on the density of roadways. For the waterway sub-sector, the emissions were allocated based on the automatic identification system, which recorded the ships' navigation speed, time, and location. For area sources, such as the service or residential buildings sector, the emissions were allocated to the grid based on the distribution of population, GDP, and land use type.

Besides, we used Moran's index (Moran 1948) to analyze the spatial autocorrelation pattern of CO_2 and air pollutants emissions. Moran's index is defined by the following equation, which is used to examine the spatial autocorrelation between the grid value and the values of neighboring grids. Higher index represent stronger spatial autocorrelations, while index equal to zero represent no less autocorrelation:

$$I = \frac{n\sum_{i=1}^{n}\sum_{j=1}^{n} w_{ij}(x_i-\bar{x})(x_j-\bar{x})}{\sum_{i=1}^{n}\sum_{j=1}^{n} w_{ij}\sum_{i=1}^{n}(x_i-\bar{x})^2} \qquad \textbf{[3-1]}$$

In the equation, I is the Moran's index, ranging between –1 and 1, n is the number of spatial units indexed by i and j (the space coordinate), x refers to the variable (CO_2, SO_2, NO_x, and $PM_{2.5}$ emissions), $\bar{x}$ denotes the mean of x, and w_{ij} is a matrix of spatial weights of unit i and j.

3.3.5 Identify the hotspots of CO_2 and air pollutants emission

After establishing the unified emission inventory at a high spatial resolution, we identified the grids of both high CO_2 and air pollutants emissions spatially, namely the "co-hotspots". Taking CO_2 and SO_2 emissions as an example, we first ranked all the grids from high to low according to their CO_2 or SO_2 emissions across all grids in the city, independently. Based on the ranks of CO_2 or SO_2 emissions, we classified the grids into four categories, including category 1: top 5%, category 2: top 6% – 10%, category 3: top 11% – 15%, and category 4: top 16% – 20% emission grids. Based on the categories of CO_2 and SO_2 emissions, we identified the grids in which CO_2 and SO_2 were both in category 1 – 4 as category 1 – 4 co-hotspots of CO_2 and SO_2.

3.4 Results

3.4.1 Characteristics of the unified emission inventory

Figure 3. 3 presents the classification of the unified emission inventory. In **Figure 3. 3**, the blue shadings represent the sectors of the air pollutants emission inventory, the green shadings represent the sectors of the CO_2 emission inventory, the grey shadings represent the sub-sectors, and the orange shadings represent the unified emission inventory.

Specifically, the stationary combustion sector of air pollutants emission inventory corresponded to the industrial energy sector (including the sub-sectors of power and heat generation, power transmission, mining and manufacturing, and other industries) and residential buildings sector (including the sub-sectors of urban and rural buildings) of the CO_2 emission inventory. The industrial processes sector of the air pollutants emission inventory covered a wider range of sub-sectors compared to the CO_2 emission inventory. CO_2 emissions from the industrial processes sector were mainly attributed to iron and steel production and cement production, and thus the contributions from other sub-sectors such as nonferrous metal production and paper industry were not included. The on-road transportation sector for both inventories were consisted of same sub-sectors, including cars, taxis, buses, and motorbikes. For the off-road transportation sector, both inventories covered waterways, aviation, railways, and engineering machinery. It should be noted that agriculture in the CO_2 emission inventory represented the emission from agriculture machinery, and thus belonged to the off-road transportation sector of the air pollutants emission inventory.

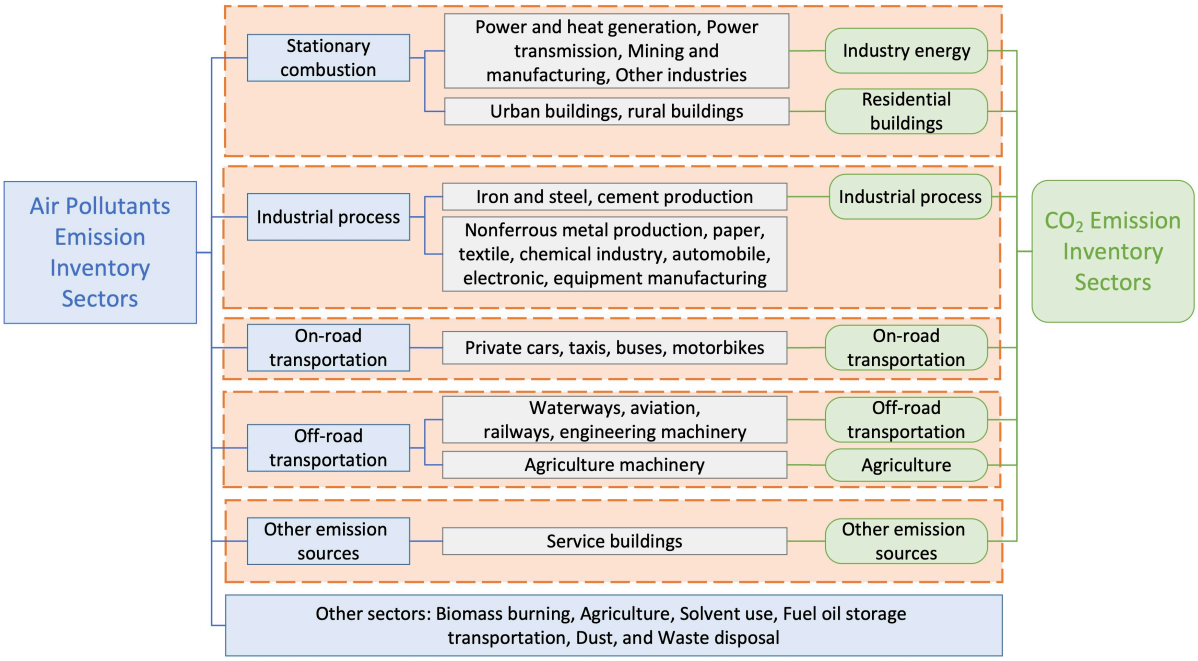

Figure. 3 Reclassification of the air pollutants (blue shading) and CO_2 emission inventory (green shading) by sub-sectors (grey shading)

Based on the unified emission inventory, the sectoral contribution to CO_2 and air pollutants emissions in Guangzhou in 2018 could be obtained, as shown in **Figure 3. 4**. We found sectors contributed substantially to both CO_2 and air pollutants emissions, particularly the stationary combustion sector and the transportation sector. In 2018, these two sectors contributed to 95%, 67%, and 93% of total CO_2, SO_2, and NO_x emissions in Guangzhou, respectively. Specifically, stationary combustion was a major contributor to both CO_2 and SO_2 emissions, which accounted for 63% and 35% of total CO_2 and SO_2 emissions, respectively. The transportation sector was the dominant contributor to NO_x emission (81%) and the second-largest contributor (32%) to CO_2 emissions. Recently, the CO_2 emissions from the transportation sector increased rapidly from 12 Mt in 2015 to 20 Mt in 2018 in Guangzhou. The transportation sector also contributed to 33% and 32% of total VOCs and SO_2 emissions, respectively. We also found sectors that mainly contributed to air pollutants emissions. For example, the industrial processes sector was a major contributor to

total VOCs (13%), $PM_{2.5}$ (19%), and PM_{10} (13%) emissions. Nevertheless, it accounted for only 2.5% of total CO_2 emissions. Therefore, mitigations aiming at controlling the emissions of the stationary combustion and the transportation sectors would have great potential to achieve the co-reduction of both CO_2 and air pollutants emissions (Mao et al. 2012; Zhou et al. 2013).

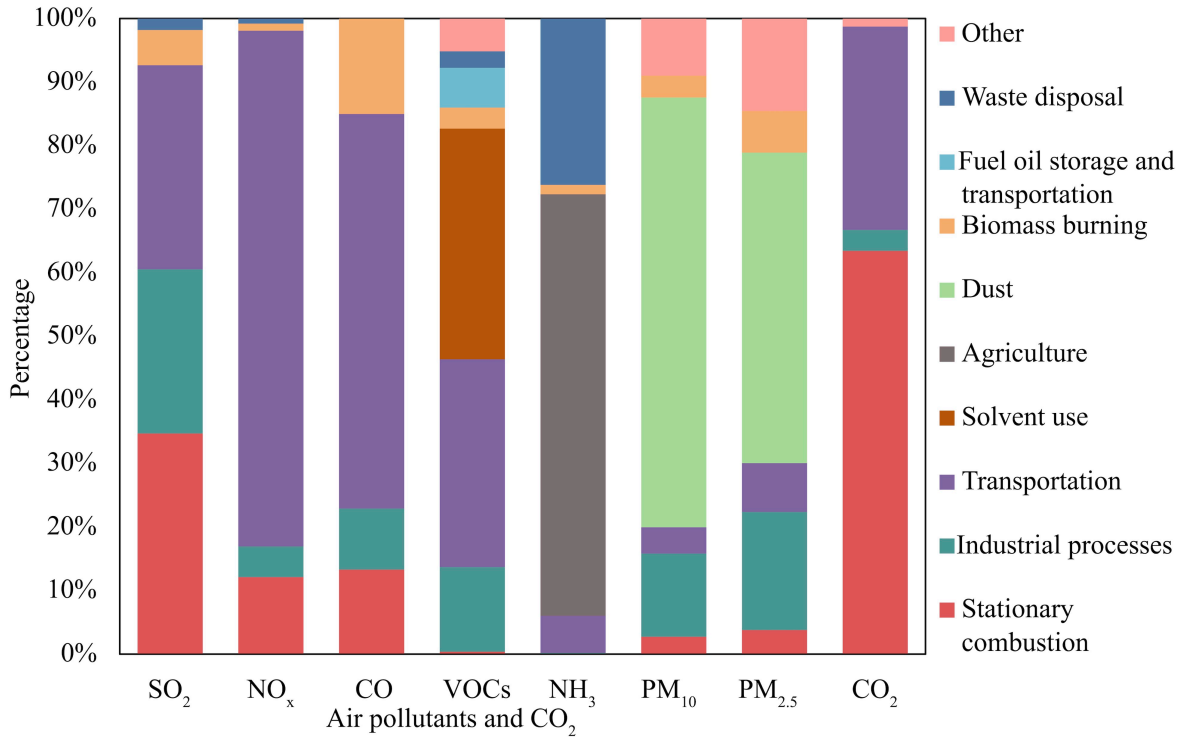

Figure 3. 4 Sectoral contribution to CO_2 and air pollutants emissions in Guangzhou in 2018

3.4.2 The spatial distribution of the unified emission inventory

Figure 3. 5 presents the spatial distributions of air pollutants (SO_2, NO_x, and $PM_{2.5}$) and CO_2 emissions in Guangzhou in 2018. For SO_2 emission (**Figure 3. 5A**), the spatial distribution was characterized by extremely large point sources mainly located in the Nansha and Huangpu districts. Specifically, grids with more than 100 tons of SO_2 emissions per year (N = 64, the red and light red grids) mainly represented the emissions from the stationary combustion or industrial processes

sectors (the power and heat generation, papermaking, and cement production industries). For NO_x (**Figure 3. 5B**), high-emission grids were found at the airport, waterways, and road intersections, which were densely distributed in the downtown area (Yuexiu, Tianhe, and Haizhu districts) and near the Baiyun International Airport. For $PM_{2.5}$ (**Figure 3. 5C**), high-emission grids were represented by the point sources of major construction sites and the line sources of road transportation. As shown in **Figure 3. 5D**, the spatial distribution of CO_2 emissions staggered in points, lines, and areas. High emission grids from point sources (attributed to industrial enterprises in the stationary combustion sector) were mainly located in the Nansha and Huangpu districts, while grids from line sources (attributed to the transportation sector) were distributed in the downtown area. The above results showed air pollutants (SO_2, NO_x, and $PM_{2.5}$) and CO_2 emissions were unevenly distributed in Guangzhou city.

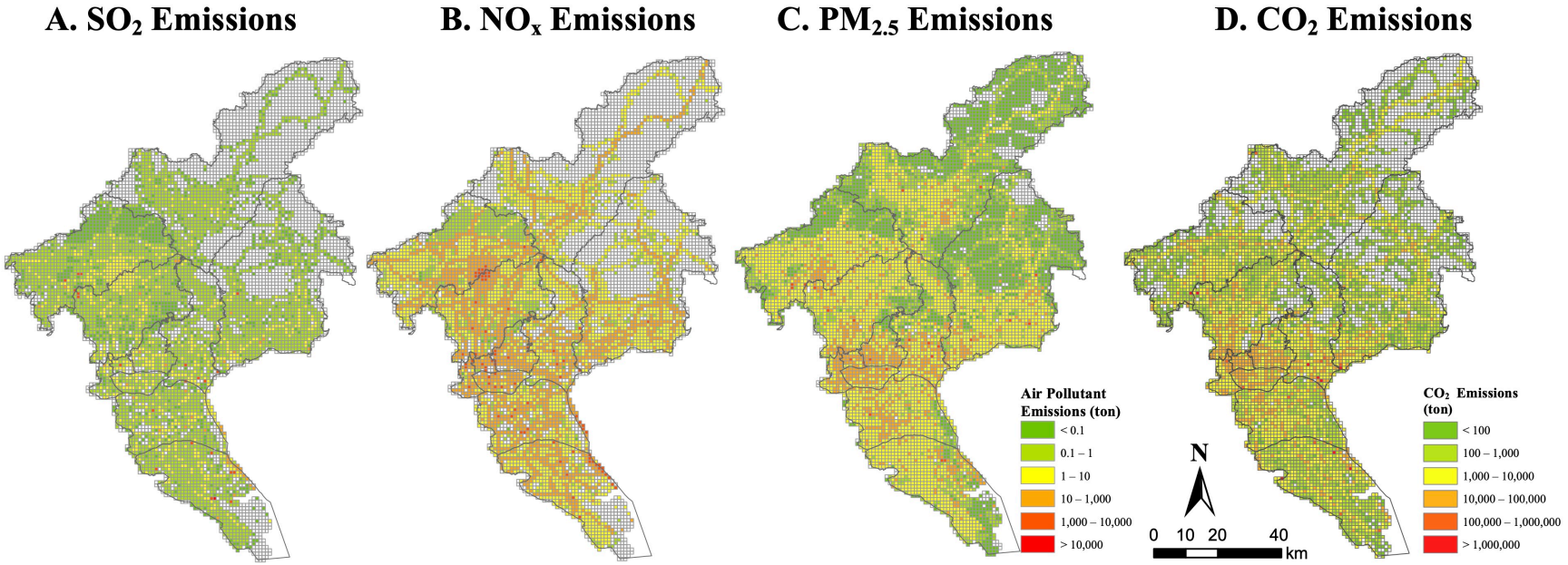

Figure 3. 5 The spatial distribution of air pollutants (A) SO_2, (B) NO_x, (C) $PM_{2.5}$, and (D) CO_2 annual emissions in Guangzhou in 2018

To better understand the characteristics of air pollutants and CO_2 emissions in Guangzhou, we analyzed the percent distribution of four categories of grids on total grids and total SO_2, NO_x, $PM_{2.5}$, and CO_2 emissions (**Figure 3. 6**). As illustrated in **Figure 3. 6A – D**, we found top 10% emission grids (Categories 1 and 2, see **Method** for details) contributed to 86%, 66%, 72%, and 86% of total SO_2, NO_x, $PM_{2.5}$, and CO_2 emissions, respectively. For example, for CO_2, there were 23 grids with more than 0.1 Mt (**Figure 3. 5D**, the red grids), which accounted for almost all CO_2 emissions in the stationary combustion sector. These emission grids mainly represented the power and heat generation, cement production, iron and steel production, and oil refining industries. Besides, the grid covering the Baiyun International Airport contributed almost 4 Mt, which accounted for 20% of total CO_2 emissions in the transportation sector. Other grids with over 10 thousand tons of CO_2 emission were distributed along the major roads in Yuexiu, Tianhe, and Haizhu districts. In addition, high-emission grids were also found in the southeast of Nansha district, representing the emissions from waterway transportation.

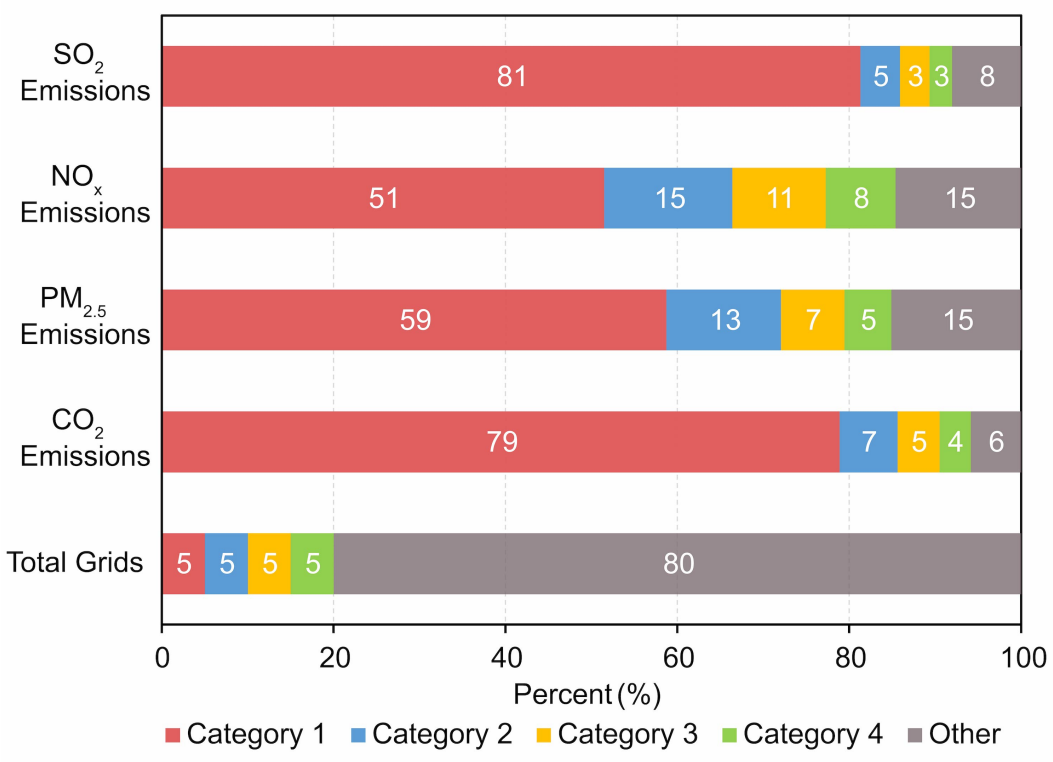

Figure 3. 6 The percent distribution of four categories of grids on total grids, total air pollutants (SO_2, NO_x, and $PM_{2.5}$) emissions, and total CO_2 emissions in Guangzhou in 2018. According to the emission ranks across all spatial grids, Category 1 represents the top 5% emission grids, Category 2 represents the top 6% – 10% emission grids, Category 3 represents the top 11% – 15% emission grids, Category 4 represents the top 16% – 20% emission grids, and Other represents the remaining emission grids.

The percent distribution suggested that more than 66% of total CO_2 or air pollutants emissions were attributable to top 10% emission grids (**Figure 3. 6**). Thus, specialized mitigation controls, such as conducting site-specific management on these high-emission grids, are critical to lowering the total emissions. We used the Moran's index to explore the spatial autocorrelation pattern of CO_2 and air pollutants emissions in Guangzhou (see **Method** for the details), in which higher Moran's indices suggest stronger spatial autocorrelations, whereas indices equal to zero represent no such autocorrelation. Our results showed that the Moran indices of SO_2, NO_x, $PM_{2.5}$, and CO_2 emissions were all smaller than 0.2, showing weak spatial

autocorrelation in the distribution of CO_2 or air pollutants (SO_2, NO_x, and $PM_{2.5}$) emissions (Glazier et al. 2004; Putra et al. 2020), respectively. The weak spatial autocorrelation suggested that the high emission grid was not surrounded by other high emissions grids in the neighboring, thus those high emissions grids were not located in a specific spatial area.

3.4.3 Identification of the hotspots

To conduct site-specific management that controls both CO_2 and air pollutants emissions efficiently, we identified the high emission grids of both air pollutants and CO_2, namely the "co-hotspots", at a spatial resolution of 1 × 1 km^2, and the results were shown in **Figure 3. 7**. Four kinds of co-hotspots were identified, including (1) SO_2 and CO_2, (2) NO_x and CO_2, (3) $PM_{2.5}$ and CO_2, and (4) SO_2, NO_x, $PM_{2.5}$, and CO_2. The co-hotspots were divided into four categories from category 1 (top 5%) to category 4 (top 16% – 20%) (see **Method** for details) according to their ranks across all spatial grids.

The co-hotspots of SO_2 and CO_2 emissions (**Figure 3. 7A**) were mainly located in the downtown area (Yuexiu, Tianhe, Liwan, and Haizhu districts), while the rural area (Conghua and Zengcheng districts) generally showed low emission levels. The identified grids were mostly comprised by point sources in the stationary combustion sector and line sources in the transportation sector as these sectors accounted for 67% and 95% of total SO_2 and CO_2 emissions, respectively (**Figure 3. 4**). In the top 10% class, 112 grids with over 2 tons of SO_2 emission and 14 thousand tons of CO_2 emissions were identified. The emissions of these 112 girds contributed to 31% and 35% of the total SO_2 and CO_2 emissions in Guangzhou,

respectively. The "top 10% class" of SO_2 and CO_2 co-hotspots represented the point sources in power and heat generation and cement production industries. For example, the hotspot grid of Zhujiang Power Plant emitted 293 tons of SO_2 and 6 Mt of CO_2 in 2018, which was considered a very large amount for both SO_2 and CO_2.

The co-hotspots of NO_x and CO_2 (**Figure 3. 7B**) were mainly distributed along major roadways and from the major point sources of the Baiyun International Airport, Huarun thermal power station, and Maxi industrial park. The combustions of fossil fuel from industrial boilers, diesel vehicles, and aircraft were the main contributors to both NO_x and CO_2 emissions in Guangzhou.

Similar to the spatial pattern of the co-hotspots of NO_x and CO_2, the co-hotspots of $PM_{2.5}$ and CO_2 (**Figure 3. 7C**) showed an overall pattern of high emissions in the downtown area (Yuexiu, Tianhe, Liwan, and Haizhu districts), where high-density roadways were constructed. Grids that covered extremely large point sources were identified, including the power and heat generation and cement production industries, suggesting that the stationary combustion sector was also an important emitter of both $PM_{2.5}$ and CO_2.

The co-hotspots of SO_2, NO_x, $PM_{2.5}$, and CO_2 (**Figure 3. 7D**) represented the grids with high emissions of multiple air pollutants (SO_2, NO_x, and $PM_{2.5}$) and CO_2.The co-hotspots were mainly distributed in the downtown area, with scattered grids distributed in the Baiyun and Huangpu districts. The co-hotspots identified in Guangzhou were mostly accompanied by high population density (**Figure 3. 2A**), which suggests that a vast majority of people were being exposed to high CO_2 and air pollutant emissions. As a result, mitigation policies such as site-

specific emission controls should be prioritized to the co-hotspots to protect the health of the public.

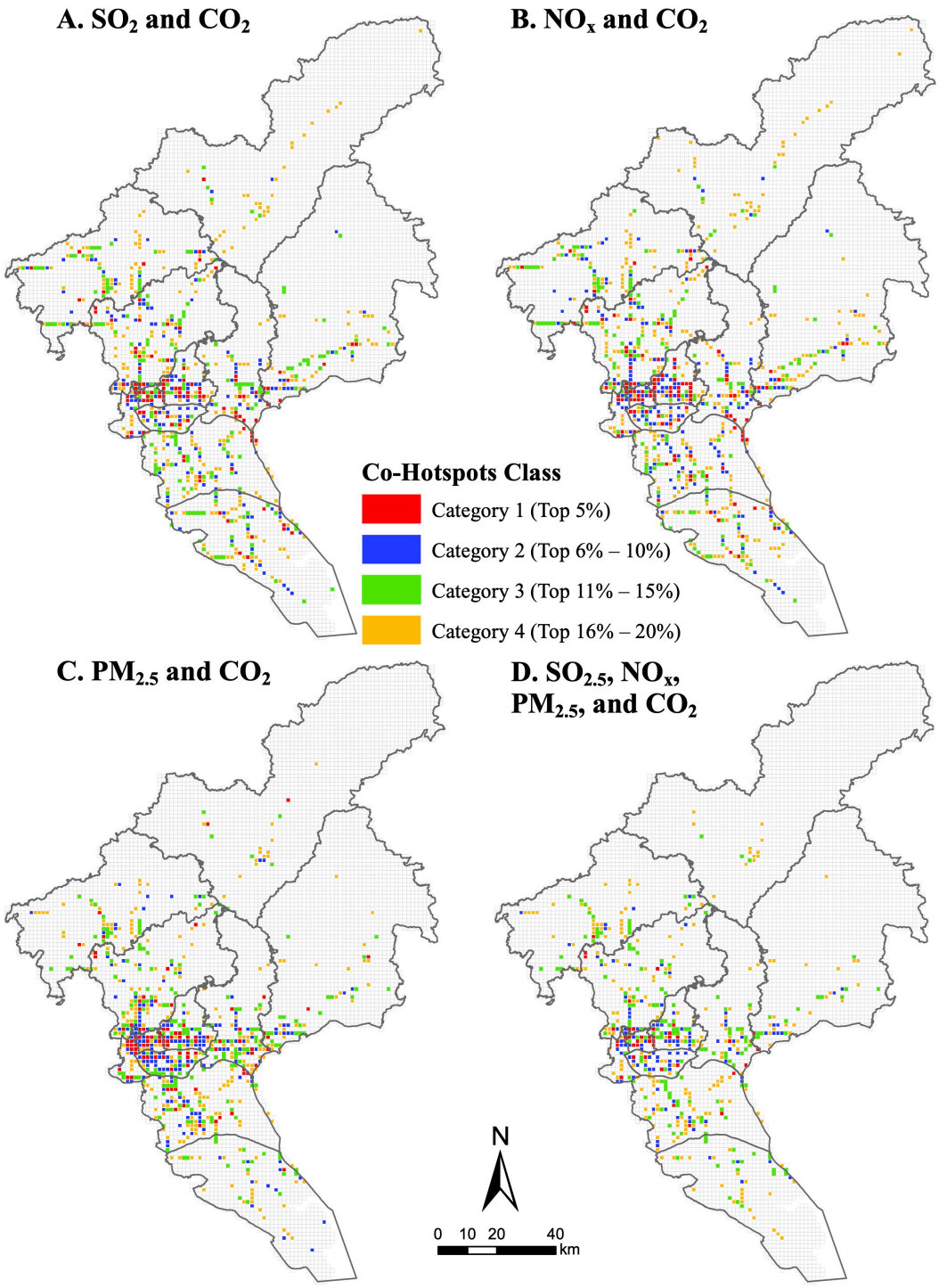

Figure 3. 7 The co-hotspots of (A) SO_2 and CO_2, (B) NO_x and CO_2, (C) $PM_{2.5}$ and CO_2, and (D) SO_2, NO_x, $PM_{2.5}$, and CO_2 in Guangzhou in 2018

3.5 Discussion

The unbalanced development in constructing CO_2 and air pollutants emission inventories was an issue. To address this problem, our study presented one of the first attempts to establish a unified emission inventory including both CO_2 and air pollutants. Based on the unified inventory and spatial mapping methods, we identified the high emission grids of both CO_2 and air pollutants and further identified the co-hotspots spatially at a high resolution (1×1 km^2). The method developed in this Chapter could be easily applied to other cities in China and other counties to develop a unified emission inventory and identify emission co-hotspots. At present, Chinese cities face strict challenges of CO_2 emission reduction and air quality improvement. Previous studies suggested that many CO_2 and air pollutants are emitted from the same sources (Oh et al. 2019; Lu et al. 2020), which was supported by our findings in Guangzhou. Co-hotspots in Guangzhou were mainly attributed to the point or line sources in the industry and transportation sectors. Besides, the high degree of overlapping in spatial distribution of both CO_2 and air pollutant emissions indicated a great potential for the city to achieve co-reductions.

Our study has several important policy implications. First, our study proposed a method to develop the unified emission inventory that integrated CO_2 and air pollutants, which addressed the inconsistency in the structures and classification of current emission inventories. Facing the challenges of both climate change and air pollution, environmental researchers, and policymakers can use the unified emission inventory to directly assess the local emission characteristics (Qi et al. 2017; Bai et al. 2020), the contribution from different sectors (D'Avignon et al. 2010; Bai et al. 2020), which provides a basis to evaluate the effectiveness of previous control measures (Zhang et al. 2013) and design collaborative control strategies

and policies in the future. Our method was also supported by IPCC Inventory Guidelines, which suggested that the integration of compiling GHG and air pollutants inventories can help decision makers understand the benefits of control measures and pool resources efficiently (IPCC 2019).

Besides, by using on our method, detailed information including CO_2 and air pollutants emissions, sectoral contribution, and major emission sources (such as the power and heat generation plants, the transportation hub) could be identified at each spatial grid. In comparison, previous studies only presented the spatial distribution of either air pollutants (Qi et al. 2017; Bai et al. 2020) or CO_2 (Cai et al. 2018a), and thus, lacked a comprehensive assessment of both emissions spatially. The identified co-hotspots allow us to discover the distribution pattern of grids with high CO_2 and air pollutants emissions (Glazier et al. 2004; Putra et al. 2020). Previous experience of site-specific management, such as the pollution control based on hotspots and regions, proved effective in air pollution prevention and control (Zhao 2018). By using our method, such practices could also be utilized to reduce both CO_2 and air pollutants emissions, considering the noticeable contribution of co-hotspots grids to total emissions. Thus, areas with densely distributed co-hotspots are of high priority to conduct site-specific management (Cai et al. 2018b; Jiang et al. 2020), which could improve the efficiency in resource allocation and lower the cost of environmental enforcement (Wu 2020).

In addition, the spatial resolution of CO_2 and air pollutants emissions was 1×1 km^2, which was greatly improved compared to the existing EDGAR (Emissions Database for Global Atmospheric Research, 10×10 km^2) (Crippa et al. 2018) and MEIC (27×27 km^2) inventory

(MEIC 2021). The improved spatial resolution allowed us to accurately identify the city-level high-emission areas and associated population suffering from unequal exposure to multiple air pollutants. For example, those people living in the downtown area of Guangzhou (**Figure 3. 2A**) may be exposed to higher levels of air pollutants. The improved spatial resolution will help the government to realize the environmental inequity issue and design mitigation policies accordingly (Wilson et al. 2010).

Chapter 4

The pathway for Chinese cities to achieve dual targets of CO_2 emission reduction and air quality improvement: a case study in Yantai city

4.1 Abstract

Chinese cities are facing strict challenges on both climate change mitigation and air pollution reduction. Previous studies commonly investigate the co-benefit of CO_2 emission reduction and air quality improvement on global, national, or provincial scales, with few at the city level. In this Chapter, we used Yantai city as a case to propose and evaluate the pathway to reach the dual targets of CO_2 emission reduction and air quality improvement for Chinese cities. We developed an integrated assessment model that coupled emission projection, air quality, and health assessment. Results indicate that energy-related measures help Yantai meet the $PM_{2.5}$ target (35 $\mu g/m^3$) by 2030 and achieves the carbon neutrality goals by 2060. Energy-related measures exhibit an increasing potential in reduction air pollutants (contributing to 53% and 79% of $PM_{2.5}$ reduction in 2035 and 2060) and CO_2 emissions in the long term. In contrast, advanced end-of-pipe controls will only contribute to improving the air quality before 2035 (contributing to 54% and 47% of $PM_{2.5}$ reduction in 2030 and 2035). Results show that the future health benefit from improved air quality will likely compensate for the abatement cost of implementing low-carbon energy measures, with a net monetized benefit of 1.9 billion

Chinese yuan in 2060. Our analysis could provide implications for Chinese cities to deal with the dual challenges in the future.

4.2 Introduction

As the world's largest CO_2 emissions (BP 2021), China faces a great challenge in mitigating CO_2 emissions. It is estimated that CO_2 emissions will increase by 50% in the next 15 years without mitigation (Liu et al. 2015). In response, in the Nationally Determined Contribution of the Paris Agreement, China pledged to reduce its CO_2 emission intensity by 60%–65% by 2030 compared to 2005 (NDRC 2015; The Guardian 2016). In addition, during the Climate Ambition Summit, China pledged to reach its CO_2 emission peak before 2030 and carbon neutrality by 2060 (Climate Ambition Summit 2020). On the other side, China is also suffering from severe air pollution, despite the improvements in recent years (Cai et al. 2017; Ding et al. 2019; Zhang et al. 2019). In 2020, about 37% of Chinese cities exceeded the national ambient air quality standard of 35 $\mu g/m^3$ for $PM_{2.5}$ (China National Environmental Monitoring Centre 2021). To address the above challenges, cities in China play an important role as they are the fundamental units to implement reduction policies (Chen et al. 2020a). So far, more than 80 cities have proposed plans to reach the CO_2 emission peak by 2030 (Qian et al. 2019). In addition, mandatory reduction targets have been set for air pollutant concentrations at the city level under current policies (State Council of the People's Republic of China 2013, 2018).

Most CO_2 and air pollutants are emitted from the fossil fuel combustion processes of the same sources (Oh et al. 2019; Lu et al. 2020). Emission source control provides a potential opportunity to simultaneously achieve the co-reduction of CO_2 and air pollutants emissions. Previous studies have suggested that CO_2 mitigation policies can reduce air pollutant concentrations and increase health benefits (Markandya et al. 2009; Nemet et al. 2010; West et al. 2013; Dong et al. 2015; Yang and Teng 2018; Xie et al. 2018; Xing et al. 2020). In

addition, the energy-related control measures in air pollution control also lead to CO_2 emission reductions (He et al. 2010; Lu et al. 2019). To investigate the co-benefits of CO_2 emission reduction and air quality improvement, these studies have applied integrated modeling frameworks incorporating emission projections, air quality evaluations, and health effect assessment, such as the regional emissions air quality climate and health (REACH) model (Li et al. 2018) and the Greenhouse Gas and Air Pollution Interactions and Synergies (GAINS) model (Li et al. 2019d; Lu et al. 2019). The co-benefit could be achieved in major sectors through energy structure adjustment and energy efficiency enhancement on global (West et al. 2013), national (Xie et al. 2018), and provincial (Dong et al. 2015) scales. At present, few studies have investigated the co-benefit at the city level (Liu et al. 2017; Deng et al. 2017; Wu et al. 2021). Although Liu et al. and Wu et al. investigated the co-benefit of CO_2 emission reduction on air quality improvement in Suzhou city (Liu et al. 2017) and Guangzhou city (Wu et al. 2021), respectively, these studies were conducted only in the year 2020, and they neglected the long-term pathway to reduce CO_2 emissions and air pollutants. We believe it is meaningful to investigate the pathway that helps Chinese cities to understand the relationship between CO_2 emissions and air pollutants emissions and finally achieve the "dual targets" of CO_2 emission reduction and air quality improvement, which can directly support the city's design of control strategies and policies in the future.

In this Chapter, we built a comprehensive framework to assess the feasibility of achieving the dual targets at the city level. We accomplished this by integrating the Chinese Academy of Environmental Planning Carbon Pathways (CAEP-CP) model (Cai et al. 2021a, b), the Weather Research and Forecasting-Community Multiscale Air Quality (WRF-CMAQ) model,

and the integrated exposure-response (IER) model. Our approach considered the different levels of energy-related measures and end-of-pipe controls, which allowed us to identify the CO_2 emission periods (growth, plateau, and decline) and to understand their influences on reducing air pollutants under future pathways. Our study used Yantai City in Shandong Province as a case study to develop our pathway. Yantai, located in eastern China, on the northern part of the Shandong Peninsula, was one of the national pilot low-carbon cities (National Development and Reform Commission 2010). Given the fast economic development and secondary-industry orientated structure, energy consumption and air pollution emissions have increased rapidly in recent years. In addition, the heavy industry contributed 60% of the industrial output value, which posed a strict challenge to reach the dual targets. Considering Yantai City's initiative to address both challenges, this case study represented a typical city in China and proposed a pathway to achieve both the CO_2 emission reduction and air quality improvement targets. The results of this study provide support for policy design and implementation.

4.3 Method

4.3.1 Overall framework

We used the CAEP-CP model to project the future emission inventory, including CO_2 and air pollutant emissions, which considered different pathways with multiple levels of energy-related measures and end-of-pipe controls. The CAEP-CP model, used in our previous studies (Cai et al. 2021a, b), was developed based on the Long-range Energy Alternatives Planning (LEAP) framework and the CHRED 3.0 Database (Cai et al. 2018a, 2019b, a). This model was developed by combining China's medium-term and long-term planning, industrial structures, and energy structures to estimate the impacts of energy policies and mitigation measures.

4.3.2 Emission inventory

The CO_2 emission inventory was compiled by the CCG (CCG 2020) and sourced from the CHRED 3.0 Database (CHRED 2020). In this Chapter, we focused on CO_2 emissions caused by fossil fuel consumption, instead of those caused by land use, land-use change, and forestry. The CO_2 emissions were calculated as the products of the energy consumption and the emission factors shown as follows:

$$CO_2\ Emission_j = \sum_i A_{i,j} \times EF_i \qquad \textbf{[4-1]}$$

where A represents the activity rate (energy consumption), EF represents the emission factor, i represents the type of fossil fuel (coal, oil, and natural gas), and j represents emission source (specific sectors), including the power generation, industries (i.e., steel, cement,

machine-made paper and paperboards, coking, primary plastic and synthetic rubber, plain glass, and other industries), transportation, building, and agriculture.

The air pollutants emission inventory was compiled by referring to the technical guidelines issued by the Ministry of Ecology and Environment (MEE 2014a, b) and the city-level environmental statistics (National Bureau of Statistics 2020c). A total of seven air pollutants ($PM_{2.5}$, PM_{10}, SO_2, NO_x, VOCs, CO, and NH_3) from eleven emission sectors (stationary combustion, industrial processes, agriculture, on-road transportation, off-road transportation, solvent use, waste disposal, fuel oil storage and transportation, dust, biomass burning, and other emission sources) were included. The emissions of air pollutants were calculated using the following equation:

$$Air\ pollutant\ Emission_{j,k} = \sum_{i,n} A_{i,j} \times EF_{i,j,k} \times \left(1 - \eta_{i,j,k,n}\right) \quad \textbf{[4-2]}$$

where A represents the activity rate, EF represents the emission factor, η represents the removal efficiency, i represents the type of fossil fuel, j represents the emission source (specific sectors or industries), k represents the air pollutant type, and n represents the type of pollutant control device.

4.3.3 Spatial mapping methods

In addition, we used spatial mapping methods to allocate the emission inventory at a high spatial resolution for air quality modeling. The detailed methods of the spatial mapping process can be found in our previous publications (Cai et al. 2018a, 2019b). The emissions, including

point, line, and area sources, were allocated to the space grid based on the location information, the weight of the density of road network, population distribution, GDP distribution, land use type, and the automatic identification system. We validated our results using the longitude and latitude data obtained from the continuous emission monitoring system and the accurate position indicator geocoding system. The basic information in Yantai in 2019, including the districts, population, industrial enterprises, and roadway distribution, is presented in **Figure 4. 1** below.

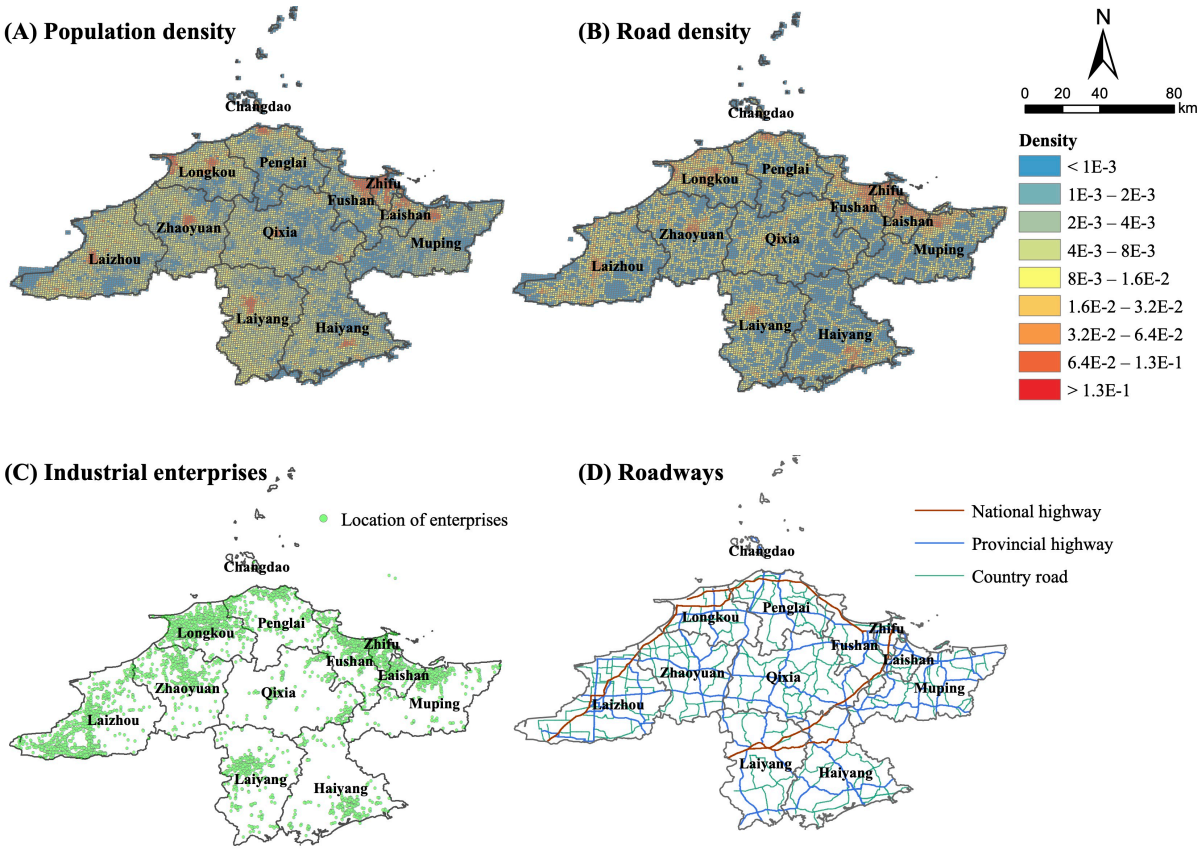

Figure 4. 1 The distribution of (A) population, (B) Road density, (C) Industrial enterprises, and (D) Road Network in Yantai in 2019.

4.3.4 Pathway projection

We investigated future CO_2 and air pollutants emissions in Yantai under three future pathways, including a Business-as-Usual pathway (BAU), an Enhanced Energy pathway (EEP), a Dual Control pathway (DCP). The base year of the CAEP-CP model was 2019. We ran the model through 2060, including the years 2030, 2035, and 2060. The details of the socioeconomic projection were provided in the Appendix B (Error! Reference source not found.). The basic socioeconomic assumptions were the same for three pathways with different levels of energy-related measures and end-of-pipe controls (**Table 4. 1**). First, we designed the BAU pathway to represent the current ongoing energy policies and end-of-pipe control measures to be conducted in Yantai without additional emission reduction measures. In the EEP pathway, aggressive low-carbon energy policies were implemented with the same level of end-of-pipe controls as in the BAU pathway. For the purpose of air pollutants control, strict end-of-pipe control policies were applied in the DCP pathway in addition to the energy policies applied in the EEP pathway. The key characteristics of the three pathways are described in detail in the **Table B 2** for comparison.

Table 4. 1 Summary table of future pathway projection

Pathways	Energy policy	End-of-pipe controls
BAU	Apply the energy policies and controls that meet the current policy requirement	Apply the end-of-pipe controls with the same stringency level as the existing control policies
EEP	Apply strict and aggressive energy policies that meet the	Same as end-of-pipe controls in the BAU pathway

	goals of CO_2 emission peak and carbon neutrality	
DCP	Same as energy policy in the EEP pathway	Maximum application of advanced and feasible end-of-pipe controls

Note: BAU represents the Business-as-Usual pathway, EEP represents the Enhanced Energy pathway, and DCP represents the Dual Control pathway.

4.3.5 WRF-CMAQ model and evaluation

We used the WRF model (version 3.6.1) to simulate the meteorological field and the CMAQ model (version 5.0.2) to simulate the pollutant concentration ($PM_{2.5}$) under three pathways. The CMAQ simulation was conducted using three nested domains with 27 km × 27 km, 9 km × 9 km, and 3 km × 3 km grid cells, covering 14 provinces in China, Shandong province and the surrounding 5 provinces, and Yantai city, respectively. We used the data from the MEIC (MEIC 2021) for the first two layers and Yantai's local emission inventory for the third layer. We assumed the same meteorological conditions as the base year under the three pathways to control the impacts of the meteorological factors on the $PM_{2.5}$ concentrations. We used the emission data in 2019 to develop the model and validated the model results with the observation data from air-monitoring sites in Yantai (China National Environmental Monitoring Centre 2021). The normalized mean bias (NMB), the normalized mean error (NME), and the correlation coefficient (R^2) were used to evaluate the fit of the model results. The NME, NME, and R^2 were 19%, 36%, and 0.76, respectively. All of them could meet the recommended benchmark (Simon et al. 2012; Huang et al. 2021), indicating a good fit of our model simulations with the observations and the reliability of the model performance.

4.3.6 Abatement cost and health benefits

We calculated the cost of implementing energy-related policies in the different sectors, including the power generation, industry (steel, cement, petrochemical, and others), building, and transportation sectors. The associated costs were estimated to be 37 – 187 US dollars (USD) per ton of CO_2 for mitigation technologies in different sectors, and the exchange rate of USD to CNY used was 1:6.6. The detailed technologies and associated costs were described in our previous study (Liu et al. 2021).

We evaluated the health effects due to long-term ambient $PM_{2.5}$ exposure using the IER model. The excess mortality due to air pollution exposure was calculated using the following equation:

$$\Delta M_d = I_d \times Pop \times \left(1 - \frac{1}{RR_d}\right) \quad \textbf{[4-3]}$$

where ΔM_d represents the attributable mortality due to $PM_{2.5}$ exposure, Pop represents the population, I_d represents the baseline mortality rate, and RR_d represents the relative risk, and d is the specific disease. The IER function was used to estimate the RR_d based on the Global Burden of Disease (GBD) study (Burnett et al. 2014), and it was calculated as follows:

$$RR_d = \begin{cases} 1 + \alpha_d\{1 - e^{[-\beta_d(z-z_0)^{\gamma_d}]}\} & for\ z > z_0 \\ 1 & for\ z \le z_0 \end{cases} \quad \textbf{[4-4]}$$

$$z = \frac{Pop_i}{Pop} \times z_i \quad \textbf{[4-5]}$$

where z is the population weighted $PM_{2.5}$ exposure ($\mu g/m^3$); z_0 is the counterfactual concentration below which there is no additional risk; and α_d, β_d, and γ_d are parameters of the

relative risk for disease d. Pop_i is the population in grid i, z_i is the simulated $PM_{2.5}$ concentrations ($\mu g/m^3$) in grid i, and Pop is the total population in Yantai. In the IER model, we calculated and added up the mortality for four diseases: chronic obstructive pulmonary disease (COPD), ischemic heart disease (IHD), lung cancer (LC), and stroke. The IER parameters z_0, α_d, β_d, and γ_d for the above four diseases were obtained from the GBD study (Burnett et al. 2014). The age-specific baseline mortality rate was obtained from Naghavi et al. (Naghavi et al. 2015). It was suggested that the predictions in China were reasonable as the observed RRs in the China cohort were similar to those predicted RRs by the GBD study (Burnett et al. 2014).

4.4 Results

4.4.1 Changes in air pollutants and CO_2 emissions

By using the CAEP-CP model and considering the end-of-pipe controls and energy-related measures, we projected the air pollutants and CO_2 emissions under the different pathways (**Figure 4. 2**). Along the BAU pathway, it is estimated that the emissions of SO_2, $PM_{2.5}$, and CO_2 in Yantai in 2030 will be 7.3E4, 7.7E4, and 6.0E7 tons, respectively, which are 11%, 9%, and 7% lower than the 2019 level. It should be noted that the NO_x emission will increase to 1.5E5 tons (by 2%) by 2030, likely because fossil fuel consumption will increase due to the demand of the transportation sector. In 2035, SO_2, NO_x, $PM_{2.5}$, and CO_2 emissions will be reduced to 5.7E4, 9.4E4, 6.3E4, and 5.7E7 tons, respectively, under the BAU pathway. Further in 2060, SO_2, NO_x, $PM_{2.5}$, and CO_2 emissions will be reduced to 2.9E4, 4.0E4, 2.6E4, and 3.3E7 tons, respectively. The above reductions in air pollutants and CO_2 emissions under the BAU pathway suggest the effectiveness of energy policies and end-of-pipe controls under the current policy design.

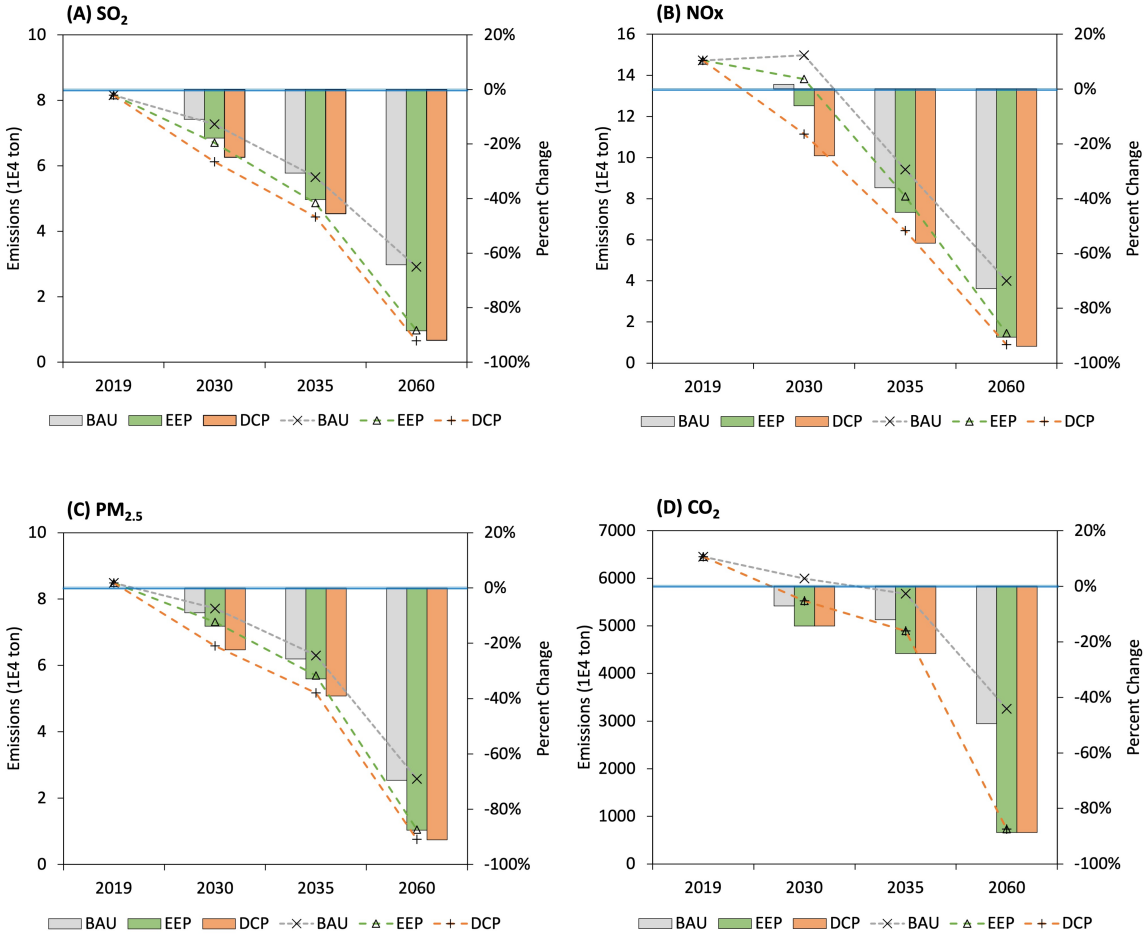

Figure 4. 2 Emissions (lines, left axis) and changes (bars, right axis, relative to 2019 level) for air pollutants and CO_2 under the Business-as-Usual pathway (BAU, grey), Enhanced Energy pathway (EEP, green), and Dual Control pathway (DCP, orange). (A) SO_2, (B) NO_x, (C) $PM_{2.5}$, and (D) CO_2.

With the application of energy-related measures under the EEP pathway, air pollutants and CO_2 emissions will be further reduced. The reductions in SO_2, NO_x, $PM_{2.5}$, and CO_2 emissions will be 40%, 45%, 33%, and 24%, respectively, in 2035 compared to the 2019 level. The energy-related measures result in substantial reductions by 2060, with emissions of SO_2, NO_x, $PM_{2.5}$, and CO_2 decreasing to 7.0E3, 9.6E3, 1.1E4, and 7.3E6 tons, respectively, which are about 91%, 93%, 88%, and 90% lower than those in 2019. DCP pathway consider the best available techniques of air pollutant control as well as the energy-related measures and most

reductions in air pollutants emissions occur. For example, in 2035, the reductions in SO_2, NO_x, and $PM_{2.5}$ emissions will reach 46%, 56%, and 39%, respectively, compared to the 2019 level.

As to the sectoral contribution, the reductions in air pollutants and CO_2 are mainly achieved through control measures in the stationary combustion, industrial process, and transportation sectors (**Figure 4. 3**). The fill and doted color bar in **Figure 4. 3** represent the emission reductions under the EEP compared to the BAU pathway and under the DCP pathway compared to the EEP pathway. When comparing the EEP pathway to the BAU pathway, the stationary combustion sector is estimated to account for 85% – 93%, 34% – 37%, 40% – 58%, and 81% – 91% of total SO_2, NO_x, $PM_{2.5}$, and CO_2 emission reductions, respectively, from 2030 to 2060, while the industrial process and the transportation sectors will account for 25% – 40% of total $PM_{2.5}$ emission reduction and 16% – 19% of total NO_x emission reduction, respectively. When comparing the DCP pathway to the BAU pathway, the transportation sector will be the dominant factor to the total NO_x emission reduction (41% – 80%).

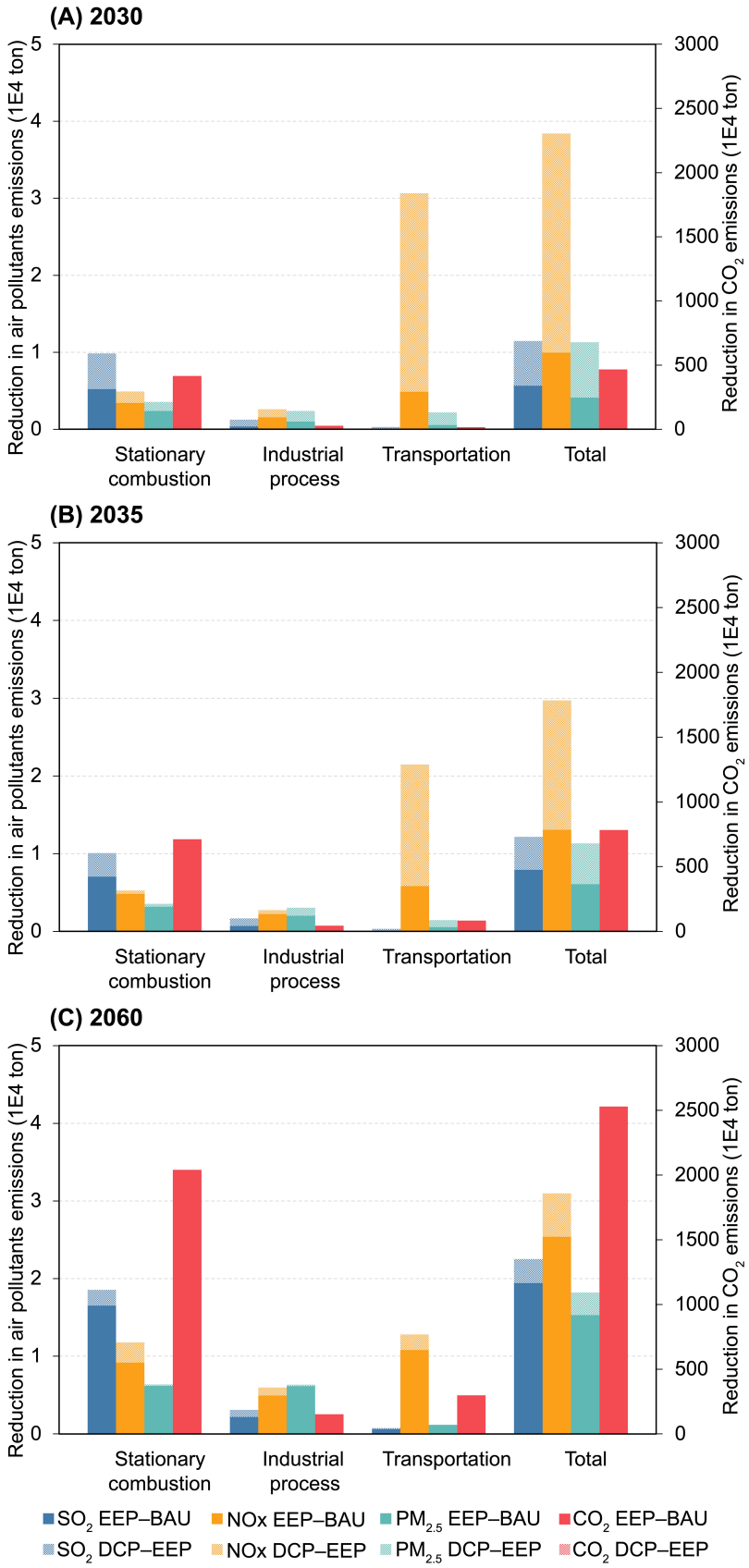

Figure 4. 3 Reduction in air pollutants (SO_2, NO_x, and $PM_{2.5}$) emissions (left axis) and CO_2 emissions (right axis) by sector under the Business-as-Usual pathway (BAU), the Enhanced

Energy pathway (EEP), and the Dual Control pathway (DCP) in (A) 2030, (B) 2035, and (C) 2060.

4.4.2 Evaluation on air quality attainment and CO_2 emission periods along future pathways

We used the WRF-CMAQ to simulate the future $PM_{2.5}$ concentrations in Yantai through 2030, 2035, and 2060 using the air pollutant emissions projected in the previous section under three different pathways. As shown in **Figure 4. 4**, Yantai will experience a substantial decrease in $PM_{2.5}$ concentrations from 2019 to 2060 due to the implementation of end-of-pipe controls and energy-related measures. The annual mean $PM_{2.5}$ concentrations will likely decrease from 37.0 μg/m^3 in 2019 to 36.0 μg/m^3, 34.7 μg/m^3, and 26.7 μg/m^3 in 2030, 2035, and 2060, respectively, under the BAU pathway. Further, the implementation of low-carbon policies under the EEP pathway will result in additional air quality improvement. The annual mean $PM_{2.5}$ concentrations will decrease to 34.8 μg/m^3, 33.1 μg/m^3, and 23.5 μg/m^3 in 2030, 2035, and 2060, respectively, which would allow Yantai city to meet the national annual ambient air quality standard (35 μg/m^3). On the other side, the end-of-pipe controls will play an important role in $PM_{2.5}$ reduction. Under the DCP pathway when stringent end-of-pipe controls are applied, the annual mean $PM_{2.5}$ concentrations will likely be 1.4 μg/m^3, 1.3 μg/m^3, and 1.0 μg/m^3 lower than the EEP pathway in 2030, 2035, and 2060, respectively. The end-of-pipe controls will be the main driver to air quality improvement before 2035. Taking the BAU pathway as a reference, the end-of-pipe controls would contribute to 54% and 47% of the $PM_{2.5}$ reduction in 2030 and 2035, respectively, while only contributing to 21% of the $PM_{2.5}$ reduction

in 2060. In contrast, the energy-related measures exhibit increasing reduction potentials, contributing 79% of the $PM_{2.5}$ reduction in 2060.

In addition, we used the time series data to identify the CO_2 emission periods and the method was described detailly in our previous study (Jiang et al. 2021). The identification of the CO_2 emission periods, including the period of decline, plateau, and growth, is important to understand the current CO_2 emission status and design pertinent reduction policies to meet future goals. Our results show that the adjustment of the energy structure and the implementation of energy conservation measures will help Yantai achieve the climate goals, including CO_2 emission peak by 2030 and carbon neutrality by 2060. Based on the identification of the CO_2 emission periods (Jiang et al. 2021), Yantai will reach the period of decline of CO_2 emission before 2030 under the EEP pathway. CO_2 emissions are expected to decrease continuously after 2035 and finally decrease to about 10% of the current emission level by 2060, which is crucial to the carbon neutrality goal.

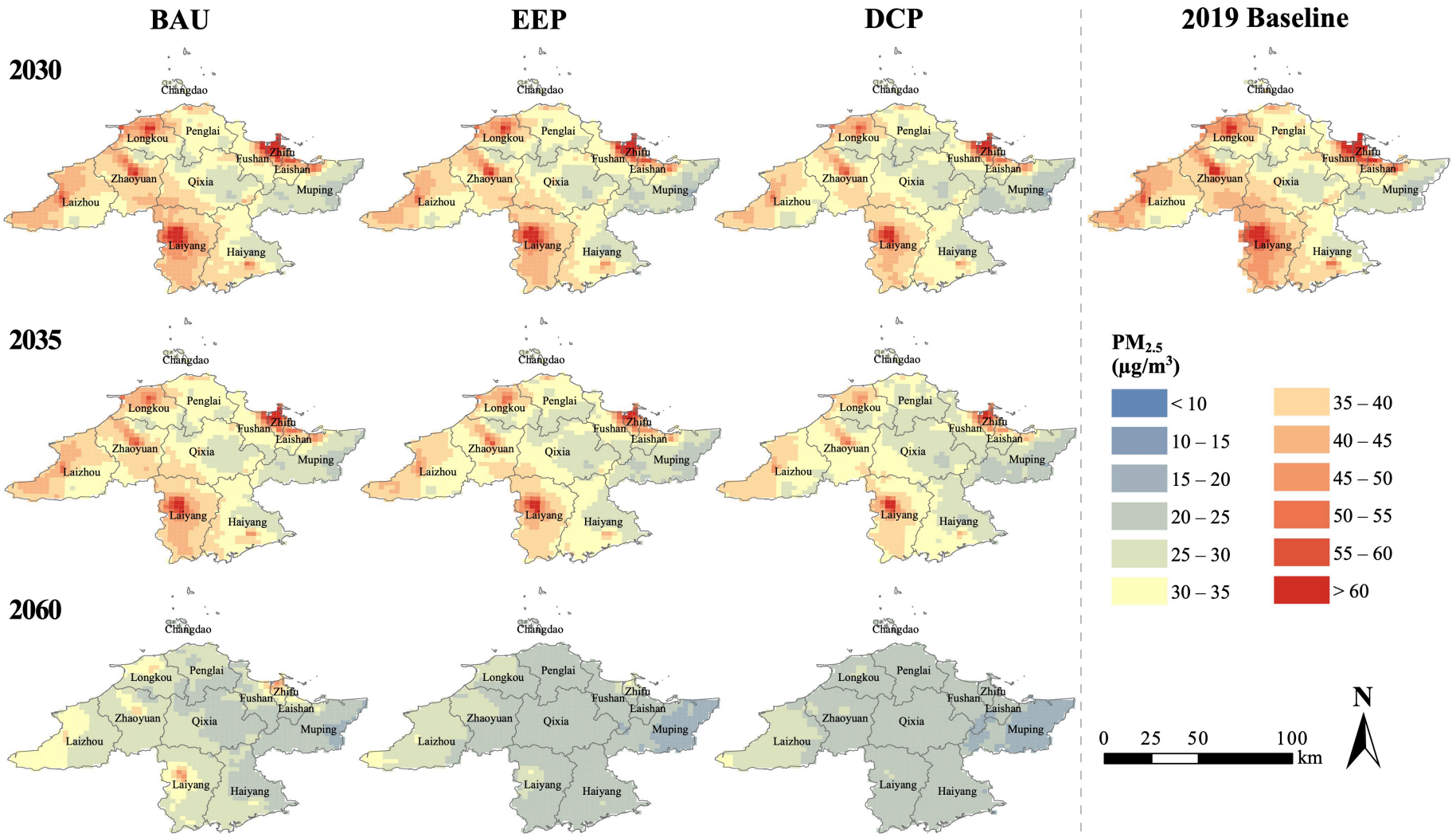
BAU
EEP
DCP
2019 Baseline
2030
2035
2060
Changdao
Longkou
Penglai
Zhifu
Fushan
Laishan
Zhaoyuan
Qixia
Muping
Laizhou
Laiyang
Haiyang
PM2.5 (μg/m3)
< 10
10 – 15
15 – 20
20 – 25
25 – 30
30 – 35
35 – 40
40 – 45
45 – 50
50 – 55
55 – 60
> 60
0 25 50 100
km
N

Figure 4. 4 $PM_{2.5}$ concentrations under the Business-as-Usual pathway (BAU), Enhanced Energy pathway (EEP), and Dual Control pathway (DCP) in Yantai in 2030, 2035, and 2060, and the Baseline in 2019.

The spatial distribution of the annual mean $PM_{2.5}$ concentrations in Yantai is shown in **Figure 4. 4** as well. In general, the $PM_{2.5}$ concentrations are higher in the Zhifu district, the central parts of Laiyang and Zhaoyuan districts, and the northern parts of Longkou and Laishan districts compared to other districts in Yantai. Although Yantai city will likely meet the national air quality standard in 2035 under the BAU pathway, many districts will still suffer from high $PM_{2.5}$ concentrations. The annual mean $PM_{2.5}$ concentrations in Zhifu, Laiyang, Laishan, Longkou, Zhaoyuan, and Laizhou districts will exceed the standard by 82%, 26%, 15%, 14%, 9%, and 9%, respectively. This is probably because of the dense distribution of industrial enterprises and road networks, leading to high air pollutants emissions in these districts. The power generation, industry, and transportation sectors are the major contributors to air pollutants emissions in Yantai, accounting for 99%, 98%, and 63% of total SO_2, NO_x, and $PM_{2.5}$ emissions, respectively (**Figure B 1**). The industrial enterprises in Yantai are mainly distributed in the Zhifu, Laishan, Laiyang, Longkou, and Laizhou districts. For example, the top 10 power plants in terms of air pollutants emissions are located in Zhifu, Laizhou, and Longkou districts. Other industries, including cement production, steel production, the chemical industry, and the food and drink industry, are also the main contributors to the emissions of air pollutants. They are mainly distributed in the Zhifu, Longkou, Laishan, Laiyang, and Laizhou districts. In addition, the transportation sector is the largest contributor to NO_x emissions (60%) and the main contributor to VOCs emissions (21%) (**Figure B 1**). The road dust sector also contributes to 10% and 24% of the total $PM_{2.5}$ and PM_{10} emissions, respectively. As can be seen from **Figure 4. 1**, the major roadways (national highway, provincial highway, country and township roads) are densely distributed in the Zhifu and

Laishan districts and parts of the Longkou, Zhaoyuan, and Laizhou districts, leading to a high degree of road network density in these districts.

Furthermore, air pollution may have severe effects due to the dense population distribution in these districts. In 2035, seven districts (Zhifu, Laiyang, Laishan, Longkou, Zhaoyuan, Laizhou, and Fushan) will not meet the national air quality standard under the BAU pathway, which affects a total of 4.6 million people (about 70%) in Yantai. The spatial distribution of the population in Yantai is presented in **Figure 4. 1A**. A high degree of overlap is found between the dense population and high $PM_{2.5}$ concentration areas, which is expected to pose a threat to the people in these districts (Zhifu, Laiyang, Longkou, and Fushan).

Fortunately, the implementation of energy-related measures will greatly decrease the $PM_{2.5}$ concentrations in the abovementioned high-concentration districts. Compared to the BAU pathway, the $PM_{2.5}$ concentrations will likely decrease by 2.8 $\mu g/m^3$, 1.7 $\mu g/m^3$, 1.6 $\mu g/m^3$, and 1.3 $\mu g/m^3$ in the Zhifu, Laiyang, Laishan, and Longkou districts, respectively, by 2030 under the EEP pathway. By 2035, the reduction is estimated to reach 3.8 $\mu g/m^3$, 2.3 $\mu g/m^3$, 2.0 $\mu g/m^3$, and 1.6 $\mu g/m^3$ in the Zhifu, Laiyang, Laishan, and Longkou districts, respectively, which represent a 4% – 7% reduction relative to the BAU pathway. The energy-related measures will likely ensure that all of the districts in Yantai meet the national air quality standard of $PM_{2.5}$ by 2060. The $PM_{2.5}$ concentrations will likely decrease to 26.4 $\mu g/m^3$, 24.1 $\mu g/m^3$, 22.1 $\mu g/m^3$, and 25.0 $\mu g/m^3$ by 2060 in the Zhifu, Laiyang, Laishan, and Longkou districts, respectively, under the EEP pathway, which is about 28%, 19%, 17%, and 12% lower than that for the BAU pathway. What's more, the application of end-of-pipe controls in the DCP pathway could bring

additional air quality improvements in the different districts. Compared to the EEP pathway, the $PM_{2.5}$ concentrations will decrease by an additional 4.1 μg/m^3, 2.2 μg/m^3, 2.1 μg/m^3, and 1.7 μg/m^3 in the Zhifu, Laiyang, Laishan, and Longkou districts, respectively, by 2030 under the DCP pathway. These reductions in the abovementioned districts will reach 1.7 μg/m^3 – 3.4 μg/m^3 by 2035, demonstrating the effectiveness of implementing strict air pollution controls before 2035.

In addition, as was previously mentioned, the population in Yantai is currently densely distributed in the relatively high $PM_{2.5}$ concentration areas (**Figs 4 and 1A**). The population weighted $PM_{2.5}$ exposure (PWE) was 45.8 μg/m^3 in 2019. The noticeable reduction could be achieved with the implementation of energy-related measures and end-of-pipe controls. The PWE will likely decrease to 42.6 μg/m^3, 39.1 μg/m^3, and 24.7 μg/m^3 by 2030, 2035, and 2060, respectively, under the EEP pathway; and it will additionally decrease to 40.4 μg/m^3, 37.1 μg/m^3, and 23.2 μg/m^3 by 2030, 2035, and 2060, respectively, under the DCP pathway. Among all of the districts, the Laiyang (about 20%), Zhifu (about 18%), Fushan (about 11%), and Longkou (about 9%) districts will contribute the most to the PWE reduction, which will help to mitigate the $PM_{2.5}$ exposure in these densely populated districts.

4.4.3 Health benefit estimate and energy policy associated cost

To quantify the health benefits from improved $PM_{2.5}$ concentrations, we estimated the mortality avoided in Yantai under future pathways due to four diseases (COPD, IHD, LC, and stroke). Compared to the Baseline in 2019, about 332 (95% Confidence level - CI: 231 – 433), 712 (95% CI: 496 – 928), and 2634 (95% CI: 1833 – 3435) premature deaths could be avoided in Yantai in 2030, 2035, and 2060, respectively, owing to the decrease in $PM_{2.5}$ concentrations under the EEP pathway (**Table 4. 2**). The above results suggest that implementing low-carbon energy policies could bring important co-benefits in reducing $PM_{2.5}$ exposure and protecting human health.

In addition, we estimated the investment costs of implementing low-carbon energy policies. The investment costs will likely be 5.1 (95% CI: 3.3 – 7.0), 6.0 (95% CI: 4.6 – 9.7), and 11.9 (95% CI: 7.6 – 16.1) billion Chinese yuan (CNY) in 2030, 2035, and 2060 (**Table 4. 2**), respectively, to which the power plant and industry sectors contribute the most (more than 70%). On a per ton of CO_2 basis, our abatement cost was higher than those reported in other studies (Liang et al. 2019; Xing et al. 2020), likely due to the different assumptions made in the cost estimation of abatement technologies. The investment costs of implementing low-carbon energy policies might be considerable at the city level. However, the costs may be compensated for by the great benefits of energy policies in reducing mortality risk in monetary term. The human health benefit of avoided premature deaths due to $PM_{2.5}$ reduction is estimated to be 1.7 (95% CI: 1.0 – 2.5), 3.7 (95% CI: 2.1 – 5.4), and 13.8 (95% CI: 7.6 – 20.0) billion CNY in 2030, 2035, and 2060 (**Table 4. 2**), respectively, assuming a value of statistical life (VSL) of 5.24 (95% CI: 3.51 – 6.98) million CNY through a survey using willingness-to-pay method (Huang et al. 2017a). In 2060, the monetized co-benefit will likely exceed the investment cost, with a net-benefit of 1.9 billion CNY. However,

the investment costs are more than the health co-benefits in the short term, with net-benefit values of -3.4 and -2.2 billion CNY in 2030 and 2035, respectively (**Table 4. 2**).

Table 4. 2 Benefits and costs of the Energy policy pathway relative to the Baseline in 2019

Year	**2030**	**2035**	**2060**
CO_2 emission reduction (1E4 ton)	927	1561	5721
Mortality avoidance	332 (231, 433)	712 (496, 928)	2634 (1833, 3435)
Monetized co-benefit (1 billion CNY)	1.7 (1.0, 2.5)	3.7 (2.1, 5.4)	13.8 (7.6, 20.0)
Investment cost (1 billion CNY)	5.1 (3.3, 7.0)	6.0 (4.6, 9.7)	11.9 (7.6, 16.1)
Net Benefit (1 billion CNY)	-3.4 (-5.4, -1.4)	-2.2 (-5.0, 0.5)	1.9 (-5.6, 9.5)

Note: the numbers in paratheses represent the 95% confidence level.

4.5 Discussion

Chinese cities face the challenges of both climate change mitigation and air pollution reduction. Our study is one of the first attempts to propose a pathway to reach the dual targets of CO_2 emission reduction and air quality improvement at the city level, which is important for achieving China's climate and clean air goals since cities are the fundamental administrative units for implementing control policies (Chen et al. 2020a). The results of our study reveal that the air quality ($PM_{2.5}$ concentrations) will be greatly improved under the future pathways (the EEP and DCP pathways) in which end-of-pipe controls and energy-related measures are implemented, allowing Yantai to meet the national $PM_{2.5}$ standard. The advanced end-of-pipe controls will still be the main contributor to improving the air quality in the short term, accounting for about 50% of the $PM_{2.5}$ reduction before 2035; while the energy-related measures will have an increasing potential in the long term, accounting for 79% of the $PM_{2.5}$ reduction in 2060. In addition, low-carbon policies will play a critical role in mitigating CO_2 emissions. Under the EEP pathway, in which aggressive low-carbon energy policies are implemented, Yantai will reach the period of decline of CO_2 emission before 2030 and reach carbon neutrality around 2060. The implementation of low-carbon policies is necessary to achieve the dual targets, and thus should be prioritized considering the reduction potential of both CO_2 and air pollutants emissions in the future (Xing et al. 2020; Geng et al. 2021).

In addition to the city's local emission control, other measures are urgently needed to improve the air quality in Yantai, especially the control of emissions from regional transport. Regional transport makes an important contribution to the PM pollutions in many Chinese cities (Sun et al. 2017; Chang et al. 2019b). As indicated by our simulation results (**Appendix B.3**), regional

transport contributed to 34% of $PM_{2.5}$ concentrations in Yantai in 2019. Thus, the annual $PM_{2.5}$ concentrations in Yantai could be further improved by implementing strict control policies in surrounding areas simultaneously, as the regional joint prevention and control policies have resulted in remarkable improvement in air quality in recent years (State Council of the People's Republic of China 2013, 2018; Ministry of Ecology and Environment of the People's Republic of China 2017).

Meanwhile, more attention should be paid to the city-level uneven spatial distribution of $PM_{2.5}$ in Yantai. The national $PM_{2.5}$ standard will be exceeded by 42% and 6% in the Zhifu and Laiyang districts, respectively, in 2035, even with aggressive low-carbon energy policies and strict end-of-pipe controls. The high $PM_{2.5}$ concentration is likely due to the emissions from the industrial and transportation sectors since the industrial enterprises and major roadways are mainly distributed in these districts (**Figure 4. 1**). In addition, the heterogeneous distribution of $PM_{2.5}$ concentrations will have a greater effect on the dense population living in the abovementioned districts since they are suffering from unequal exposure to $PM_{2.5}$. It is suggested that the land space be reasonably planned to avoid major industrial enterprises in densely populated districts. Besides, specialized control and strict monitoring of the major emission sources are needed (Wu et al. 2021) to address the environmental inequity.

Chapter 5

Conclusions and Outlook

5.1 Conclusions

In this dissertation, we systematically assess air quality and CO_2 emission changes for all Chinese cities from 2015 to 2019 by using the city-level data of $PM_{2.5}$ and O_3 concentrations and CO_2 emissions. We select important regions for air pollution control in China and categorize all cities into different classes according to their development levels. Then we make comparisons for the changes of air quality and CO_2 emissions by region or city class. Overall, we find a remarkable reduction in $PM_{2.5}$ concentrations due to effective pollution control policies with mandatory city-level reduction targets, especially for cities in the BTH and YRD regions. Nonetheless, we find that O_3 concentrations increase in 91% of Chinese cities from 2015 to 2019. This is likely because of the ineffective control of VOCs emissions, which is a major O_3 precursor. Meanwhile, we find that CO_2 emissions increase in 69% of the cities and the changes show distinct patterns among different city classes. Our results suggest that the changes in CO_2 emissions are significantly lower in developed cities compared to developing cities, which is mainly driven by the reduction in energy intensity and the improvement in energy structure. Our findings indicate a lack of synergy in air quality improvement and CO_2 emission reduction in China. Therefore, to tackle the challenges of both air pollution and CO_2 mitigation, we suggest that cities set mandatory city-level CO_2 emission reduction targets and reinforce energy policies to address both challenges holistically in the future.

To design effective and simultaneous control strategies on air pollutants and CO_2, we develop a unified emission inventory that resolves the inconsistency in the structures and classification of current air pollutants and CO_2 emission inventories. We then map air pollutants and CO_2 emissions and identify the hotspots of both emissions at a high spatial resolution. We find that CO_2 and air pollutants emissions are mainly originated from the stationary combustion and the transportation sectors, suggesting that mitigations aiming at controlling the emissions of these two sectors would have great potential to achieve co-reductions. We also find that most CO_2 and air pollutants emissions are attributed to the top 10% hotspot grids in spatial. Therefore, specialized controls on these hotspot grids should be prioritized to lower the total emissions. Our method enables accurate identification of hotspots, and thus, improved the precision and efficiency could be achieved through site-specific management.

To investigate the pathway for Chinese cities to achieve the dual targets of CO_2 emission reduction and air quality improvement, we couple an integrated assessment model that combines emission projection, air quality, and health impact analysis. We find that city-level air quality and carbon neutrality targets are feasible through energy-related measures and end-of-pipe controls. Energy-related measures exhibit an increasing potential in reducing air pollutants and CO_2 emissions in the long run; while advanced end-of-pipe controls will contribute to improving the air quality in the short term. We also find that the health benefit from improved air quality will likely compensate for the implementation cost of energy-related measures. Our findings suggest that implementing energy-related measures is necessary to achieve the dual targets and should be prioritized in the future. Our findings provide important implications for other Chinese cities to tackle climate and air quality problems in the future.

5.2 Future work

5.2.1 Investigate the influencing factors of air pollutant concentration and CO_2 emission

In this dissertation project, we systematically assess the changes in CO_2 emission reduction and air quality improvement for Chinese cities. Our analysis is based on the CO_2 emissions and air pollutant concentration data in 2015 and 2019. In the city-level pathway analysis, we consider the impacts of local emission and regional transport on air pollutant concentrations. However, the impacts of other influencing factors, such as meteorology and population growth, are not considered. For example, future climate change and intense extreme events (such as stagnation and heat waves) will likely make the meteorological conditions unfavorable that may enhance air pollution levels (Hong et al. 2019). Therefore, future research could be designed to examine their respective influence on CO_2 emission reduction and air quality improvement to complement the current findings.

5.2.2 Investigate the uncertainties of the modeling results

Uncertainties originate from the emission inventory, the socioeconomic projection, the WRF-CMAQ model simulations, and the health impact analysis. Previous studies suggest that the uncertainties of China's GHG emissions and air pollutants emissions are in the range of 7.2% to 39.8% (Cai et al. 2019a) and 12% to 107% (Zhang et al. 2009; Lei et al. 2011), respectively. Emission inventories are subject to uncertainties due to the incompleteness of activity data and emission factors (Eggleston H.S. et al. 2016). The data quality could be further improved in the

future. Also, the WRF-CMAQ model simulations could introduce uncertainty due to complex meteorology and physical and chemical processes, which is extremely difficult to quantify (Mallet and Sportisse 2006; Wang et al. 2020). Besides, the uncertainty is associated with the health impact analysis. The epidemiologic data in Chinese cities might be different from the cohort yielding the relative risk parameters and probably introduce another uncertainty. In addition, the uncertainty could come from the monetized health values and investment cost of energy policies, such as the VSL and the interest rate. Future research could be designed to investigate the uncertainties comprehensively and lower the uncertainty of the estimates.

5.2.3 Investigate temporal variations in the spatial hotspots

In our hotpot analysis, we identify the high emission grids of CO_2 and air pollutants using annual emissions. Temporal variation in the spatial pattern of hotspots could also be very meaningful. For example, future studies could utilize our developed method to conduct the analysis over multiple years. Besides, future studies may focus on the seasonal variability of both CO_2 and air pollutants emissions in the industrial sector or the weekly variability of both emissions in the transportation sector, which could provide important implications in the collaborative control of both emissions.

Appendix A

Supplementary materials for Chapter 2

A.1 The air quality data and CO_2 emission data for 335 cities in China from 2015 to 2019.

Table A 1 Air pollutant concentrations and CO_2 emissions for 335 cities in China from 2015 to 2019

Name	City Number	Region	City Class	2015 $PM_{2.5}$ ($\mu g/m^3$)	2015 O_3 (ppb)	2015 CO_2 (1E4 ton)	2019 $PM_{2.5}$ ($\mu g/m^3$)	2019 O_3 (ppb)	2019 CO_2 (1E4 ton)
Baicheng	1	Other	4	58	59	1113	26	62	1567
Hulunbuir	2	Other	4	35	49	8116	17	55	7047
Tacheng	3	Other	5	20	55	1956	10	54	2075
Hegang	4	Other	5	47	54	1792	24	51	2952
Haixi	5	Other	5	27	71	1932	14	78	2202
Beijing	6	BTH	1	78	95	10410	42	98	10532
Longnan	7	Other	4	35	55	303	19	62	484
Heihe	8	Other	5	29	52	790	16	49	771
Dezhou	9	BTH	3	96	88	5205	53	102	4845
Zunyi	10	Other	3	36	51	2912	20	63	3628
Baoding	11	BTH	2	104	86	3899	58	104	4473
Langfang	12	BTH	3	82	80	1843	46	100	2660
Xilingol	13	Other	5	16	38	5590	9	63	7054
Naqu	14	Other	5	33	47	12	19	51	60
Huangnan	15	Other	5	38	55	43	22	60	55
Baishan	16	Other	5	50	62	2724	29	66	921
Hengshui	17	BTH	3	96	86	1341	56	98	1705
Pingliang	18	Other	4	41	57	2012	24	67	2521
Siping	19	Other	4	61	75	1945	36	77	2699
Aksu	20	Other	4	66	69	2552	39	67	2670
Harbin	21	Other	2	71	50	6415	42	59	7382
Changchun	22	Other	2	64	71	5021	38	69	6343
Tonghua	23	Other	4	48	63	1829	29	53	1732

Chifeng	24	Other	3	38	50	5487	23	65	5716
Shenyang	25	Other	2	71	73	5524	43	79	7140
Liaocheng	26	BTH	3	95	80	4695	58	107	7054
Anshan	27	Other	4	70	73	4198	43	79	4291
Altay	28	Other	5	13	52	274	8	65	568
Huzhou	29	YRD	4	52	89	2042	32	96	2658
Songyuan	30	Other	4	47	60	1743	29	62	1121
Qitaihe	31	Other	5	55	42	3553	34	57	1761
Meishan	32	Chengyu	4	58	78	859	36	78	1323
Kizilsu Kirghiz	33	Other	5	45	63	128	28	70	403
Dongying	34	Other	4	77	92	2251	48	105	3090
Huangshi	35	Other	4	64	69	2154	40	86	2725
Tongliao	36	Other	4	51	71	7200	32	68	6855
Jinhua	37	YRD	3	51	77	2011	32	81	2312
Kashgar	38	Other	3	102	56	1252	64	70	1345
Xinxiang	39	BTH	3	89	73	3378	56	95	3154
Ulanqab	40	Other	4	38	66	5039	24	78	5385
Xiaogan	41	Other	3	68	73	1434	43	88	2602
Zhangjiajie	42	Other	5	49	58	285	31	63	216
Neijiang	43	Chengyu	4	55	71	3671	35	72	1868
Zhengzhou	44	BTH	2	91	75	6196	58	99	5055
Wuhai	45	Other	5	47	62	4236	30	78	8905
Liaoyuan	46	Other	5	56	58	566	36	78	1003
Jingdezhen	47	Other	5	42	48	1686	27	68	2272
Hechi	48	Other	4	42	54	399	27	54	500
Ezhou	49	Other	5	65	80	1925	42	83	2222
Jinan	50	BTH	2	85	78	5924	55	103	7424

Changdu	51	Other	5	17	54	23	11	57	99
Ningbo	52	YRD	3	43	72	13322	28	77	9314
Enshi	53	Other	4	49	52	642	32	65	1085
Heze	54	BTH	2	90	77	3152	59	92	4427
Jiuquan	55	Other	5	38	62	847	25	69	1498
Tangshan	56	BTH	2	82	86	15663	54	97	22585
Daqing	57	Other	4	44	51	4270	29	60	3052
Jilin	58	Other	3	57	72	5870	38	69	4324
Suizhou	59	Other	4	63	69	363	42	82	622
Ali	60	Other	5	12	49	12	8	62	54
Jinchang	61	Other	5	30	63	1081	20	69	1184
Hainan	62	Other	5	30	72	155	20	74	150
Xingtai	63	BTH	2	97	66	2790	65	107	6010
Wuhan	64	Other	2	67	80	7705	45	94	6435
Wuxi	65	YRD	3	58	80	5590	39	93	7032
Nantong	66	YRD	2	55	79	5203	37	80	5286
Zibo	67	BTH	3	86	86	6748	58	105	6365
Zhongwei	68	Other	5	43	66	1121	29	72	1402
Haibei	69	Other	5	28	72	482	19	75	231
Guoluo	70	Other	5	28	65	61	19	71	145
Western Hunan	71	Other	4	44	50	365	30	59	596
Zigong	72	Chengyu	4	66	56	449	45	79	809
Wenzhou	73	YRD	2	41	70	3115	28	70	3413
Wuzhong	74	Other	5	41	63	3086	28	74	2423
Benxi	75	Other	5	54	64	2462	37	69	3560
Hinggan	76	Other	5	35	55	1110	24	58	1229
Jingzhou	77	Other	3	67	81	1380	46	81	1692
Shigatse	78	Other	5	16	53	5	11	70	82

Shuangyashan	79	Other	5	42	47	1926	29	52	1645
Taizhou	80	YRD	3	39	69	2645	27	74	4012
Xianning	81	Other	4	52	81	1519	36	87	1925
Lishui	82	YRD	4	36	62	651	25	69	701
Liaoyang	83	Other	5	59	70	2192	41	72	1955
Turpan	84	Other	5	66	54	1259	46	67	1483
Binzhou	85	BTH	4	76	70	15595	53	107	13423
Chenzhou	86	Other	3	43	59	1650	30	72	1750
Hefei	87	YRD	2	63	53	3050	44	86	3966
Shanghai	88	YRD	1	50	76	22098	35	77	17732
Jiaxing	89	YRD	4	50	86	3943	35	87	4812
Mudanjiang	90	Other	4	47	57	1740	33	53	1408
Hangzhou	91	YRD	2	54	79	4460	38	93	3661
Liupanshui	92	Other	4	34	36	5422	24	56	7704
Lhasa	93	Other	5	17	67	69	12	66	138
Suzhou	94	YRD	2	55	79	12998	39	88	15757
Dandong	95	Other	4	45	56	1420	32	65	1564
Zhoushan	96	YRD	5	28	67	2169	20	67	1860
Pingxiang	97	Other	5	56	58	1219	40	80	1465
Zaozhuang	98	Other	4	84	84	3992	60	98	5157
Pingdingshan	99	Other	3	84	81	9202	60	95	4458
Huanggang	100	Other	3	56	77	1636	40	86	1656
Baoshan	101	Other	4	28	58	379	20	65	418
Xinyang	102	Other	3	67	68	1568	48	88	1509
Jining	103	BTH	2	78	81	9403	56	100	7604
Zhoukou	104	Other	2	78	59	864	56	92	1046
Suining	105	Chengyu	4	43	77	427	31	69	676
Yinchuan	106	Other	4	43	58	11189	31	75	13751

Yanbian	107	Other	4	36	55	1474	26	59	1651
Guilin	108	Other	3	47	65	865	34	70	1147
Chengde	109	Other	4	40	83	3514	29	84	4191
Baise	110	Other	4	40	55	1800	29	59	2336
Huangshan	111	YRD	5	33	37	333	24	72	371
Bortala	112	Other	5	33	40	268	24	66	558
Shaoxing	113	YRD	3	52	76	2729	38	81	3288
Zhaotong	114	Other	3	26	64	1026	19	67	1423
Zhumadian	115	Other	3	71	78	1819	52	92	1587
Cangzhou	116	BTH	2	68	79	4318	50	95	6026
Qiqihar	117	Other	3	38	51	2639	28	51	4226
Nanjing	118	YRD	2	54	80	7947	40	93	8015
Shijiazhuang	119	BTH	2	85	70	11385	63	106	8999
Ma'anshan	120	YRD	4	58	67	4113	43	91	4113
Linxia	121	Other	4	39	63	278	29	65	327
Chongqing	122	Chengyu	1	51	59	16226	38	80	13445
Tieling	123	Other	4	55	68	3654	41	76	3729
Luzhou	124	Chengyu	3	55	57	1680	41	75	1607
Tianjin	125	BTH	1	68	67	17662	51	103	14461
Huaihua	126	Other	3	48	58	879	36	67	788
Nanchong	127	Chengyu	3	56	46	679	42	66	1015
Chengdu	128	Chengyu	1	57	86	6578	43	82	4848
Yan'an	129	Other	4	41	68	3011	31	73	1415
Handan	130	BTH	2	87	66	11355	66	103	9449
Yichun	131	Other	5	29	49	720	22	48	842
Taizhou	132	YRD	3	58	78	3013	44	90	3600
Lu'an	133	YRD	3	54	43	994	41	74	1124
Dalian	134	Other	3	46	75	5994	35	79	7004

Liuzhou	135	Other	4	46	65	2465	35	68	3187
Ganzhou	136	Other	2	38	56	1227	29	80	2127
Shiyan	137	Other	4	51	52	1067	39	72	1131
Shantou	138	Other	3	30	66	2153	23	75	2676
Shangqiu	139	Other	2	73	74	5005	56	88	1867
Jiaozuo	140	BTH	4	82	70	3706	63	102	2745
Xuchang	141	Other	3	78	77	2808	60	92	1923
Linyi	142	Other	2	74	89	5609	57	97	6260
Kumul	143	Other	5	35	29	3369	27	60	4234
Heyuan	144	Other	4	31	64	771	24	67	1116
Bayannur	145	Other	5	40	65	1789	31	73	2630
Chaozhou	146	Other	4	36	76	1655	28	75	2096
Luohe	147	Other	4	77	84	863	60	93	847
Rizhao	148	Other	4	59	75	2735	46	85	3797
Dazhou	149	Chengyu	3	59	51	1725	46	65	2111
Panjin	150	Other	5	50	77	5806	39	80	1685
Qingdao	151	Other	2	50	69	6304	39	78	4307
Ankang	152	Other	4	50	60	400	39	63	422
Shangrao	153	Other	3	41	57	1595	32	75	1913
Loudi	154	Other	4	51	56	3030	40	77	3780
Huai'an	155	YRD	3	56	77	3419	44	83	2904
Ganzi	156	Other	5	14	46	244	11	48	299
Fuxin	157	Other	5	47	65	2075	37	77	1740
Yichang	158	Other	3	66	57	2766	52	83	2772
Dingxi	159	Other	4	33	62	398	26	66	579
Xinzhou	160	Other	4	52	60	3015	41	88	4142
Nanning	161	Other	2	38	55	1403	30	65	2030
Guang'an	162	Chengyu	4	43	74	1883	34	70	1206

Baiyin	163	Other	5	34	57	1712	27	61	1863
Hotan	164	Other	4	78	55	477	62	62	502
Yongzhou	165	Other	3	49	60	986	39	73	859
Shaoyang	166	Other	2	54	63	980	43	75	1339
Suqian	167	YRD	3	59	73	912	47	92	757
Sanmenxia	168	FWP	4	69	69	4118	55	83	3444
Quzhou	169	YRD	4	40	71	2336	32	72	2180
Wuhu	170	YRD	4	55	33	2853	44	89	3312
Zhangye	171	Other	5	35	67	626	28	71	670
Guyuan	172	Other	5	30	57	663	24	66	600
Zhenjiang	173	YRD	4	56	87	4539	45	94	5024
Lianyungang	174	YRD	3	52	75	3258	42	86	2445
Nanping	175	Other	4	26	52	1254	21	64	1301
Shanwei	176	Other	4	26	63	1610	21	73	2017
Dali	177	Other	4	21	53	728	17	62	875
Shizuishan	178	Other	5	42	73	6719	34	77	2952
Jinzhou	179	Other	4	58	75	1791	47	80	1760
Hezhou	180	Other	4	37	48	957	30	65	779
Weifang	181	Other	2	69	91	6374	56	95	8029
Yancheng	182	YRD	2	48	77	3489	39	81	4142
Meizhou	183	Other	3	32	56	2217	26	67	1868
Chuzhou	184	YRD	3	59	30	945	48	86	1664
Bayingolin	185	Other	5	43	53	1270	35	60	1931
Gannan	186	Other	5	27	65	130	22	62	205
Anyang	187	BTH	3	87	70	3291	71	104	3369
Puyang	188	BTH	4	77	69	1150	63	96	1084
Guiyang	189	Other	3	33	56	3207	27	64	2771
Hengyang	190	Other	2	51	64	1780	42	75	1870

Leshan	191	Chengyu	4	51	63	1784	42	68	2048
Changzhou	192	YRD	3	57	77	2908	47	93	3121
Changsha	193	Other	2	57	69	1506	47	88	1877
Yangzhou	194	YRD	3	52	83	2975	43	91	3746
Chongzuo	195	Other	4	35	63	538	29	61	566
Zhangjiakou	196	Other	3	30	75	5384	25	83	6310
Alxa	197	Other	5	30	68	1406	25	75	2682
Suzhou	198	YRD	3	60	54	1436	50	92	2103
Xiangyang	199	Other	3	72	73	1959	60	83	2463
Guangzhou	200	PRD	1	36	68	5425	30	91	5445
Foshan	201	PRD	2	36	66	2990	30	95	3587
Maoming	202	Other	3	30	59	1581	25	77	1525
Deyang	203	Chengyu	4	48	73	1057	40	75	1033
Tianshui	204	Other	4	36	60	578	30	65	539
Yushu	205	Other	5	12	54	144	10	59	162
Urumqi	206	Other	4	60	57	5289	50	65	5284
Bengbu	207	YRD	4	61	60	1595	51	79	1632
Haidong	208	Other	5	43	65	583	36	71	661
Wenshan	209	Other	4	31	58	618	26	60	986
Shangluo	210	Other	4	38	65	365	32	71	450
Jiangmen	211	PRD	3	32	69	2643	27	101	3574
Yantai	212	Other	2	45	71	5667	38	83	6783
Jingmen	213	Other	4	66	64	1611	56	83	2261
Haikou	214	Other	4	20	48	188	17	74	391
Wuwei	215	Other	5	34	58	489	29	69	657
Nanchang	216	Other	3	41	62	1818	35	77	1885
Changzhi	217	BTH	4	55	75	3940	47	96	6433
Tongling	218	YRD	5	55	49	2499	47	77	2843

Ningde	219	Other	4	28	58	1634	24	63	2259
Lanzhou	220	Other	4	42	62	5360	36	77	2751
Kaifeng	221	BTH	3	71	62	1614	61	97	1178
Yueyang	222	Other	3	50	72	3464	43	84	2721
Weihai	223	Other	4	36	69	2426	31	86	2154
Jieyang	224	Other	3	36	65	1794	31	75	1863
Putian	225	Other	4	29	56	874	25	71	1895
Zhuhai	226	PRD	4	29	67	2157	25	86	1949
Baotou	227	Other	4	44	70	7792	38	73	9284
Tai'an	228	Other	3	66	81	6168	57	97	3819
Fushun	229	Other	4	52	70	5988	45	81	2807
Shuozhou	230	Other	5	45	88	3992	39	81	4963
Karamay	231	Other	5	30	57	3904	26	65	1251
Fuzhou	232	Other	4	38	64	936	33	80	1753
Great Khingan	233	Other	5	23	44	295	20	50	219
Nanyang	234	Other	2	69	68	2559	60	93	2580
Zhongshan	235	PRD	4	31	68	1475	27	101	1595
Ji'an	236	Other	3	39	51	1333	34	78	1538
Laibin	237	Other	4	40	56	1010	35	74	1411
Qinzhou	238	Other	4	33	57	3245	29	64	2213
Jiayuguan	239	Other	5	25	67	2693	22	71	2307
Dehong	240	Other	5	26	65	111	23	62	223
Hanzhong	241	Other	4	52	64	917	46	62	964
Yibin	242	Chengyu	3	53	58	2289	47	75	2163
Fuzhou	243	Other	2	27	56	4771	24	71	4947
Xiamen	244	Other	3	27	45	1424	24	70	1418
Sanming	245	Other	4	27	40	2196	24	61	2648
Shenzhen	246	PRD	2	27	60	3404	24	80	3857

Zhaoqing	247	PRD	3	36	69	1404	32	84	2269
Qinhuangdao	248	Other	4	46	51	2456	41	93	4157
Xuancheng	249	YRD	4	46	47	1069	41	69	1407
Yingkou	250	Other	4	48	86	3154	43	85	4549
Guigang	251	Other	3	39	60	1535	35	73	1758
Ziyang	252	Chengyu	4	39	74	604	35	75	706
Jinzhong	253	FWP	4	50	58	4807	45	98	5978
Anqing	254	YRD	3	50	38	2404	45	85	2410
Chaoyang	255	Other	4	41	43	2505	37	80	2480
Jiamusi	256	Other	4	31	54	1558	28	53	1371
Huludao	257	Other	4	52	75	2786	47	81	2804
Zhuzhou	258	Other	4	52	66	1027	47	83	1738
Tongchuan	259	FWP	5	52	62	1561	47	81	1055
Xiangtan	260	Other	4	53	68	3589	48	86	2564
Zhangzhou	261	Other	3	32	46	3642	29	73	3657
Wuzhou	262	Other	4	33	54	294	30	66	668
Hebi	263	BTH	5	67	68	3018	61	101	1398
Luoyang	264	FWP	3	68	63	7302	62	96	4129
Qujing	265	Other	3	23	63	4624	21	73	5810
Bozhou	266	YRD	3	58	53	506	53	90	1314
Datong	267	Other	4	35	65	5886	32	75	5236
Xining	268	Other	4	37	59	2088	34	66	1704
Xuzhou	269	YRD	2	62	72	7904	57	92	7406
Mianyang	270	Chengyu	3	41	65	1227	38	70	1539
Lvliang	271	FWP	4	42	52	1936	39	84	9210
Honghe	272	Other	3	28	63	2810	26	69	2913
Fangchenggang	273	Other	5	29	49	1258	27	65	2183
Sanya	274	Other	5	15	53	166	14	60	308

Shaoguan	275	Other	4	31	63	2525	29	74	3518
Yunfu	276	Other	4	31	42	1397	29	71	1502
Ya'an	277	Chengyu	5	32	37	452	30	67	654
Xinyu	278	Other	5	37	42	1917	35	74	585
Yulin	279	Other	3	37	60	785	35	68	865
Yichun	280	Other	3	38	50	3455	36	79	4290
Yingtan	281	Other	5	39	64	829	37	81	1093
Liangshan	282	Other	3	21	65	1220	20	74	1449
Ordos	283	Other	4	23	74	12528	22	79	21026
Longyan	284	Other	4	23	56	1850	22	60	2309
Jiujiang	285	Other	3	48	63	2000	46	77	4139
Anshun	286	Other	4	24	62	1128	23	60	1372
Quanzhou	287	Other	2	26	57	4648	25	74	5122
Beihai	288	Other	5	27	62	685	26	73	909
Qiandongnan	289	Other	4	27	50	1370	26	54	1604
Huaibei	290	YRD	4	56	80	8668	54	95	3468
Yangjiang	291	Other	4	29	68	1546	28	79	1890
Qingyang	292	Other	4	31	59	390	30	68	501
Dongguan	293	PRD	2	33	80	5980	32	98	5047
Bazhong	294	Other	4	33	60	273	32	56	648
Hohhot	295	Other	4	38	68	5933	37	75	7610
Yuncheng	296	FWP	3	61	72	6563	61	93	6998
Suihua	297	Other	3	36	56	1008	36	59	1539
Changde	298	Other	3	48	66	1551	48	82	1774
Zhanjiang	299	Other	2	26	65	3042	26	80	3832
Huizhou	300	PRD	3	25	65	4705	25	74	2923
Qiannan	301	Other	4	19	56	1461	19	59	1642
Lijiang	302	Other	5	11	50	296	11	59	291

Linzhi	303	Other	5	7	54	1	7	56	70
Shannan	304	Other	5	10	54	39	10	64	65
Baoji	305	FWP	4	51	63	2273	51	71	1939
Weinan	306	FWP	3	56	62	3387	56	87	5228
Taiyuan	307	BTH	3	55	62	7845	56	95	6822
Qingyuan	308	Other	4	31	57	1955	32	78	2859
Bijie	309	Other	3	25	51	3754	26	64	7160
Fuyang	310	YRD	2	49	54	1931	51	90	1530
Jincheng	311	BTH	4	51	44	2085	54	103	4829
Huainan	312	YRD	4	50	54	5613	53	89	6149
Yulin	313	Other	4	33	67	16897	35	81	15205
Yangquan	314	BTH	5	48	62	1948	51	95	1669
Xi'an	315	FWP	2	53	68	2679	57	85	2095
Jixi	316	Other	5	28	44	1576	31	42	2436
Kunming	317	Other	3	23	52	2711	26	69	2155
Yili	318	Other	3	37	56	2227	42	63	4205
Xianyang	319	FWP	3	58	65	3338	66	83	1992
Aba	320	Other	5	14	40	249	16	56	343
Linfen	321	FWP	3	54	53	16467	62	105	6700
Yiyang	322	Other	3	47	71	1267	54	77	1311
Panzhihua	323	Other	5	26	55	1947	30	72	2051
Diqing	324	Other	5	11	36	74	13	59	74
Xishuangbanna	325	Other	5	26	62	186	31	68	260
Pu'er	326	Other	4	20	58	370	24	72	534
Chuxiong	327	Other	4	17	40	594	21	66	802
Tongren	328	Other	4	25	54	1089	31	62	998
Qianxinan	329	Other	4	16	43	1847	20	59	2299
Chizhou	330	YRD	5	33	49	1073	42	88	1056

Yuxi	331	Other	4	18	41	1524	23	72	814
Changji	332	Other	5	44	53	7400	57	63	17919
Guangyuan	333	Other	4	21	64	789	28	52	876
Lincang	334	Other	4	23	51	251	31	68	339
Nujiang	335	Other	5	18	45	65	25	52	72

A.2 The comparison of CO_2 emission changes between China's pilot low-carbon cities and non-pilot cities

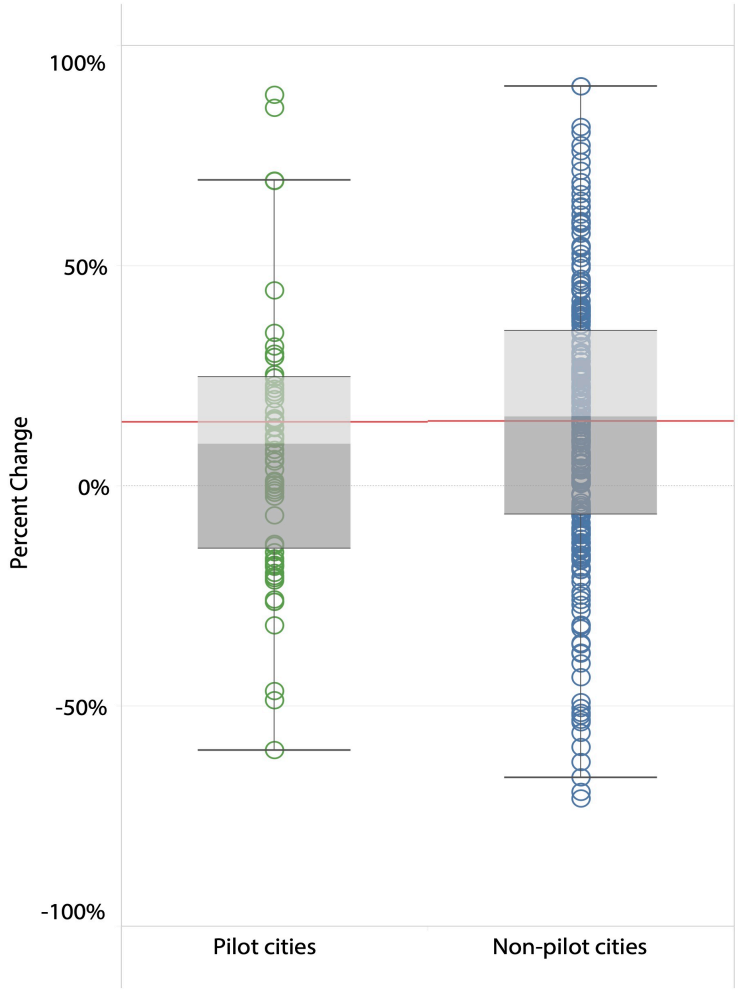

Figure A 1 The comparison of percent changes of CO_2 emissions for China's pilot low-carbon cities and non-pilot cities

Appendix B

Supplementary materials for Chapter 4

B.1 Socioeconomic projection in Yantai

GDP and the population are two important inputs for the CAEP-CP model. The GDP and population in base year 2019 was obtained from Yantai's statistical yearbook (National Bureau of Statistics 2020b). The future projection of GDP and population referred to the city, provincial or national plans (People's Government of Shandong 2021; People's Government of Yantai 2021). The projection results of GDP and population were compared in **Table B 1**. In Chapter 4, the growth rate of the GDP was set at 5.0%, 4.5%, 3.7%, 2.0%, and 1.5% during 2020 – 2025, 2025 – 2030, 2030 – 2035, 2035 – 2050, and 2050 – 2060, respectively. The growth rate of the population was set at 0.24%, 0.08%, -0.06%, -0.28%, and -0.75% during 2020 – 2025, 2025 – 2030, 2030 – 2035, 2035 – 2050, and 2050 – 2060, respectively.

Table B 1 Predictions of the (A) GDP growth rate and (B) population growth rate in Yantai city

(A) GDP growth rate (%) (SSP 2017; OECD 2021; People's Government of Shandong 2021; People's Government of Yantai 2021)

Studies	2020–2025	2025–2030	2030–2035	2035–2050	2050–2060
Yantai 14th five-year plan	5.0	N/A	N/A	N/A	N/A
Provincial 14th five-year plan	5.5	N/A	N/A	N/A	N/A

Organisation for Economic Co-operation and Development	4.4	3.5	2.7	1.7	1.4
SSP database	6.0	4.3	3.0	1.8	0.8
CAEP	5.5	5.0	4.2	2.2	1.6
This study	5.0	4.5	3.7	2.0	1.5

(B) population growth rate (%) (United Nations 2019; IEA 2021; OECD 2021; World Bank 2021)

Studies	2020–2025	2025–2030	2030–2035	2035–2050	2050–2060
United Nation	0.26	0.08	-0.04	-0.27	-0.50
International Energy Agency	0.25	0.10	-0.04	-0.27	N/A
World Bank	0.24	0.07	-0.06	-0.30	N/A
Organisation for Economic Co-operation and Development	0.10	-0.06	-0.22	-0.30	-1.13
This study	0.24	0.08	-0.06	-0.28	-0.75

B.2 Key characteristics of three pathway for projecting future emissions in Yantai

All pathways were projected under the same socioeconomic assumptions but different assumptions of energy policies and end-of-pipe controls. The key characteristics of the three pathways are summarized in detail in **Table B 2**.

Table B 2 Key assumptions of the pathways in Yantai city

<table>
<tr><th>Sector</th><th>BAU</th><th>EEP</th><th>DCP</th></tr>
<tr><td rowspan="3">Power</td><td colspan="3">▪ Reduce coal power plants
▪ Develop renewable energy power plants
▪ Reduce coal consumption
▪ Apply ultralow emission standard to existing coal power plants</td></tr>
<tr><td></td><td colspan="2">▪ More strict control on coal consumption
▪ Improve the efficiency of electricity generation
▪ Increase the capacity of renewable energy power plants, such as offshore wind and photovoltaic</td></tr>
<tr><td></td><td></td><td>▪ Apply the maximal desulfurization and denitrification controls</td></tr>
<tr><td>Industry</td><td colspan="3">▪ Control the industrial productions, such as cement, non-ferrous metal, and plate glass
▪ Eliminate and upgrade on the industrial boilers and kilns
▪ Control on coal consumption
▪ Apply the ultralow emission standard to key industries</td></tr>
</table>

		▪ Replace coal by natural gas and electricity ▪ More strict control on coal consumption ▪ Improve the efficiency of industrial productions and decrease the energy intensity	
			▪ Apply the maximal ultralow emission standard to industries, including desulfurization, denitrification, and dedusting controls
Building	▪ Promote the design standard for energy efficiency of new buildings, public buildings, and existing building reconstruction		
		▪ Increase the implementation of clean heating, especially in urban areas ▪ Increase the proportion of clean coal use ▪ Increase the construction of natural gas pipeline network in rural areas ▪ Decrease the energy intensity of buildings	
			▪ Apply advanced cookstoves with low emissions
Transport	▪ Improve the management on on-road, off-road, and waterway transport.		
		▪ Replace the freight service from on-road transport to railway and waterway transport ▪ Promote the fuel substitution to clean and new-energy vehicles ▪ Promote the use of shore power for waterway transport ▪ Eliminate the outdated vehicles and ships	

			▪ Improve the oil quality for vehicles ▪ Apply advanced emission standard for vehicles and ships

Note: BAU represents the Business-as-Usual pathway, EEP represents the Enhanced Energy pathway, and DCP represents the Dual Control pathway.

B.3 Contributions from local emission and regional transport in Yantai

We categorized the emissions affecting the $PM_{2.5}$ in Yantai into two groups: Yantai local emissions and emissions from surrounding areas, excluding Yantai. Three emission inventories were then developed. Inventory 1, the baseline inventory, included both Yantai local emissions and emissions from surrounding areas. Inventory 2, the hypothetical emission inventory, included the Yantai local emissions only and turned off the emissions from surrounding areas. Inventory 3, the hypothetical emission inventory, included the emissions from surrounding areas only and turned off the Yantai local emissions.

We simulated the $PM_{2.5}$ concentrations in 2019 based on the above three inventories using the WRF-CMAQ model. Then, we compared the $PM_{2.5}$ concentrations between the baseline inventory and each of the hypothetical inventory and calculated the relative contribution of each emission group to total $PM_{2.5}$ concentration. Our results showed that the local emissions and emissions from regional transport contributed to 70% and 34% of the $PM_{2.5}$ concentration in Yantai in 2019, respectively. The simple add-up of the relative contributions of two emission groups was not 100% because of the nonlinear emission-concentration relationship.

B.4 Sectoral contributions to air pollutants and CO_2 emissions in Yantai

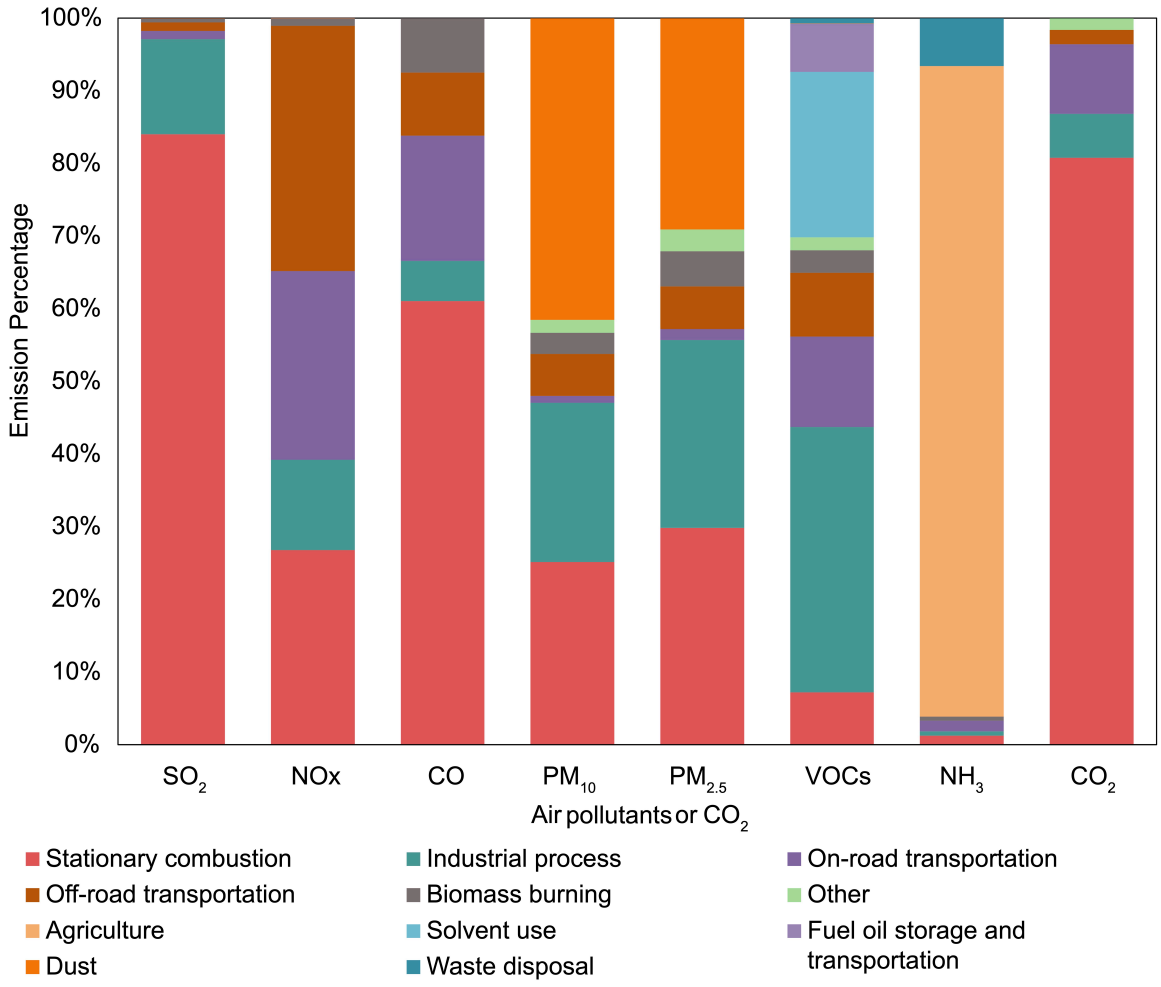

Figure B 1 Sectoral contribution to air pollutants and CO_2 emissions in Yantai in 2019

References

Ang BW (2005) The LMDI approach to decomposition analysis: a practical guide. Energy Policy 33:867–871. https://doi.org/10.1016/J.ENPOL.2003.10.010

Bai L, Lu X, Yin S, et al (2020) A recent emission inventory of multiple air pollutant, $PM_{2.5}$ chemical species and its spatial-temporal characteristics in central China. J Clean Prod 269:122114. https://doi.org/10.1016/j.jclepro.2020.122114

BP (2021) Statistical Review of World Energy. https://www.bp.com/en/global/corporate/energy-economics/statistical-review-of-world-energy.html. Accessed 22 Feb 2021

Brunekreef B, Holgate ST (2002) Air pollution and health. Lancet 360:1233–1242. https://doi.org/10.1016/S0140-6736(02)11274-8

Burnett R, Chen H, Szyszkowicz M, et al (2018) Global estimates of mortality associated with long-term exposure to outdoor fine particulate matter. Proc Natl Acad Sci U S A 115:9592–9597. https://doi.org/10.1073/pnas.1803222115

Burnett RT, PopeIII CA, Ezzati M, et al (2014) An Integrated Risk Function for Estimating the Global Burden of Disease Attributable to Ambient Fine Particulate Matter Exposure. Environ Health Perspect 122:397–403. https://doi.org/10.1289/EHP.1307049

C40 (2018) 27 Cities Have Reached Peak Greenhouse Gas Emissions whilst Populations Increase and Economies Grow. https://www.c40.org/press_releases/27-cities-have-reached-peak-greenhouse-gas-emissions-whilst-populations-increase-and-economies-grow. Accessed 18 May 2021

C40 Cities (2021) C40 Open Data Portal. https://www.c40.org/research/open_data. Accessed 18 Mar 2021

Cai B, Cao L, Lei Y, et al (2021a) China's carbon emission pathway under the carbon neutrality target (In Chinese). China Popul Environ 31:7–14. https://doi.org/10.12062/cpre.20210101

Cai B, Cui C, Zhang D, et al (2019a) China city-level greenhouse gas emissions inventory in 2015 and uncertainty analysis. Appl Energy 253:113579. https://doi.org/10.1016/j.apenergy.2019.113579

Cai B, Guo H, Ma Z, et al (2019b) Benchmarking carbon emissions efficiency in Chinese cities: A comparative study based on high-resolution gridded data. Appl Energy 242:994–1009. https://doi.org/10.1016/j.apenergy.2019.03.146

Cai B, Liang S, Zhou J, et al (2018a) China high resolution emission database (CHRED) with point emission sources, gridded emission data, and supplementary socioeconomic data.

Resour Conserv Recycl 129:232–239. https://doi.org/10.1016/j.resconrec.2017.10.036

Cai B, Zhang L, Xia C, et al (2021b) A new model for China's CO_2 emission pathway using the top-down and bottom-up approaches (In Press). Chinese J Popul Resour Environ

Cai S, Li Q, Wang S, et al (2018b) Pollutant emissions from residential combustion and reduction strategies estimated via a village-based emission inventory in Beijing. Environ Pollut 238:230–237. https://doi.org/10.1016/j.envpol.2018.03.036

Cai S, Wang Y, Zhao B, et al (2017) The impact of the "Air Pollution Prevention and Control Action Plan" on $PM_{2.5}$ concentrations in Jing-Jin-Ji region during 2012–2020. Sci Total Environ 580:197–209. https://doi.org/10.1016/j.scitotenv.2016.11.188

CAS Institute of Geographic Sciences and Natural Resources Research (2021) Resource and Environment Science and Data Center. http://www.resdc.cn/. Accessed 7 Nov 2019

CCG (2020) China City Greenhouse Gas Working group. http://www.cityghg.com/. Accessed 30 Dec 2020

CDP (2021) Carbon Disclosure Project Data. https://www.cdp.net/zh/data. Accessed 18 Mar 2021

Chang X, Wang S, Zhao B, et al (2019a) Contributions of inter-city and regional transport to PM2.5 concentrations in the Beijing-Tianjin-Hebei region and its implications on regional joint air pollution control. Sci Total Environ 660:1191–1200. https://doi.org/10.1016/J.SCITOTENV.2018.12.474

Chang X, Wang S, Zhao B, et al (2019b) Contributions of inter-city and regional transport to $PM_{2.5}$ concentrations in the Beijing-Tianjin-Hebei region and its implications on regional joint air pollution control. Sci Total Environ 660:1191–1200. https://doi.org/10.1016/j.scitotenv.2018.12.474

Chen H, Chen W, He J (2020a) Pathway to meet carbon emission peak target and air quality standard for China (In Chinese). China Popul Environ 30:12–18

Chen L, Zhu J, Liao H, et al (2020b) Meteorological influences on $PM_{2.5}$ and O_3 trends and associated health burden since China's clean air actions. Sci Total Environ 744:140837. https://doi.org/10.1016/j.scitotenv.2020.140837

China Ministry of Ecology and Environment (2018) China Second Biennial Update Report on Climate Change. https://unfccc.int/sites/default/files/resource/China 2BUR_English.pdf. Accessed 15 Sep 2021

China National Environmental Monitoring Centre (2021) Real-time data. http://www.cnemc.cn/sssj/. Accessed 30 Dec 2020

CHRED (2020) China high spatial resolution grid data. https://wxccg.cityghg.com/geo/#!g_vs=!13000248.55768378 3!4831691.550907453!1031.991808400932!0. Accessed 18 Feb 2021

Climate Ambition Summit (2020) Climate Ambition Summit 2020. https://www.climateambitionsummit2020.org/index.php#home. Accessed 18 Feb 2021

Crippa M, Guizzardi D, Muntean M, et al (2018) Gridded emissions of air pollutants for the period 1970-2012 within EDGAR v4.3.2. Earth Syst. Sci. Data 10:1987–2013

Crippa M, Solazzo E, Huang G, et al (2020) High resolution temporal profiles in the Emissions Database for Global Atmospheric Research. Sci Data 7:1–17. https://doi.org/10.1038/s41597-020-0462-2

D'Avignon A, Carloni FA, Rovere EL La, Dubeux CBS (2010) Emission inventory: An urban public policy instrument and benchmark. Energy Policy 38:4838–4847. https://doi.org/10.1016/j.enpol.2009.10.002

Deng HM, Liang QM, Liu LJ, Anadon LD (2017) Co-benefits of greenhouse gas mitigation: A review and classification by type, mitigation sector, and geography. Environ Res Lett 12:123001. https://doi.org/10.1088/1748-9326/aa98d2

Development and Reform Commission of Shenzhen Municipality (2012) Notice on issuing the mid-term and long-term plan for low-carbon development in Shenzhen (2011-2020). http://fgw.sz.gov.cn/zwgk/ghjh/zxgh/content/post_4561905.html. Accessed 18 Feb 2021

Ding D, Xing J, Wang S, et al (2019) Estimated Contributions of Emissions Controls, Meteorological Factors, Population Growth, and Changes in Baseline Mortality to Reductions in Ambient $PM_{2.5}$ and $PM_{2.5}$-Related Mortality in China, 2013-2017. Environ Health Perspect 127:67009. https://doi.org/10.1289/EHP4157

Dong H, Dai H, Dong L, et al (2015) Pursuing air pollutant co-benefits of CO_2 mitigation in China: A provincial leveled analysis. Appl Energy 144:165–174. https://doi.org/10.1016/j.apenergy.2015.02.020

Dunn OJ (1964) Multiple Comparisons Using Rank Sums. Technometrics 6:241–252

Eggleston H.S., L. B, K. M, et al (2016) IPCC 2006, 2006 IPCC Guidelines for National Greenhouse Gas Inventories, Prepared by the National Greenhouse Gas Inventories Programme

Ge B, Wang Z, Lin W, et al (2018) Air pollution over the North China Plain and its implication of regional transport: A new sight from the observed evidences. Environ Pollut 234:29–38. https://doi.org/10.1016/J.ENVPOL.2017.10.084

Geng G, Zheng Y, Zhang Q, et al (2021) Drivers of $PM_{2.5}$ air pollution deaths in China 2002–

2017. Nat Geosci 14:645–650. https://doi.org/10.1038/s41561-021-00792-3

Glazier RH, Creatore MI, Gozdyra P, et al (2004) Geographic methods for understanding and responding to disparities in mammography use in Toronto, Canada. J Gen Intern Med 19:952–961. https://doi.org/10.1111/j.1525-1497.2004.30270.x

Hartigan JA, Wong MA (1979) Algorithm AS 136: A K-Means Clustering Algorithm. Appl Stat 28:100. https://doi.org/10.2307/2346830

He K, Lei Y, Pan X, et al (2010) Co-benefits from energy policies in China. Energy 35:4265–4272. https://doi.org/10.1016/j.energy.2008.07.021

Hong C, Zhang Q, Zhang Y, et al (2019) Impacts of climate change on future air quality and human health in China. Proc Natl Acad Sci 116:17193–17200. https://doi.org/10.1073/PNAS.1812881116

Huang D, Andersson H, Zhang S (2017a) Willingness to pay to reduce health risks related to air quality: evidence from a choice experiment survey in Beijing. J Environ Plan Manag 61:2207–2229. https://doi.org/10.1080/09640568.2017.1389701

Huang J, Pan X, Guo X, et al (2017b) Health impact of China's Air Pollution Prevention and Control Action Plan: an analysis of national air quality monitoring and mortality data. Lancet Planet Heal 2:e313–e323. https://doi.org/10.1016/S2542-5196(18)30141-4

Huang L, Zhu Y, Zhai H, et al (2021) Recommendations on benchmarks for numerical air quality model applications in China - Part 1: $PM_{2.5}$ and chemical species. Atmos Chem Phys 21:2725–2743. https://doi.org/10.5194/ACP-21-2725-2021

IEA (2021) Net Zero by 2050. https://www.iea.org/reports/net-zero-by-2050#

IPCC (2019) 2019 Refinement to the 2006 IPCC Guidelines for National Greenhouse Gas Inventories. https://www.ipcc.ch/report/2019-refinement-to-the-2006-ipcc-guidelines-for-national-greenhouse-gas-inventories/. Accessed 28 Dec 2020

Jiang H, Duan Y, Zhang Z, et al (2021) Study on peak CO_2 emissions of typical large cities in China (in Chinese). Clim Chang Res 2.

Jiang P, Chen X, Li Q, et al (2020) High-resolution emission inventory of gaseous and particulate pollutants in Shandong Province, eastern China. J Clean Prod 259:120806. https://doi.org/10.1016/j.jclepro.2020.120806

Jiang P, Chen Y, Geng Y, et al (2013) Analysis of the co-benefits of climate change mitigation and air pollution reduction in China. J Clean Prod 58:130–137. https://doi.org/10.1016/j.jclepro.2013.07.042

Lei Y, Zhang Q, He KB, Streets DG (2011) Primary anthropogenic aerosol emission trends for

China, 1990-2005. Atmos Chem Phys 11:931–954. https://doi.org/10.5194/ACP-11-931-2011

Levin K, Rich D (2017) Turning points: trends in countries' reaching peak greenhouse gas emissions over time. https://www.wri.org/research/turning-points-trends-countries-reaching-peak-greenhouse-gas-emissions-over-time

Li K, Jacob DJ, Liao H, et al (2019a) Anthropogenic drivers of 2013–2017 trends in summer surface ozone in China. Proc Natl Acad Sci U S A 116:422–427. https://doi.org/10.1073/pnas.1812168116

Li K, Jacob DJ, Liao H, et al (2019b) A two-pollutant strategy for improving ozone and particulate air quality in China. Nat Geosci 12:906–910. https://doi.org/10.1038/s41561-019-0464-x

Li M, Liu H, Geng G, et al (2017) Anthropogenic emission inventories in China: A review. Natl. Sci. Rev. 4:834–866

Li M, Zhang D, Li CT, et al (2018) Air quality co-benefits of carbon pricing in China. Nat Clim Chang 8:398–403. https://doi.org/10.1038/s41558-018-0139-4

Li M, Zhang Q, Zheng B, et al (2019c) Persistent growth of anthropogenic non-methane volatile organic compound (NMVOC) emissions in China during 1990-2017: Drivers, speciation and ozone formation potential. Atmos Chem Phys 19:8897–8913. https://doi.org/10.5194/acp-19-8897-2019

Li N, Chen W, Rafaj P, et al (2019d) Air Quality Improvement Co-benefits of Low-Carbon Pathways toward Well below the 2 °C Climate Target in China. Environ Sci Technol 53:5576–5584. https://doi.org/10.1021/acs.est.8b06948

Liang X, Zhang S, Wu Y, et al (2019) Air quality and health benefits from fleet electrification in China. Nat Sustain 2019 210 2:962–971. https://doi.org/10.1038/s41893-019-0398-8

Liu H, Cai B, Zhang L, et al (2021) Research on carbon dioxide abatement technology and cost in China's power industry (In Chinese). Environ Eng 39:8–14. https://doi.org/10.13205/j.hjgc 202110000

Liu M, Huang Y, Jin Z, et al (2017) Estimating health co-benefits of greenhouse gas reduction strategies with a simplified energy balance based model: The Suzhou City case. J Clean Prod 142:3332–3342. https://doi.org/10.1016/j.jclepro.2016.10.137

Liu Z, Guan D, Moore S, et al (2015) Climate policy: Steps to China's carbon peak. Nature 522:279–281

Lu X, Zhang S, Xing J, et al (2020) Progress of Air Pollution Control in China and Its Challenges and Opportunities in the Ecological Civilization Era. Engineering 6:1423–1431

Lu Z, Huang L, Liu J, et al (2019) Carbon dioxide mitigation co-benefit analysis of energy-related measures in the Air Pollution Prevention and Control Action Plan in the Jing-Jin-Ji region of China. Resour Conserv Recycl X 1:100006. https://doi.org/10.1016/j.rcrx.2019.100006

Mallet V, Sportisse B (2006) Uncertainty in a chemistry-transport model due to physical parameterizations and numerical approximations: An ensemble approach applied to ozone modeling. J Geophys Res Atmos 111:1302. https://doi.org/10.1029/2005JD006149

Mao X, Xing Y, Hu T, et al (2012) An environmental-economic analysis of carbon, sulfur and nitrogen co-reduction path for China's power industry (In Chinese). China Environ Sci 32:748–756

Markandya A, Armstrong BG, Hales S, et al (2009) Public health benefits of strategies to reduce greenhouse-gas emissions: low-carbon electricity generation. Lancet 374:2006–2015

Martínez DM, Ebenhack BW, Wagner TP (2019) Energy efficiency: Concepts and calculations. Elsevier

Masson-Delmotte V, Zhai P, A. Pirani, et al (2021) IPCC, 2021: Summary for Policymakers. In: Climate Change 2021: The Physical Science Basis. Contribution of Working Group I to the Sixth Assessment Report of the Intergovernmental Panel on Climate Change (In press)

MEE (2014a) Technical Guidelines for Compiling the Primary Source Emission Inventory of Inhalable Particulate Matter. In: Minist. Ecol. Environ. People's Repub. China. http://www.mee.gov.cn/gkml/hbb/bgg/201501/t20150107_293955.htm?COLLCC=4091198132&. Accessed 12 Mar 2020

MEE (2014b) The guidelines for preparing an emission inventory of atmospheric fine particulate matter from primary sources. In: Minist. Ecol. Environ. People's Repub. China. http://www.mee.gov.cn/gkml/hbb/bgg/201408/t20140828_288364.htm. Accessed 12 Mar 2020

MEIC (2021) MEIC Model – Tracking Athropogenic Emissions in China. http://meicmodel.org/. Accessed 18 Mar 2021

Miao Y, Che H, Zhang X, Liu S (2021) Relationship between summertime concurring $PM_{2.5}$ and O3 pollution and boundary layer height differs between Beijing and Shanghai, China. Environ Pollut 268:115775. https://doi.org/10.1016/j.envpol.2020.115775

Ministry of Ecology and Environment of the People's Republic of China (2018) Notice on issuing the Fenwei Plain 2018-2019 Autumn and Winter Comprehensive Air Pollution Control Action Plan. https://www.mee.gov.cn/xxgk2018/xxgk/xxgk03/201810/t20181029_667650.html

Ministry of Ecology and Environment of the People's Republic of China (2017) Notice on issuing the Beijing-Tianjin-Hebei and the surrounding region 2017-2018 Autumn and Winter Comprehensive Air Pollution Control Action Plan. http://www.mee.gov.cn/gkml/hbb/bwj/201708/t20170824_420330.htm

Moran PAP (1948) The Interpretation of Statistical Maps. J R Stat Soc Ser B 10:243–251. https://doi.org/10.1111/j.2517-6161.1948.tb00012.x

Naghavi M, Wang H, Lozano R, et al (2015) Global, regional, and national age–sex specific all-cause and cause-specific mortality for 240 causes of death, 1990–2013: a systematic analysis for the Global Burden of Disease Study 2013. Lancet 385:117–171. https://doi.org/10.1016/S0140-6736(14)61682-2

National Bureau of Statistics (2020a) China's economic and social big data research platform. https://data.cnki.net/Yearbook/Navi?type=type&code=A. Accessed 18 Feb 2021

National Bureau of Statistics (2020b) Statistical yearbook. http://www.stats.gov.cn/. Accessed 18 Feb 2021

National Bureau of Statistics (2020c) China Statistical Yearbook on Environment. https://data.cnki.net/trade/Yearbook/Single/N2019030257?z=Z008.

National Development and Reform Commission (2010) Pilot projects for low-carbon provinces and cities. http://www.ncsc.org.cn/SY/dtsdysf/202003/t20200319_769716.shtml. Accessed 18 Feb 2021

NDRC (2015) China's Intended Nationally Determined Contribution Document. In: Natl. Dev. Reform Comm. China. https://www4.unfccc.int/sites/submissions/indc/Submission Pages/submissions.aspx.

NDRC (2011) Guidelines for Provincial Greenhouse Gas Inventory. http://www.ncsc.org.cn/SY/tjkhybg/202003/t20200319_769763.shtml.

Nemet GF, Holloway T, Meier P (2010) Implications of incorporating air-quality co-benefits into climate change policymaking. Environ Res Lett 5:014007. https://doi.org/10.1088/1748-9326/5/1/014007

OECD (2021) OECD data. https://data.oecd.org

Oh I, Yoo WJ, Yoo Y (2019) Impact and interactions of policies for mitigation of air pollutants and greenhouse gas emissions in Korea. Int J Environ Res Public Health 16. https://doi.org/10.3390/ijerph16071161

People's Government of Shandong (2021) Notice of the People's Government of Shandong on issuing the 14th Five year Plan and the Vision 2035. http://www.shandong.gov.cn/art/2021/4/25/art_107851_111958.html

People's Government of Yantai (2021) Notice of the People's Government of Yantai on issuing the 14th Five year Plan and the Vision 2035. http://www.yantai.gov.cn/art/2021/6/12/art_43632_2943830.html

Putra A, Tong G, Pribadi D (2020) Spatial Analysis of Socio-Economic Driving Factors of Food Expenditure Variation between Provinces in Indonesia. Sustainability 12:1638. https://doi.org/10.3390/su12041638

Qi J, Zheng B, Li M, et al (2017) A high-resolution air pollutants emission inventory in 2013 for the Beijing-Tianjin-Hebei region, China. Atmos Environ 170:156–168. https://doi.org/10.1016/j.atmosenv.2017.09.039

Qian L, Lu Z, Fang Q (2019) Establishing Climate Investment and Financing Mechanisms to Boost Achieving to the Local Carbon Emission Peak (In Chinese). Environ Prot 47:15–19. https://doi.org/10.14026/j.cnki.0253-9705.2019.24.004

Richard O. Gilbert (1987) Statistical Methods for Environmental Pollution Monitoring | Wiley. John Wiley and Sons, New York

Royston JP (1982) An Extension of Shapiro and Wilk's W Test for Normality to Large Samples. J R Stat Soc Ser C (Applied Stat 31:115–124. https://doi.org/10.2307/2347973

Simon H, Baker KR, Phillips S (2012) Compilation and interpretation of photochemical model performance statistics published between 2006 and 2012. Atmos Environ 61:124–139. https://doi.org/10.1016/J.ATMOSENV.2012.07.012

SSP (2017) The Shared Socioeconomic Pathways and their energy, land use, and greenhouse gas emissions implications: An overview. Glob Environ Chang 42. https://doi.org/110.1016/j.gloenvcha.2016.05.009

State Council Information Office of the People's Republic of China (2021) Responding to Climate Change: China's Policies and Actions. http://www.scio.gov.cn/zfbps/32832/Document/1715506/1715506.htm. Accessed 9 Nov 2021

State Council of the People's Republic of China (2013) Notice of the general office of the state council on issuing the air pollution prevention and control action plan. http://www.gov.cn/zwgk/2013-09/12/content_2486773.htm. Accessed 18 Feb 2021

State Council of the People's Republic of China (2018) Notice of the state council on issuing the three-year action plan for winning the Blue Sky defense battle. http://www.gov.cn/zhengce/content/2018-07/03/content_5303158.htm. Accessed 18 Feb 2021

State Council of the People's Republic of China (2016) Notice of the state council on issuing the

work plan for controlling greenhouse gas emissions during the 13th Five-Year Plan. http://www.gov.cn/zhengce/content/2016-11/04/content_5128619.htm. Accessed 18 Feb 2021

Stocker TF, Qin D, G.-K.Plattner, et al (2013) IPCC, 2013: Summary for Policymakers. In: Climate Change 2013: The Physical Science Basis. Contribution of Working Group I to the Fifth Assessment Report of the Intergovernmental Panel on Climate Change. Cambridge

Sun J, Huang L, Liao H, et al (2017) Impacts of Regional Transport on Particulate Matter Pollution in China: a Review of Methods and Results. Curr Pollut Reports 2017 33 3:182–191. https://doi.org/10.1007/S40726-017-0065-5

The Guardian (2016) China ratifies Paris climate change agreement ahead of G20 . https://www.theguardian.com/world/2016/sep/03/china-ratifies-paris-climate-change-agreement. Accessed 29 Dec 2020

UNEP (2018) Emissions Gap Report 2018. Nairobi

United Nations (2019) 2019 Revision of World Population Prospects. https://population.un.org/wpp/

Wang H, Lu X, Deng Y, et al (2019) China's CO_2 peak before 2030 implied from characteristics and growth of cities. Nat Sustain 2:748–754. https://doi.org/10.1038/s41893-019-0339-6

Wang S, Zhao B, Wu Y, Hao J (2015) Target and measures to prevent and control ambient fine particle pollution in China. China Environ Manag 37–43

Wang T, Jiang Z, Zhao B, et al (2020) Health co-benefits of achieving sustainable net-zero greenhouse gas emissions in California. Nat Sustain 2020 38 3:597–605. https://doi.org/10.1038/s41893-020-0520-y

West JJ, Smith SJ, Silva RA, et al (2013) Co-benefits of mitigating global greenhouse gas emissions for future air quality and human health. Nat Clim Chang 3:885–889. https://doi.org/10.1038/nclimate2009

Wilson SM, Richard R, Joseph L, Williams E (2010) Climate Change, Environmental Justice, and Vulnerability: An Exploratory Spatial Analysis. https://home.liebertpub.com/env 3:13–19. https://doi.org/10.1089/ENV.2009.0035

World Bank (2021) Population estimates and projections Database. https://databank.worldbank.org/source/population-estimates-and-projections

World Health Organization (2021) WHO global air quality guidelines: particulate matter ($PM_{2.5}$ and PM_{10}), ozone, nitrogen dioxide, sulfur dioxide and carbon monoxide. Geneva

WRI China (2015) Greenhouse Gas Accounting Tool for Chinese Cities (Pilot Version 1.0).

https://www.wri.org.cn/en/publication/greenhouse-gas-accounting-tool-chinese-citiespilot-version-10. Accessed 18 Mar 2021

Wu P, Guo F, Cai B, et al (2021) Co-benefits of peaking carbon dioxide emissions on air quality and health, a case of Guangzhou, China. J Environ Manage 282:111796. https://doi.org/10.1016/j.jenvman.2020.111796

Wu S (2020) Problems and countermeasures of grid for environmental supervision (In Chinese). Environ Dev 32:213, 215. https://doi.org/10.16647/j.cnki.cn15-1369/X.2020.06.120

Xie Y, Dai H, Xu X, et al (2018) Co-benefits of climate mitigation on air quality and human health in Asian countries. Environ Int 119:309–318. https://doi.org/10.1016/j.envint.2018.07.008

Xing J, DIng Di, Wang S, et al (2019) Development and application of observable response indicators for design of an effective ozone and fine-particle pollution control strategy in China. Atmos Chem Phys 19:13627–13646. https://doi.org/10.5194/acp-19-13627-2019

Xing J, Lu X, Wang S, et al (2020) The quest for improved air quality may push China to continue its CO_2 reduction beyond the Paris Commitment. Proc Natl Acad Sci U S A 117:29535–29542. https://doi.org/10.1073/pnas.2013297117

Xinhua (2020) CPC sets targets through 2035 to basically achieve China's socialist modernization. http://www.xinhuanet.com/english/2020-10/29/c_139476284.htm. Accessed 18 Feb 2021

Xu L (2018) A brief summary on city carbon emission accounting (In Chinese). China Econ Stat Q 02:15–37

Yang X, Teng F (2018) The air quality co-benefit of coal control strategy in China. Resour Conserv Recycl. https://doi.org/10.1016/j.resconrec.2016.08.011

Zhang Q, Streets DG, Carmichael GR, et al (2009) Asian emissions in 2006 for the NASA INTEX-B mission. Atmos Chem Phys 9:5131–5153. https://doi.org/10.5194/acp-9-5131-2009

Zhang Q, Zheng Y, Tong D, et al (2019) Drivers of improved $PM_{2.5}$ air quality in China from 2013 to 2017. Proc Natl Acad Sci U S A 116:24463–24469. https://doi.org/10.1073/pnas.1907956116

Zhang S, Wu Y, Liu H, et al (2013) Historical evaluation of vehicle emission control in Guangzhou based on a multi-year emission inventory. Atmos Environ 76:32–42. https://doi.org/10.1016/j.atmosenv.2012.11.047

Zhao H, Ma W, Dong H, Jiang P (2017) Analysis of Co-Effects on Air Pollutants and CO_2 Emissions Generated by End-of-Pipe Measures of Pollution Control in China's Coal-Fired

Power Plants. Sustainability 9:499. https://doi.org/10.3390/SU9040499

Zhao S (2018) Analysis and Enlightenment on Atmospheric Hot Grid Construction in Jing-Jin-Ji Region (In Chinese). J EMCC 28:67–69. https://doi.org/10.13358/j.issn.1008-813x.2018.0825.03

Zheng B, Tong D, Li M, et al (2018) Trends in China's anthropogenic emissions since 2010 as the consequence of clean air actions. Atmos Chem Phys 18:14095–14111. https://doi.org/10.5194/acp-18-14095-2018

Zheng Y, Xue T, Zhang Q, et al (2017) Air quality improvements and health benefits from China's clean air action since 2013. Environ Res Lett 12:114020. https://doi.org/10.1088/1748-9326/AA8A32

Zhou Y, Liu L, Cao D (2013) Synergistical emission control of carbon dioxide and conventional pollutants in thermal power plants (In Chinese). Therm Power Gener 42:63–65. https://doi.org/10.3969/j.isn.1002-3364.2013.09.063